Operating machines at the nanoscale

Effects of electron-electron interactions and strong system-bath coupling on the working principles of electronic nanomachines

Dissertation

zur Erlangung des Grades eines Doktors
der Naturwissenschaften (Dr. rer. nat.)

am Fachbereich Physik der Freien Universität Berlin

vorgelegt von

Anton Bruch

Berlin, 2017

Gutachter

Erstgutachter: Prof. Felix von Oppen, PhD (Freie Universität Berlin)
Zweitgutachter: Prof. Dr. Piet W. Brouwer (Freie Universität Berlin)
Tag der Disputation: 11.12.2017

Abstract

The advancement of nanofabrication leads to the realization of machines on ever smaller scales, which utilize the coupling between mechanical degrees of freedom and electrons to perform a specific task. Upon this miniaturization, two fundamental properties of the participant electrons become increasingly important: First, they are charged particles that repel each other via Coulomb interactions, and second, they are fermionic quantum particles properly described by wavefunctions whose time-evolution is governed by the Schrödinger equation. In this thesis we investigate how these two fundamental features of the electrons modify the working principle of electronic nanomachines.

In the first part we examine an adiabatic quantum motor in which coupling to a one-dimensional electron system generates directed motion. Due to their confinement to a single dimension, the interactions between the electrons become important in this system. The motor is based on an electron pump, which is operated in reverse. We show that on the one hand the interactions enhance the robustness of the motor against 'leakages' through the electron pump, which would reduce the output power of the motor. On the other hand, the interactions also increase the friction of the motor. We show, however, that putting the one-dimensional electron system into contact with macroscopic electronic reservoirs, such as a battery to drive the motor, reduces the dissipation at steady velocity to the non-interacting value.

In the second part, we investigate how the thermodynamic laws, being extremely successful in describing the operation of macroscopic machines, can be applied to tiny electronic machines which are strongly coupled to their surrounding. We show for the simplest possible model, a single slowly driven electronic level coupled to a metallic bath, how to properly take the coupling energy and hybridization between system and bath into account. Thereby we derive the full thermodynamic description of this simple electronic nanomachine beyond the quasistatic equilibrium. Subsequently, we show the strong limitations of developed approach, which necessitates a splitting of the coupling Hamiltonian between effective system and bath to derive the thermodynamics of finite velocity transformations. We demonstrate that this splitting does not capture the fluctuations of the internal energy correctly and breaks down beyond the wide band limit. This motivates a new thermodynamic formulation on the basis of the Landauer-Büttiker theory of electronic transport to describe more complex nanoelectronic machines. Instead of calculating the thermodynamic functions of the strongly coupled subsystem directly, which are complicated by the strong hybridization and the proper placement of the coupling energy, we look at the thermodynamic evolution from an outside perspective, i.e. considering the associated currents in the attached leads. With this approach we provide a clear understanding of the general connection between heat and entropy currents generated when operating an electronic nanomachine, and show their connection to the occurring dissipation. The developed formalism is applicable to arbitrary non-interacting electron systems which are slowly driven. Finally, we show the validity of the Jarzynski equality in these systems, which characterizes work fluctuations.

Zusammenfassung

Fortschritte in der Herstellung von Nanostrukturen führen zur experimentellen Realisierung von immer kleineren Maschinen, welche die Kopplung zwischen Elektronen und mechanischen Freiheitsgraden nutzen um bestimmte Aufgaben zu erfüllen. Je kleiner die Strukturen dabei werden, umso mehr treten zwei fundamentale Eigenschaften der beteiligten Elektronen in den Vordergrund: erstens tragen die Elektronen Ladung und stoßen sich gegenseitig ab. Und zweitens handelt es sich bei Elektronen um fermionische Quantenteilchen, welche mithilfe von Wellenfunktionen und der Schrödingergleichung beschrieben werden. In dieser Arbeit untersuchen wir, wie diese fundamentalen Eigenschaften der Elektronen das Wirkungsprinzip von elektronischen Nanomaschinen beeinflussen.

Im ersten Teil analysieren wir einen adiabatischen Quantenmotor, in welchem die Kopplung an ein eindimensionales Elektronensystem zu gerichteter Bewegung führt. Aufgrund ihrer Beschränkung auf eine einzelne Dimension spielen die Wechselwirkung zwischen den Elektronen eine große Rolle in diesem System. Der Motor basiert auf einer Elektronenpumpe, welche umgekehrt als Elektromotor betrieben wird. Wir zeigen, dass einerseits die Wechselwirkungen den Motor stabilisieren. Andererseits führen die Wechselwirkungen auch zu einer erhöhten Reibung, was auf den ersten Blick den Wirkungsgrad des Motors verringert. Eine genauere Untersuchung zeigt jedoch, dass die Dissipation bei stationärer Geschwindigkeit auf den Wert von nicht wechselwirkenden Elektronen reduziert wird sobald das eindimensionale Elektronensystem an makroskopische Reservoirs angeschlossen wird, um den Motor zum Beispiel über eine Batterie zu betreiben.

Im zweiten Teil untersuchen wir, wie die Gesetze der Thermodynamik, welche extrem erfolgreich dabei sind makroskopische Maschinen zu beschreiben, auf sehr kleine elektronische Maschinen angewendet werden können die stark an ihre Umgebung gekoppelt sind. Wir zeigen im einfachst möglichen System, das aus einem einzelnen langsam getriebenen Niveau in Kontakt zu einem metallischen Bad besteht, wie man die Hybridisierung und die Kopplungsenergie in der thermodynamischen Beschreibung richtig berücksichtigt und erlangen eine vollständige Charakterisierung dieser elektronischen Nanomaschine über das quasistatische Regime hinaus. Anschließend leiten wir her, dass das symmetrische Aufspalten des Hamiltonoperators der Kopplung zwischen effektivem System und Bad, welches benötigt wird um Prozesse mit endlicher Geschwindigkeit zu beschreiben, die Anwendbarkeit des Formalismus stark beschränkt. Erstens prognostiziert diese effektive Aufspaltung die falschen Fluktuationen der inneren Energie, und zweitens lässt sie sich bei energieabhängiger Kopplung zwischen System und Bad, das heißt außerhalb der 'wide band' Approximation, überhaupt nicht anwenden. Daher entwickeln wir einen neuen Zugang zu stark gekoppelter Thermodynamik auf Basis der Landauer-Büttiker-Theorie zu Quantentransport, welcher die Beschreibung von komplexeren nanoelektronischen Maschinen ermöglicht. Anstatt die thermodynamischen Größen des stark gekoppelten Subsystems direkt zu berechnen, nehmen wir dabei die assoziierten Ströme in den angeschlossenen Leitern in den Fokus und beschreiben die Zustandsänderungen aus einer Aussenperspektive. Das führt zu einem klaren Verständnis vom Zusammenhang zwischen Entropie- und Wärmeströmen und ihrer Verbindung zu der auftretenden Dissipation. Unsere Theorie ermöglicht eine vollständige Beschreibung der thermodynamischen Zustandsänderungen von beliebigen, langsam getriebenen Elektronensystemen, in denen die Wechselwirkungen zwischen den Elektronen vernachlässigt werden können. Abschließend zeigen wir für solche Systeme die Gültigkeit der Jarzynsikigleichung, welche die Fluktuationen der Arbeit beschreibt.

Contents

1 | Introduction: Nanomachines on the move

The miniaturization of electronic devices has drastically changed modern life. Calculations that used to be done by room size computers, can now be performed in smart phones – at a multiple of the speed [Wolf, 2015]. This is primarily driven by the strongly enhanced complexity of the involved semiconductor chips, said to double every two years by Moore's law. But not only computer chips become increasingly sophisticated as fabrication gets more and more refined. Also tiny machines that utilize the coupling between electronic and mechanical degrees of freedom get integrated into the electronic circuits of modern devices, forming an important cornerstone of state-of-the-art technology. In today's smartphones they are in use for motion sensing (gyroscopes and accelerators), stabilization, and filtering (bulk acoustic wave filters). Upon further miniaturization of these devices, currently commercially operated at the micron scale, new opportunities open up arising from their reduced dimension and mass, high resonance frequencies, small force constants, and high quality factors [Craighead, 2000; Ekinci and Roukes, 2005; Zhang et al., 2013]. Mass sensing of single molecules [Naik et al., 2009], force detection of single spins [Rugar et al., 2004], and explorations of the quantum regime of mechanical oscillators [O'Connell et al., 2010] point to exciting technological advances and allow for new insights into the coupling between electrons and mechanical modes from a fundamental science perspective.

One challenge to building future nanotechnology is to generate directed motion on the nanoscale – a nanomotor. Modern life is influenced by an immense variety of motors in all forms and sizes, driven by energy sources ranging from heat, as in a combustion engine, through chemical energy in biological motors to electrical energy in electric motors. As the miniaturization of modern devices moves forward, the need for control over mechanical motion at these scales becomes increasingly pressing. The advances in experiments and nanofabrication are impressive: nanomechanical motion was already realized using chemical energy [Collins et al., 2016; Wilson et al., 2016], light [Koumura et al., 1999; Klok et al., 2008], and electrons [Tierney et al., 2011; Kudernac et al., 2011] as driving agents. And the design and synthesis of the involved molecular machines earned

Jean-Pierre Sauvage, Sir J. Fraser Stoddart and Ben Feringa the Nobel Prize in Chemistry in 2016.

We focus here on nano-electromechanical machines, which utilize the coupling between mechanical modes and many electrons to perform a prescribed task. As these devices become very small, the theoretical description of their operation moves to exciting new frontiers: the quantum mechanical nature of the electrons plays an increasing role as do the interactions between them. In this thesis we focus on two key aspects: First, the influence of the interactions between electrons on the working principle of electronic nanomachines. Second, how to extend the thermodynamic laws, the ruling description of machines since the industrial revolution, to analyze their operation.

1.1 Electromechanical coupling

Nano-electromechanical machines rely fundamentally on the coupling between electrons and mechanical modes at these small scales. This coupling becomes manifest in the dependence of the electronic current through a nanostructure on mechanical deformations, e.g. vibrations of the nanostructure, and in the inverse effect in a modification of the mechanical dynamics by an electric current. In general these couplings fall into two different regimes, depending on the involved time scales.

In the regime of slow electrons, the time that the electrons spend in the nanostructure is long compared to typical mechanical periods. This is typically realized for the transport through molecular junctions, where the vibrations are fast and the coupling between the molecule and the adjacent metallic lead is small [Galperin et al., 2007]. In this regime one can observe vibrational side-bands in the conductance spectra, induced by the absorption or emission of one or several vibrational quanta in an electronic tunneling event when the electro-mechanical coupling is weak [Park et al., 2000; Yu et al., 2004]. If the coupling becomes strong, the transport through the nanostructure can be strongly suppressed by an effect known as Franck-Condon blockade [Koch and von Oppen, 2005; Koch et al., 2006], analogous to the suppression of certain electronic-vibrational transitions in molecular spectroscopy.

In the opposite regime of fast electrons, the electrons spend a very short time in the nanostructure compared to the vibration period and observe an almost static configuration of the mechanical modes. This regime is typically realized for slower, collective mechanical modes for example in suspended carbon nanotubes [Steele et al., 2009; Lassagne et al., 2009; Benyamini et al., 2014]. We focus on this adiabatic regime in the present thesis.

The theoretical analysis of the adiabatic regime was in the past executed assuming non-interacting electrons in a Fermi liquid theory, treated with a combination of non-equilibrium Green's functions and scattering theory [Bode et al., 2011, 2012b; Thomas et al., 2012], and field theoretic treatments on the basis

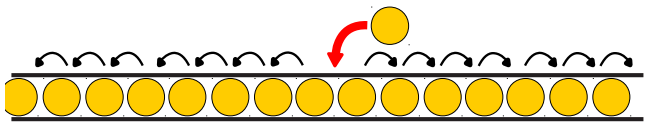

Figure 1.1: In a 1d electron systems any motion of an electron, such as the addition of an extra electron depicted here, necessitates a reaction of all other electrons in the system. This excludes quasi-particle-like excitations and leads to a description of the system in terms of the collective modes.

of the Feynman-Vernon influence functional [Lü et al., 2012]. However, the assumption of non-interacting electrons can be violated when the electrons become strongly confined to small nanostructures.

1.2 Interaction effects due to reduced dimensionality

Even a small piece of metal ($\sim [1\text{mm}]^3$) contains a huge number ($\sim 10^{20}$) of free electrons. Since these are charged particles, they all interact with each other via Coulomb interactions – a horrendously complicated problem already in the static case, not even speaking of coupling them to time-dependent potentials to make use of them to drive a nanomotor. Luckily things are not so bad: the Fermi liquid theory provides a drastic simplification of the multi-particle problem. In its essence it shows that the low energy excitations of the interacting many-body system behave like free quasi-particles [Landau, 1957]. It is so successful, and its application ubiquitous that deviations from it are considered exotic and exciting.

Strong deviations from the Fermi liquid behavior occur when electrons are confined to lower-dimensional regions. When they are constrained to a 0-dimensional structure, a quantum dot, with a sufficiently small coupling to the surrounding, the energy needed to add an additional electron to the dot (charging energy) becomes important [Kouwenhoven et al., 1997]. Therefore in this situation the description of the excitations as non-interacting quasi-particles breaks down. The coupling to mechanical modes in this regime has in the past been treated on the basis of the Pauli master equation, which treats the electronic occupations in terms of classical probabilities and is valid at sufficiently small couplings to the surrounding and sufficiently high temperatures so that quantum mechanical coherences can be neglected [Koch and von Oppen, 2005; Koch et al., 2006].

Another situation which strongly deviates from the Fermi liquid behavior is when the electrons are confined to a single spatial dimension, like in a quantum wire with sufficiently low diameter. The fermionic nature of the electrons (and with it the Pauli principle) forbids independent motion of an electron in the

system regardless of the effective strength of Coulomb interactions between the electron, see Fig. 1.1. Therefore any motion in the one-dimensional structure is necessarily collective. Coming as a drawback at first sight, since one has to give up the beloved picture of essentially free quasi-particles, this collective nature of all excitations turns out to be a virtue: an exactly solvable *bosonic* description in terms of the collective excitations is possible for the low energy excitations [Haldane, 1981]. This kind of one-dimensional (1d) electron system is called a Luttinger liquid.

The behavior of a Luttinger liquid deviates significantly from a Fermi liquid in several aspects. In a Luttinger liquid, spin and charge excitations can move independently at different velocities, while they are tied together in the quasi-particle excitations of a Fermi liquid. This was observed, e.g., in quantum wires [Tserkovnyak et al., 2002; Auslaender et al., 2002; Tserkovnyak et al., 2003; Auslaender et al., 2005]. The same effect that lets all excitations be collective also suppresses the tunneling conductance into a Luttinger liquid at low energies (zero-bias anomaly): since the electrons cannot pass each other, addition of an extra electron into the wire requires a movement of all the other electrons of the 1d system (Fig. 1.1). Experimentally this was found, e.g., in carbon nanotubes [Dekker et al., 1999] and quantum wires [Auslaender et al., 2000, 2002].

To make use of a one-dimensional electron system as fuel for a nanomachine, a good understanding of the coupling between mechanical degree of freedom and Luttinger liquid is needed. One goal of this thesis is thus to investigate the effect of electron-electron interactions in such a one-dimensional system on the electro-mechanical coupling. Thereby we want to find out, how electron-electron interactions affect the working principles of nano-electromechanical motors.

1.3 Thermodynamic laws describing the operation of nanomachines

Classical machines such as heat engines and refrigerators are described by thermodynamic laws which characterize how a subsystem exchanges energy – in the form of both heat and work – and particles with its environment. The theory of thermodynamics, founded by Nicolas Léonard Sadi Carnot in 1824 [Carnot, 1824] in the desire to defeat the British in the Napoleonic wars by increasing the efficiency of steam engines at the time, is extremely successful: it describes very complex systems containing $\sim 10^{22}$ particles with just a few parameters such as temperature, pressure, and volume. In an idealization of a heat engine, the classical Carnot cycle describes heat-to-work conversion by considering expansion and compression of a gas in contact to either a hot or a cold reservoir respectively–or being isolated from both (see Fig. 1.2).

Once one leaves the macroscopic world towards smaller scales, several things change. The surface-to-volume ratio becomes drastically enhanced in nanostructures. In macroscopic thermodynamics this ratio vanishes, which justifies

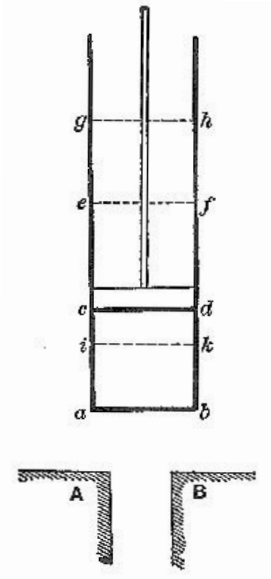

Figure 1.2: Carnot's heat engine: a movable piston compresses and expands a gas while being in contact to a hot (A) or a cold (B) reservoir, or being isolated from both [Carnot, 1824].

the practice of disregarding the system-bath coupling in the thermodynamic description. In contrast, when considering the thermodynamics of small systems, special attention has to be given to both the definition of the 'system' and consequently the 'bath', and their mutual interaction. This issue is furthermore closely connected to the quantum nature of the electrons. At sufficiently low temperatures and strong couplings, the hybridization with the surrounding necessitates a full quantum treatment of the problem, including the coherent evolution of the electronic wave functions. These issues have been the subject of several earlier papers, which addressed quantum particles strongly coupled to a harmonic oscillator bath [Allahverdyan and Nieuwenhuizen, 2000; Hänggi et al., 2008; Hilt and Lutz, 2009] and also simple models for the electronic nanomachines considered here [Ludovico et al., 2014; Esposito et al., 2015b].

In an elementary thermodynamic transformation, an external agent performs work on a system by changing its Hamiltonian, constituting a stroke of a quantum engine, analogous to the compression and expansion of a gas in the Carnot engine above. For electronic nanomachines, this is achieved by changing the potential in a finite region which is coupled to electronic reservoirs. This type of machine can be realized by a quantum dot connected to leads and subject to a time-dependent gate potential (see Fig. 1.3). In the presence of strong coupling between the quantum dot and the surrounding electronic reservoirs, the hybridization between the electronic levels of the dot and the bath com-

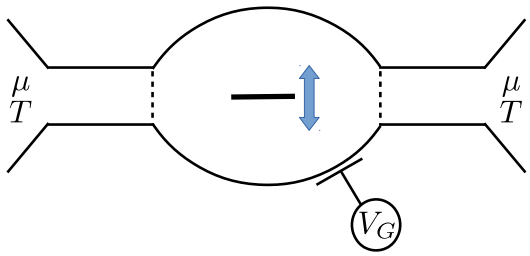

Figure 1.3: Quantum dot engine: a quantum dot open to electronic reservoirs of temperature T and chemical potential μ is subject to a changing gate voltage V_G. The gate voltage changes the energy levels of the dot, thereby doing work on the system and acting as a "nano-piston".

plicates the thermodynamic description: The system-bath distinction becomes fuzzy and quantum mechanical coherences become important. Even for the simplest possible case of just a single time-dependent level coupled to metallic leads, i.e. the resonant level model, the thermodynamic description in the strong coupling regime is nontrivial and sparked a lot of discussion in the community [Ludovico et al., 2014; Esposito et al., 2015a,b; Bruch et al., 2016; Ochoa et al., 2016]. The present thesis introduces our contribution that overcomes flaws in earlier approaches for this model [Esposito et al., 2015b] in Chapter 3. This treatment of the simplest possible electronic nanomachine builds a solid basis for the development of a new approach in Chapter 5 that yields a general thermodynamic theory of strongly coupled electronic nanomachines applicable to arbitrary non-interacting electron systems. Thereby we aim at better understanding the working principles of electronic nanomachines.

The problem of system-bath distinction in the strong coupling regime is not the only issue that arises when one tries to describe small quantum systems thermodynamically. While for macroscopic systems fluctuations around the mean are strongly suppressed by the huge number of participant particles, the thermodynamic quantities necessarily acquire strong fluctuations at small scales. Remarkably, the entire probability distribution of these fluctuating quantities can be characterized elegantly for very general thermodynamic transformations, also far from equilibrium. This development started with classical systems [Jarzynski, 1997; Crooks, 1999], and was later generalized to quantum systems with arbitrarily strong system-bath coupling [Campisi et al., 2009]. These laws go under the name of fluctuation theorems, which gained considerable attention in recent years [[Talkner et al., 2007; Jarzynski, 2011; Hänggi and Talkner, 2015]. Experimentally the fluctuation theorems were confirmed for systems ranging from classical zipping-unzipping experiments of DNA hairpins [Mossa et al., 2009; Junier et al., 2009], electrons in a single-electron box [Saira et al., 2012; Koski et al., 2013, 2014], trapped ions [An et al., 2014], to nuclear spins [Batalhão et al., 2014]. In Chapter 6 we show the validity of the work fluctuation theorem within our developed formalism for slow transformations of non-interacting

electron systems.

1.4 Outline of this thesis

We organize the present thesis as follows:

To investigate the effect of electron-electron interactions on the working principle of electronic nanomachines, which gain importance due reduced dimensionality, we consider a model for a quantum motor based on a 1d electron pump operating in reverse [Qi and Zhang, 2009; Bustos-Marún et al., 2013] in Chapter 2. In such a pump, the cyclic variations of parameters, here effected by a mechanical degree of freedom, lead to a net charge transport through the device [Brouwer, 1998]. In the reverse mode a *dc* bias is applied and the forces exerted by the scattered electrons drive the coupled mechanical degree of freedom [Bode et al., 2011, 2012b; Thomas et al., 2012], realizing a motor. We present a field theoretic treatment of an adiabatic quantum motor in which coupling to a one-dimensional interacting electron system generates directed motion. The system is based on a Thouless electron pump operating in reverse. When the sliding periodic potential of the pump is associated with the motor degree of freedom, a bias voltage applied to the 1d electron channel sets the motor in motion. To investigate the effects of electron-electron interactions we model the leads of the Thouless motor as Luttinger liquids. We show that interactions enhance the energy gap opened by the periodic potential and the robustness of the Thouless motor against variations in chemical potential. Thereby interactions support the working principle of the motor. While in the case of an infinite Luttinger liquid the coupling induced friction is enhanced by electron-electron interactions, the connection to Fermi liquid reservoirs results in a reduction of the dissipation at steady velocity to the non-interacting value. We show that our results can be readily applied to the model of a nanomagnet coupled to a quantum spin Hall edge. The manuscript for a publication about the content of this chapter is in preparation.

To study the thermodynamics for strongly coupled electronic nanomachines, we consider the simplest possible example in Chapter 3: the resonant level model. We present a consistent thermodynamic theory for the resonant level model in the wide band limit, whose level energy is driven slowly by an external force. The problem of defining 'system' and 'bath' in the strong coupling regime is circumvented by considering as the 'system' everything that is influenced by the externally driven level. The thermodynamic functions that are obtained to first order beyond the quasistatic limit fulfill the first and second law with a positive entropy production, successfully connect to the forces experienced by the external driving, and reproduce the correct weak coupling limit of stochastic thermodynamics. This chapter is based on Ref. [Bruch et al., 2016].

Subsequently we investigate the limitation of this approach. The treatment of Chapter 3 demands the representation of the internal energy in terms of an expectation value of a split Hamiltonian to take proper account of the coupling

energy. Only on this basis the non-equilibrium Green's function formalism can be employed to find the thermodynamic functions beyond the quasistatic limit. We demonstrate in Chapter 4 that this splitting of the coupling Hamiltonian in the resonant level model has a very limited applicability: First, already in wide band limit and in equilibrium, the fluctuations of the internal energy are not properly captured by a split Hamiltonian, narrowing its use to the mean of the internal energy. Second, beyond the wide band limit, no splitting of the system-bath interaction can properly describe the thermodynamic functions of the strongly coupled level. This chapter is based on Ref. [Ochoa et al., 2016].

In Chapter 5 we overcome these limitations and develop an approach to strongly coupled thermodynamics from an outside perspective that is applicable to arbitrary non-interacting electron systems. For that we develop a Landauer-Büttiker theory of entropy evolution in time-dependent strongly coupled electron systems. This formalism naturally avoids the problem of system-bath distinction caused by the strong hybridization of central system and surrounding reservoirs. In an adiabatic expansion up to first order beyond the quasistatic limit, it provides a clear understanding of the connection between heat and entropy currents generated by time-dependent potentials and shows their connection to the occurring dissipation. Combined with the work required to change the potential, the developed formalism provides a full thermodynamic description from an outside perspective. This chapter is based on Ref. [Bruch et al., 2017].

In the final Chapter 6 we show the validity of the Jarzynski equality characterizing the non-equilibrium work distribution for slowly driven non-interacting electron systems.

Throughout this thesis we use units in which the reduced Planck constant $\hbar = 1$ and the Boltzmann constant $k_B = 1$ are set to unity.

2 | An interacting adiabatic quantum motor

To study the effects of electron-electron interactions on electronic nanomachines, we consider a device, in which electrons in a one-dimensional (1d) wire are coupled to a slowly sliding periodic potential. The sliding periodic potential is associated with the mechanical degree of freedom of the motor as depicted in Fig. 2.1. This device exhibits the essential features of an ancient Archimedean screw. When operating the Archimedean screw as a pump, turning of the screw leads to water transport. The same happens in the electronic system, where the sliding periodic potential pumps electrons through the 1d conductor, forming a Thouless pump [Thouless, 1983]. When the Archimedean screw is operated in reverse, the water pushed through makes it work as a turbine. Similarly, in the electronic system a current pushed through the 1d conductor by an applied *dc* bias voltage slides the periodic potential associated with the slow mechanical degree of freedom, turning the device into a Thouless motor [Qi and Zhang, 2009; Bustos-Marún et al., 2013].

Possible physical realizations of the Thouless motor were proposed based on a nanoscale helical wire placed in between capacitor plates [Qi and Zhang, 2009] and on a quantum spin Hall (QSH) edge coupled to a nanomagnet [Meng et al., 2014; Arrachea and von Oppen, 2015; Silvestrov et al., 2016]. In the case of the helical wire, a slowly rotating transverse electric field leads to charge pumping, while in the inverse mode an applied *dc* bias in the presence of a static field leads to a rotation of the helix. Similarly the precession of the magnetization of the nanomagnet pumps charge along the QSH edge, while in the inverse mode an applied bias leads to a spin transfer torque acting on the nanomagnet and driving its precession, cf. Fig. 2.1b).

The earlier theoretical description of adiabatic quantum motors assumed non-interacting electrons. When the electrons are confined to 1d, as in the present case of the quantum wire, the low energy behavior is modified by electron-electron interactions in essential ways. In this paper we investigate how these interaction effects modify the dynamics of adiabatic quantum motors. We describe the 1d electronic system as a Luttinger liquid (LL), which provides an exact description of its low energy excitations in terms of bosonic collective

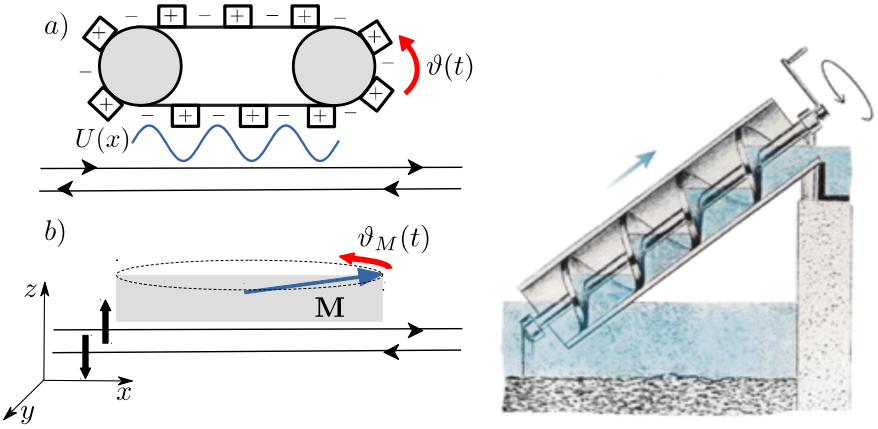

Figure 2.1: a) Model for a Thouless motor based on a single channel quantum wire in proximity to a chain of alternating charges. The sliding periodic potential $U(x)$ is associated with the rotational degree of freedom $\vartheta(t)$ of the quantum motor. b) A Nanomagnet with magnetization **M** is coupled to a single edge of a quantum spin Hall insulator in the x-y-plane, where $\vartheta_M(t)$ (angle of the in-plane magnetization) is associated with the motor degree of freedom. The Thouless motor resembles an Archimedean screw water pump (on the right, figure taken from [Altshuler and Glazman, 1999]).

excitations [Giamarchi, 2004]. LL theory has proven a useful description of both quantum wires [Fisher and Glazman, 1997; Auslaender et al., 2005] and QSH edges [Wu et al., 2006], covering the possible physical realizations of the Thouless motor mentioned above. Furthermore, our LL approach leads to a field theoretic description of quantum motors, complementing the earlier analysis on the basis of Landauer-Büttiker theory [Bustos-Marún et al., 2013]. For definiteness we base our discussion on the Thouless motor and give an explicit translation of the results to the magnetic system in Sec. 2.5.

We introduce the model of the Thouless pump in Sec. 2.1. In Sec. 2.3 we investigate the coupling of the LL to the periodic potential and derive the effective gap size in the presence of electron-electron interactions. Section 2.4 is devoted to the derivation of the effective field theory of the motor degree of freedom that leads to an interaction dependent effective Langevin equation for the motor dynamics. In the case of an infinite LL the friction is enhanced by repulsive interactions, as shown in Sec. 2.4.2. The connection to Fermi liquid (FL) leads yields an effective equation of motion including memory and restores the reduced non-interacting dissipation at steady velocity, as presented in Sec. 2.4.4. In the final section 2.5 we give the explicit translation of the obtained results to the nanomagnet coupled to a QSH edge.

2.1 Model

Our model of a quantum motor is based on a finite length Thouless pump operating in reverse. A toy model realizing such a pump is sketched in Fig. 2.1. A single channel quantum wire is placed next to a chain of fixed, periodically alternating charges. These charges move with respect to the quantum wire when turning the wheel and advancing the angular degree of freedom ϑ. This causes a slowly sliding periodic potential for the electrons, thereby forming a Thouless pump [Thouless, 1983].

The sliding periodic potential U (cf. Fig. 2.1) is of the form

$$U(x) = 2\,V_0 \cos\left(q\,x - \vartheta(t)\right)\,\Theta\left(\frac{L}{2} - |x|\right)\,, \tag{2.1}$$

where q is the wavevector of the potential of strength $2V_0$. For $q \approx 2k_F$ (k_F is the Fermi momentum), the periodic potential causes backscattering between right and left moving electrons in the wire. The analysis of the system on the basis of Landauer-Büttiker theory for non-interacting electrons showed that, to exponential accuracy in the length L, the backscattering induced gap leads to a vanishing normal conductance, quantized charge pumping per cycle, and unit efficiency, i.e., a conversion of the entire electronic energy provided by the bias into mechanical energy associated with the degree of freedom ϑ [Bustos-Marún et al., 2013]. To include the interaction effects when confining the electrons to the 1d quantum wire, we model the electrons as a spinless LL [Haldane, 1981; Giamarchi, 2004]. We introduce the Luttinger liquid formalism in the following technical section, which can be skipped by readers either familiar with the topic or uninterested in technical details.

2.2 Technical section: Luttinger liquid

In the following we introduce the basic concepts needed to treat the interacting one-dimensional electron system, based on the books by Giuliani and Vignale [Giuliani and Vignale, 2005] and Giamarchi [Giamarchi, 2004]. A detailed derivation of all required quantities and relations is beyond the scope of this work. Instead, we try to sketch the most important steps in the derivation of the Luttinger model and provide the necessary relations needed in this thesis.

Above in Sec. 1.2 we already gave an intuitive picture why a bosonized description of the one-dimensional electron system might be useful: since the electrons can not pass each other in 1d, a movement of a single electron is necessarily accompanied by a reaction of all the other electrons of the system. Therefore all fundamental excitations are collective, hence bosonic, and quasi-particle-like fermionic excitations are forbidden unlike in 2d and 3d.

To describe the low-energy excitations of the system, the Luttinger model assumes a one-dimensional electron system with a linearized dispersion around

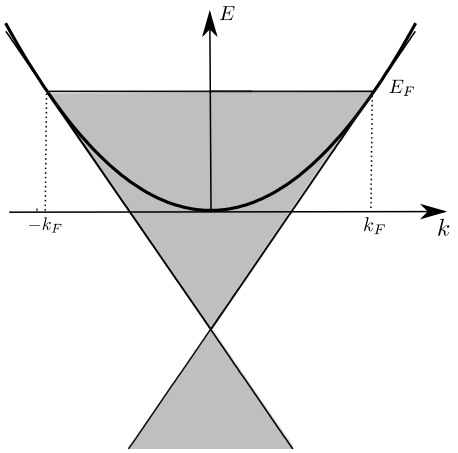

Figure 2.2: Linearized electron dispersion of the Luttinger model in the vicinity of $\pm k_F$.

the Fermi energy E_F (Fig. 2.2). By linearizing the spectrum, the band bottom is removed, which yields an infinite number of states with arbitrarily large negative energies. This needs to be accounted for by working with normal-ordered occupation numbers $\hat{N}_{k,\tau} = :a^\dagger_{k,\tau} a_{k,\tau}:$. Here $a^\dagger_{k,\tau}$ ($a_{k,\tau}$) is the creation (annihilation) operator of a right- ($\tau = 1$) or left-moving ($\tau = -1$) electron with wave vector k. The normal ordering is executed with respect to the vacuum, i.e. with all electronic states filled up to $\pm k_F$ for right and left movers, respectively, e.g.

$$:a^\dagger_{k,R} a_{k,R}: = \begin{cases} a^\dagger_{k,R} a_{k,R} & \text{for} \quad k > k_F \\ -a_{k,R} a^\dagger_{k,R} & \text{for} \quad k < k_F \,. \end{cases} \tag{2.2}$$

This yields the non-interacting Hamiltonian as $H_0 = v_F \sum_{k,\tau} (k\,\tau - k_F) :a^\dagger_{k,\tau} a_{k,\tau}:$, while interactions between the electrons take the form $\hat{H} = \frac{1}{2L} \sum_{q \neq 0} v_q \hat{n}_q \hat{n}_{-q}$. Here v_q is the Fourier transform of the interaction potential and $\hat{n}_q = \sum_k a^\dagger_{k-q} a_k$ is the electron density operator.

The normal ordering for the operators leads to an anomalous commutator for the density fluctuation operators $[\hat{n}_{q,\tau}, \hat{n}_{-q',\tau'}] = \frac{qL}{2\pi} \tau \delta_{q,q'} \delta_{\tau,\tau'}$. This shows that the electron density operators can serve as bosonic creation and annihilation operators

$$\hat{b}_q = \sqrt{\frac{2\pi}{L|q|}} \left(\Theta(q) \hat{n}_{q,R} + \Theta(-q) \hat{n}_{q,L} \right) \tag{2.3}$$

$$\hat{b}^\dagger_q = \sqrt{\frac{2\pi}{L|q|}} \left(\Theta(q) \hat{n}_{-q,R} + \Theta(-q) \hat{n}_{-q,L} \right) , \tag{2.4}$$

where Θ is the Heaviside step function. Furthermore one can show that the operators $\hat{b}^\dagger{}_q$ ($\hat{b}_q$) raise (lower) the energy of an eigenstate of H_0 by $v_F|q|$, leading to an interacting Hamiltonian in which all contributions are quadratic in the bosonic operators

$$H = \sum_{q\neq 0} \left[\left(v_F + \frac{V_1(q)}{2\pi} \right) |q| \hat{b}_q^\dagger \hat{b}_q + \frac{V_2(q)}{2\pi} |q| \left(\hat{b}_q^\dagger \hat{b}_{-q}^\dagger + \hat{b}_{-q} \hat{b}_q \right) \right] , \tag{2.5}$$

with $V_1(q) = v_q$ and $V_2(q) = v_q - v_{2k_F}$.
For our purpose it is beneficial to introduce a real space representation in terms of displacement field $\phi(x)$ and phase field $\theta(x)$

$$\phi(x) = \frac{1}{2i} \sum_{q\neq 0} \sqrt{\frac{2\pi}{L|q|}} \ \mathrm{sign}(q)\, \mathrm{e}^{iqx} \ \left(\hat{b}_q + \hat{b}_{-q}^\dagger \right) , \tag{2.6}$$

$$\theta(x) = \frac{1}{2i} \sum_{q\neq 0} \sqrt{\frac{2\pi}{L|q|}} \ \mathrm{e}^{iqx} \ \left(\hat{b}_q - \hat{b}_{-q}^\dagger \right) . \tag{2.7}$$

The displacement field $\phi(x)$ describes the local density fluctuations through

$$:n_R(x) + n_L(x): = \frac{\partial_x \phi(x)}{\pi} \tag{2.8}$$

and the phase field $\theta(x)$ is associated with the difference in density between right and left movers,

$$n_R(x) - n_L(x) = \frac{\partial_x \theta(x)}{\pi} . \tag{2.9}$$

These bosonic fields obey the commutation relations $[\theta(x), \nabla\phi(x')] = -i\pi\delta(x - x')$, which shows that the gradient of one field is the canonical conjugate momentum to the other up to a factor of $-\pi$ [Giamarchi, 2004]. In terms of these fields the Hamiltonian of the Luttinger model takes the form

$$H = \frac{v_c}{2\pi} \int \mathrm{d}x \left\{ \frac{1}{K} \left(\partial_x \phi(x) \right)^2 + K \left(\partial_x \theta(x) \right)^2 \right\} , \tag{2.10}$$

$$K = \sqrt{\frac{2\pi v_F + V_1(0) - V_2(0)}{2\pi v_F + V_1(0) + V_2(0)}} , \tag{2.11}$$

$$v_c = \sqrt{\left(v_F + \frac{V_1(0)}{2\pi} \right)^2 - \left(\frac{V_2(0)}{2\pi} \right)^2} , \tag{2.12}$$

where K is the dimensionless interaction parameter, with $K < 1$ for repulsive electron-electron interactions ($K = 1$ for a non-interacting system), and v_c is the charge velocity. Thus, one arrived at a remarkably elegant result: the low

energy excitations of the 1d electron system can be described by a quadratic (i.e., exactly solvable) bosonic theory, irrespective of the interaction strength. With that, the effect of electron-electron interactions in the model is reduced to the Luttinger parameter K and the charge velocity v_c.

One can also express the fermionic fields in terms of the bosonic ones as

$$\psi(x) = \psi_R(x) + \psi_L(x)\,, \tag{2.13}$$

$$\psi_{R/L}(x) = \frac{1}{\sqrt{2\pi\lambda}} \mathrm{e}^{\pm i k_F x} \mathrm{e}^{i[\theta(x) \pm \phi(x)]}\,, \tag{2.14}$$

where we neglect the Klein factors (which change the total number of left or right moving electrons in the system respectively) and λ is a short distance cutoff due to the finite band width [Giamarchi, 2004].

The basis of our field theoretic treatment is the canonical partition function of the Luttinger liquid

$$Z = \mathrm{Tr}\left\{\mathrm{e}^{-\beta H}\right\}\,, \tag{2.15}$$

which can be evaluated as a functional integral

$$Z = \int \mathbf{D}\left[\Pi, \phi\right] \exp\left(-S[\Pi, \phi]\right)\,. \tag{2.16}$$

Here, the Euclidean (imaginary time) action is obtained as [Giamarchi, 2004]

$$-S\left[\Pi, \phi\right] = \int_0^\beta \mathrm{d}\tau \int \mathrm{d}x \left[i\Pi(x,\tau)\partial_\tau \phi(x,\tau) - H\left(\phi(x,\tau), \Pi(x,\tau)\right)\right]\,, \tag{2.17}$$

where Π is the conjugate momentum of ϕ. Due to the commutation relations of the bosonic fields we can write this as

$$-S\left[\theta, \phi\right] = \int_0^\beta \mathrm{d}\tau \int \mathrm{d}x \left[-\frac{i}{\pi}\partial_x\theta\,\partial_\tau\phi - \frac{v_c}{2\pi}\left(\frac{1}{K}\left(\partial_x\phi\right)^2 + K\left(\partial_x\theta\right)^2\right)\right]\,, \tag{2.18}$$

where we dropped the time and space labels for better readability.

After integrating out the θ-field (since ϕ and θ are hermitian operators, the associated fields in functional integral representation are real), one obtains the action of the bare LL in the ϕ-representation [Fisher and Glazman, 1997; Kane and Fisher, 1992]

$$S_0 = \int d\mathbf{r} \frac{1}{2\pi K}\left[\frac{1}{v_c}\left(\partial_\tau\phi\right)^2 + v_c\left(\partial_x\phi\right)^2\right]\,. \tag{2.19}$$

Here we introduced the short hand notations $(x,\tau) = \mathbf{r}$ and $\int_0^\beta d\tau \int dx = \int d\mathbf{r}$.

The coupling to the sliding periodic potential in Eq. (2.1) gives the following contribution to the Hamiltonian for $q \sim 2k_F$

$$\begin{aligned} H_U &= \int dx\, \psi^\dagger(x) U(x) \psi(x) \\ &= V_0 \int dx \left[\mathrm{e}^{iqx + i\vartheta} \psi_R^\dagger(x) \psi_L(x) + \mathrm{e}^{-iqx - i\vartheta} \psi_L^\dagger(x) \psi_R(x) \right] , \end{aligned} \tag{2.20}$$

where we omitted the terms that oscillate rapidly in space and hence vanish in the integral.

Using the expression for the fermionic fields in Eqs. (2.13) and (2.14), and the commutation relations $[\phi(x), \theta(x')] = i\pi\,\mathrm{sgn}(x - x')/2$, the periodic potential contributes the sine-Gordon term

$$S_U = \frac{2V_0}{2\pi\lambda} \int d\mathbf{r} \cos\left[2\phi(x) + (2k_F - q)\, x + \vartheta(t)\right] \tag{2.21}$$

for $x \in [-L/2, L/2]$ to the action, which we analyze thoroughly in the following. The cosine in Eq. 2.21 couples the ϕ-field at different energies. Thereby higher energy modes influence the effective properties of the lower energy ones, which we are ultimately interested in. This causes the effective strength of the periodic potential to be dependent on the energy scale of interest, which makes this a suitable problem to be treated by a renormalization group (RG) approach, as detailed below.

2.3 Coupling to periodic potential

2.3.1 Energy gap

The unit efficiency of the Thouless motor depends crucially on the presence of an energy gap at the Fermi energy. In the absence of interactions, this gap has size $\Delta_{\text{non-int.}} = 2V_0$. Interactions modify this gap. To start with, the sine-Gordon term is a relevant perturbation over a wide range of interaction strengths, indicating the formation of a gap. Consider $\vartheta(t) = 0$ and perfect backscattering, $q = 2k_F$, and employ the usual momentum shell renormalization group (RG) procedure for the sine-Gordon term in Eq. (2.21) [Giamarchi, 2004]. We show the explicit derivation of the flow equation in a short technical interlude, which can be skipped by readers either familiar with the technique or uninterested in technical details.

2.3.2 Technical interlude: RG perfect backscattering

We start with the LL action $S_0 + S_U$ in the presence of the static perfect backscattering potential, i.e. $\vartheta(t) = 0$ and $q = 2k_F$, in Eqs. (2.19) and (2.21). The calculation here is analogous to the RG treatment of the sine-Gordon term, e.g. in [Giamarchi, 2004]. We split the displacement field ϕ into slow and fast modes $\phi_<$ and $\phi_>$

$$\phi(\mathbf{r}) = \phi_<(\mathbf{r}) + \phi_>(\mathbf{r})\,, \tag{2.22}$$

where $\phi_<$ contains frequencies and momenta inside the shell $||\mathbf{q}|| = \sqrt{k_m^2 + (\omega_n/v_c)^2} < \gamma/b$ with $b > 1$ and γ being the ultraviolet momentum cutoff, and $\phi_>$ contains $\gamma/b < ||\mathbf{q}|| < \gamma$. We integrate out the fast modes by averaging $\cos[2\phi(x)]$ over the fast modes up to first order in the cumulant expansion

$$\langle S_U[\phi_<, \phi_>]\rangle_{0,>} = \int d\mathbf{r} \frac{V}{2\pi\lambda}\Big(\mathrm{e}^{2i\phi_<(\mathbf{r})}\,\langle \mathrm{e}^{2i\phi_>(\mathbf{r})}\rangle_{0,>} + \text{h.c.}\Big)\,,$$

where $\langle ...\rangle_{0,>}$ means averaging over the fast modes of the free LL action, which is done in the Fourier decomposition

$$\langle \mathrm{e}^{\pm 2i\phi_>(\mathbf{r})}\rangle_{0,>} = \frac{1}{Z_{0,>}} \prod_{n,m>} \int d\phi_{n,m} \exp\Big\{ - \sum_{n,m>} \Big(\frac{1}{2\pi K}(\frac{1}{v_c}\omega_n^2 + v_c k_m^2)|\phi_{n,m}|^2 \pm \frac{2i}{\sqrt{\beta L}}\phi_{n,m}\mathrm{e}^{i\mathbf{q}\cdot\mathbf{r}}\Big)\Big\}\,, \tag{2.23}$$

where $(n, m >)$ is a shorthand notation for the fast Fourier modes. Doing the Gaussian integral we obtain

$$\langle \mathrm{e}^{\pm 2i\phi_>(\mathbf{r})}\rangle_{0,>} = \exp\left\{ - \sum_{n,m>} \frac{2K\pi}{v_c\,\beta\,L\,((\omega_n/v_c)^2 + k_m^2)} \right\}\,. \tag{2.24}$$

For low temperatures and large volumes the sum over the fast momentum shell can be evaluated as a two-dimensional integral leading to

$$\sum_{n,m>} \frac{2K\pi}{v_c\,\beta\,L\,((\omega_n/v_c)^2 + k_m^2)} = \frac{K}{2\pi}\int d\varphi \int dq \frac{q}{q^2} = K\,\ln(b)\,, \tag{2.25}$$

where $q = |\mathbf{q}|$ and $\varphi = \arg(k_m + i(\omega_n/v_c))$ is the angle in the $\mathbf{q}$ -plane. This leads to the effective action

$$\langle S_U[\phi_<, \phi_>]\rangle_{0,>} = \int d\mathbf{r} \frac{2V}{2\pi\lambda} \mathrm{e}^{-K\,\ln(b)} \cos[2\phi(\mathbf{r})]\,, \tag{2.26}$$

from which we derive the flow equation (2.27).

Figure 2.3: Oscillations of the electron density around the minima of the periodic potential corresponding to the action Eq. (2.28). Quantum fluctuations of the electrons around the minima position lead to a down-scaling of the strength of the periodic potential V as described by Eq. (2.34), resulting in the renormalized gap given by Eq. (2.36).

Integrating out the fast modes of the action $S_0 + S_U$ in Eqs. (2.19) and (2.21) in a momentum shell $\gamma/b < |q| < \gamma$ (γ is the momentum cutoff, and rescaling time $\tau' = \tau/b$ and space $x' = x/b$, with $b = \mathrm{e}^l$, yields the familiar flow equation

$$\frac{dV(l)}{dl} = (2 - K)\, V(l)\,, \tag{2.27}$$

for the strength of the periodic potential, while the free action S_0 remains unchanged to first order in the cumulant expansion. Thus the periodic potential is a relevant perturbation for all $K < 2$ and the system flows to strong coupling.

For a large coupling strength V, the displacement field ϕ is trapped near a minimum of the cosine. The electron density is commensurate and oscillates about the minima of the periodic potential in Fig. 2.3.

The effective dynamics of ϕ can be obtained by expanding the action about this minimum,

$$\begin{aligned} S &\simeq S_0 + \int d\mathbf{r} \frac{2V_0}{2\pi\lambda}\, \phi^2 \\ &= \sum_{n,m} \frac{1}{2\pi K} \left(\frac{1}{v_c}\omega_n^2 + v_c q_m^2 + \frac{4V_0 K}{\lambda} \right) |\phi_{n,m}|^2\,, \end{aligned} \tag{2.28}$$

where ω_n is a bosonic Matsubara frequency and q_m is the wave vector. Thus, the system has a bare energy gap of size

$$\Delta_0 = \sqrt{\frac{4V_0 K\, v_c}{\lambda}}\,, \tag{2.29}$$

which can be understood as the pinning frequency of the classical Wigner crystal, as we show explicitly in a short interlude.

2.3.3 Interlude: Pinning frequency of Wigner crystal

The bare gap size $\Delta_0 = \sqrt{\frac{4V_0 K\, v_c}{\lambda}}$ Eq. (2.29) has an immediate physical meaning in the classical Wigner crystal limit $K \to 0$, where the interactions between the electrons are so strong that already an arbitrarily small potential is strong enough to pin the Wigner crystal into the minima of the potential.
We can directly calculate the oscillation frequency of the electrons around the minima for the $q = 0$ mode of the collective excitations. In this mode, all electrons oscillate in phase and hence the potential stemming from electron-electron interactions does not contribute to the equations of motion of the electrons. Expanding the potential around a minimum

$$U \simeq V_0 \left[2k_F x\right]^2 \tag{2.30}$$

leads to the equation of motion for each electron

$$m\ddot{x} = -\partial_x V_0 \left[2k_F x\right]^2 = -8k_F^2 x\,. \tag{2.31}$$

Hence, the oscillation frequency of the $q = 0$ mode has a frequency

$$\omega_{\text{pin}} = \sqrt{\frac{8k_F^2}{m} V_0}\,. \tag{2.32}$$

The $q = 0$ excitation is the lowest available mode, since all $q \neq 0$ modes have higher energy due to electron-electron interactions, and therefore ω_{pin} is the energy gap of the Wigner crystal.
Using $\lambda = \frac{2\pi}{k_F}$ as the initial short distance cutoff in the bare gap size Δ_0 reproduces ω_{pin} up to a numerical prefactor stemming from the uncertainty in choosing the initial cutoff

$$\Delta_0 = \sqrt{\frac{4V_0 K\, v_c}{\lambda}} \simeq \sqrt{\frac{4V_0 k_F^2}{2\pi m}}\,, \tag{2.33}$$

where we used $v_c K \simeq v_F$.

Quantum fluctuations of the electron density about the commensurate configuration (cf. Fig. 2.3) effectively decrease the restoring force of the potential and thus result in a downscaling of the effective gap. This effect is present even for non-interacting electrons. Indeed, for non-interacting electrons $K \to 1$, the bare gap in Eq. (2.29) is different from $\Delta_{\text{non-int.}} = 2V_0$. Repulsive interactions suppress the density fluctuations so that the downward renormalization becomes weaker as the repulsive interactions increase. In the Wigner crystal limit $K \to 0$ fluctuations are fully suppressed, so that the bare gap Eq. (2.29) represents the actual gap of the system.

We account for the quantum fluctuations by integrating out the high energy

modes while retaining the original units, so energies can be compared. This leads to

$$\frac{dV(l)}{dl} = -KV(l)\,. \tag{2.34}$$

We can see that, as anticipated, the downwards scaling is stronger for less repulsively interacting systems.

Integrating out modes down to the gap leads to a self-consistent equation for the renormalized energy gap $\Delta = \sqrt{4VK\,v_c/\lambda}$, with V obtained by integrating the flow equation (2.34),

$$V = V_0 \left(\frac{2\pi v_c}{\lambda\Delta}\right)^{-K}. \tag{2.35}$$

The resulting self-consistent equation for Δ has the solution

$$\Delta = \left(\frac{4V_0K\,v_c}{(2\pi v_c\lambda^{-1})^K\,\lambda}\right)^{1/(2-K)}. \tag{2.36}$$

This formula reproduces $\Delta_{\text{non-int.}} = 2V_0$ for non-interacting electrons (up to a numerical prefactor, as before). We also see explicitly that the gap is enhanced for repulsive electron-electron interactions ($K < 1$),

$$\frac{\Delta(K)}{\Delta\,(K=1)} = K\left(\frac{\pi^2 v_c/\lambda}{2V_0K}\right)^{(1-K)/(2-K)} > 1\,. \tag{2.37}$$

Here we used that $\pi v_c/\lambda \gg V_0$ is an energy of the order of the Fermi energy.

We can use the expanded action Eq. (2.28) to calculate the correlation function $\langle\phi(r)\phi(0)\rangle$, which decays exponentially for $r/\xi \gg 1$

$$\langle\phi(r)\phi(0)\rangle \sim \exp\left(-\frac{r}{\xi}\right)\left\{r^{-1/2} + \mathcal{O}\left(r^{-3/2}\right)\right\}. \tag{2.38}$$

Hence, as long as the region in which the periodic potential is applied exceeds $\xi = v_c/\Delta$, the fields at both ends can be regarded as uncorrelated.

2.3.4 Variations of the chemical potential

While the previous section considered the case of perfect commensurability $q = 2k_F$ at the center of the gap $\mu = 0$, the non-interacting Thouless motor maintains optimal efficiency as long as the chemical potential remains within the gap $|\mu| \lesssim V_0$ [Bustos-Marún et al., 2013]. In the following we investigate the robustness of the gapped interacting system against variations of the chemical potential.

A uniform chemical potential term $H_\mu = -\mu\int dx\,\partial_x\phi(x)/\pi$ can be absorbed into the free LL Hamiltonian Eq. (2.10) by shifting the field

$$\tilde{\phi}(x) = \phi(x) - \mu\frac{K}{v_c}x\,. \tag{2.39}$$

This yields a compressed liquid with a changed density $\Delta n = \mu K/(v_c\pi)$. The resulting density mismatch between the compressed LL and the applied periodic potential leads to the coupling in Eq. (2.21)

$$S_U\left[\phi\right] = \frac{2V}{2\pi\lambda}\int d\mathbf{r}\cos\left[2\tilde{\phi}(x) + 2\mu\frac{K}{v_c}\,x\right]. \tag{2.40}$$

The chemical potential μ thus introduces a constant gradient into the solutions of $\tilde{\phi}$ that minimize the cosine in order to adapt to the density dictated by the periodic potential. The Hamiltonian of the compressed Luttinger liquid Eq. (2.10) gives the associated elastic energy cost per unit length

$$\epsilon_{el} = \frac{1}{2\pi K}v_c\left(\mu\frac{K}{v_c}\right)^2. \tag{2.41}$$

This cost increases with μ and eventually leads to a depinning of $\tilde{\phi}$ beyond a critical μ_c, when adapting to the applied potential becomes too costly. To take proper account of the renormalization of the potential due to quantum fluctuations, we use the effective theory for the lowest available excitations developed in Sec. 2.3.1. Since μ does not alter the renormalization of the potential Eq. (2.34) (up to first order in the cumulant expansion), we can express the effective potential V for the lowest available modes in terms of the effective gap size $\Delta = \sqrt{4VK\,v_c/\lambda}$, with Δ given in Eq. (2.36). This leads to the effective low energy action S_{eff}

$$S_{\text{eff}}[\tilde{\phi}] = S_0[\tilde{\phi}] + \int d\mathbf{r}\frac{\Delta^2}{4\pi K v_c}\cos\left[2\tilde{\phi}(x) + 2\mu\frac{K}{v_c}\,x\right]. \tag{2.42}$$

The elastic energy cost Eq. (2.41) can be reduced by inserting a finite density n_s of π phase slips in $\tilde{\phi}$, which are described by soliton solutions of $\tilde{\phi}$. This leads to a reduced average gradient

$$g' = -\frac{\mu K}{v_c} + \pi n_s\,. \tag{2.43}$$

Under assumption of a low soliton density the total energy cost of this configuration can be estimated by adding the elastic energy cost of the reduced average gradient g' and the cost of n_s solitons,

$$\epsilon = \epsilon_{el}(g') + n_s E_{sol}\,. \tag{2.44}$$

The soliton solution and its energy $E_{sol} = 2\Delta/(\pi K)$ can be derived from Eq. (2.42) in the standard way [Rajaraman, 1987]. Using g' Eq. (2.43), we find the optimal soliton density by minimizing the total energy cost given by Eq. (2.44) for a given chemical potential μ,

$$n_{s,\text{opt}} = \frac{\mu K}{\pi v_c} - \frac{2\Delta}{\pi^2 v_c}\,. \tag{2.45}$$

This soliton density becomes positive at the critical chemical potential

$$\mu_c = \frac{2}{\pi}\frac{\Delta}{K}\,, \tag{2.46}$$

at which the system leaves the pinned regime. Since repulsive interactions enhance the effective gap size Δ Eq. (2.36), electron-electron interactions also increase the robustness of the system against variations of the chemical potential. Note that the limit of vanishing electron-electron interactions $K \to 1$ reproduces the critical chemical potential $\mu_c(K=1) \sim V_0$ of the non-interacting case.

2.3.5 Sliding periodic potential

So far, we considered the motor degree of freedom to be at rest. In the absence of interactions, the adiabatic variation of ϑ pumps a unit charge per cycle. The same occurs in the interacting system. Restoring the time dependence of the motor degree of freedom $\vartheta(\tau)$ in Eq. (2.21), the coupling to the periodic potential is

$$S_U\left[\phi\right] = \frac{2V}{2\pi\lambda}\int d\mathbf{r}\cos\left[2\phi(x)+\vartheta(\tau)\right]\,. \tag{2.47}$$

This introduces an explicit time dependence into the solutions $\phi_{\min}$ that minimize the cosine

$$\phi_{\min}(x,\tau) = -\frac{\vartheta(\tau)}{2} \tag{2.48}$$

(up to a constant that picks the specific minimum of the cosine). A time-dependent displacement field ϕ implies current flow. Using the continuity equation, we obtain the current density

$$j(x,t) = -\frac{e}{\pi}\partial_t\phi(x,t) = \frac{e}{2\pi}\partial_t\vartheta(t)\,, \tag{2.49}$$

which describes pumping of a quantized charge

$$Q_P = \int_0^T dt\, j(t) = e \tag{2.50}$$

when advancing the periodic potential by one period.

The interaction-enhanced gap also implies a larger range of validity of this adiabatic treatment. Comparing the kinetic term in the Lagrangian to the energy gain due to the gap formation, we conclude that the adiabatic approximation remains valid as long as $|\dot{\vartheta}| \ll \Delta$, where Δ is the renormalized gap of the interacting system.

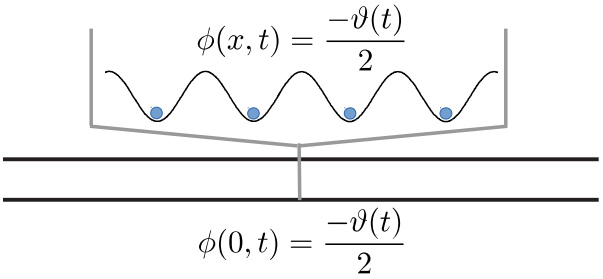

Figure 2.4: The pinning condition $\phi = -\vartheta/2$ within the area of the periodic potential reduces the coupling between motor degree of freedom and electrons to a free LL with a constrained boundary condition $\phi(0,t) = -\vartheta(t)/2$ when the area of the periodic potential is shrunk to a single point $x = 0$.

2.4 Reduced dynamics of the motor degree of freedom

2.4.1 Bias voltage

As long as $|\mu| < \mu_c$ and $|\dot{\vartheta}| < \Delta$, the displacement field is locked to $\phi = -\mu K\, x/(2v_c) - \vartheta/2$ and the spectrum is gapped. Within the region of the periodic potential, the electrons are locked to its minima, cf. Fig. 2.4, and the electronic dynamics is effectively frozen out. As long as the length of the periodic potential L is larger than $\xi = v_c/\Delta$, the fields ϕ at the two ends of the periodic potential lock to $\phi(x = \pm L/2) = -\vartheta/2$, where we neglected the ϑ-independent offset $\propto L$ for an incommensurate potential. Effectively, this allows us to shrink the length of the periodic potential to a single point $x = 0$, at which the pinned displacement field interacts with the free LL, as shown schematically in Fig. 2.4.

In a motor setup, the energy provided by the applied bias voltage V is used to drive the motor degree of freedom. When ϕ is locked and the electronic dynamics in the region of the periodic potential is frozen out, we can also shrink the voltage drop to the point $x = 0$, which yields a contribution to the action

$$S_{\text{bias}} = -\frac{eV}{2}\int d\mathbf{r}\,\text{sgn}(x)\frac{\partial_x\phi}{\pi} = \frac{eV}{\pi}\int d\tau\phi(0,\tau)\,. \tag{2.51}$$

Here we used the bosonized form of the normal ordered electron density given in Eq. (2.8).

Integrating out all electronic degrees of freedom away from $x = 0$ under the constraint $\phi(0,t) = -\vartheta(t)/2$, analogous to the treatment of a local impurity in a LL [Kane and Fisher, 1992; Castro Neto and Fisher, 1996], leads to an effective description of the dynamics of the motor degree of freedom, including

a non-conservative mean force stemming from the electronic bias, friction, and a fluctuating force.

2.4.2 Motor dynamics for an infinite Luttinger liquid

We first treat the coupling to an infinite LL. Following earlier work [Kane and Fisher, 1992], the LL can be integrated out. This calculation is shown in Appendix A.1 and leads to the effective action

$$S_{\text{eff}} = \sum_n \left(\frac{\mathcal{I}\omega_n^2}{2} + \frac{|\omega_n|}{4\pi K} \right) |\vartheta_n|^2 - \int_0^\beta d\tau \frac{eV}{2\pi} \vartheta \,, \tag{2.52}$$

where we added the kinetic energy of the motor with some associated moment of inertia $\mathcal{I}$. The second term describes a dissipative contribution to the motor dynamics and the third term a potential induced by the applied bias.

To obtain the explicit equation of motion we analytically continue the effective action to the Keldysh contour [Kamenev, 2011]. The effective action then acquires the form

$$\begin{aligned} S_{\text{eff}} &= \int \frac{d\omega}{2\pi} (\bar{\vartheta}_\omega^{cl}, \bar{\vartheta}_\omega^{q}) \, \hat{K}(\omega) \begin{pmatrix} \vartheta_\omega^{cl} \\ \vartheta_\omega^{q} \end{pmatrix} + \frac{eV}{\pi} \int dt \, \vartheta^q(t) \\ \hat{K}(\omega) &= \begin{pmatrix} 0 & K^A(\omega) \\ K^R(\omega) & K^K(\omega) \end{pmatrix} . \end{aligned} \tag{2.53}$$

We performed a Keldysh rotation into the quantum $\vartheta^q = (\vartheta^+ - \vartheta^-)/2$ and classical component $\vartheta^{cl} = (\vartheta^+ + \vartheta^-)/2$ of ϑ. The kernels $K^{R(A)}(\omega)$ are the analytical continuations of the Matsubara correlator $\mathcal{K}(\omega_n) = \mathcal{I}\omega_n^2/2 + |\omega_n|/(4\pi K)$ in Eq. (2.52) to real frequencies $K^{R(A)}(\omega) = -2\mathcal{K}(i\omega_n \to \omega \pm i\eta)$ [Kamenev, 2011]. The Keldysh component follows from the fluctuation dissipation theorem $K^K(\omega) = \big(K^R(\omega) - K^A(\omega)\big) \coth(\omega/2T)$ [1]. Fourier transforming the action Eq. (2.53) to real time we obtain

$$\begin{aligned} S = \int dt \Bigg\{ &- 2\vartheta^q(t) \left[\mathcal{I}\ddot{\vartheta}^{cl}(t) + \frac{\dot{\vartheta}^{cl}(t)}{2\pi K} - \frac{eV}{2\pi} \right] \\ &+ \int dt' K^K(t-t') \vartheta^q(t) \vartheta^q(t') \Bigg\} , \end{aligned} \tag{2.54}$$

where we performed an integration by parts. The Fourier transform of the Keldysh component reads

$$K^K(t) = \frac{iT^2}{K \cosh\left(\pi T t\right)^2} \,, \tag{2.55}$$

[1] Due to the pinned LL on the length of the periodic potential, the free LL's on the left and right side are isolated and act as independent equilibrium baths for the motor degree of freedom.

yielding a coupling of the quantum fields nonlocal in time. This action determines the reduced dynamics of the motor degree of freedom including all quantum fluctuations.

The contribution quadratic in the quantum components leads to the fluctuating Langevin force in the classical equation of motion of the motor. Its explicit form can be obtained by decoupling the quantum components by a Hubbard-Stratonovich transformation [Kamenev, 2011]

$$\exp\left(i\int\frac{d\omega}{2\pi}\,K^K(\omega)|\vartheta^q(\omega)|^2\right)= \\ \int\mathbf{D}\left[\xi\right]\exp\left(\int\frac{d\omega}{2\pi}\left[\frac{|\xi(\omega)|^2}{i\,K^K(\omega)}+2i\bar{\xi}(\omega)\vartheta^q(\omega)\right]\right)\,, \tag{2.56}$$

where $\xi(t)$ is a real field. Introducing the integral over ξ Eq. (2.56) into the Keldysh partition function $Z=\int\mathbf{D}\left[\vartheta\right]\exp(iS)$ corresponding to the action S Eq. (2.54) leads to the classical saddle point equation for ϑ

$$\mathcal{I}\ddot{\vartheta}^{cl}(t)=\frac{eV}{2\pi}-\frac{1}{2\pi K}\dot{\vartheta}^{cl}(t)+\xi(t) \tag{2.57}$$

with

$$\langle\xi(t)\xi(t')\rangle=\frac{K^K(t'-t)}{2i}=\frac{T^2}{2K\cosh\left(\pi T\left[t'-t\right]\right)^2}\,. \tag{2.58}$$

In the classical limit for large T we can approximate $\cosh\left(\pi T\left[t'-t\right]\right)^{-2}\simeq 2(\pi T)^{-1}\delta(t-t')$ and hence the fluctuating force becomes delta-correlated, with the magnitude of the correlator determined by temperature and the friction coefficient

$$\langle\xi(t)\xi(t')\rangle=2\gamma T\delta(t-t')\,. \tag{2.59}$$

We see that while the mean force is unaffected by the electron-electron interactions, the friction $\gamma=(2\pi K)^{-1}$ and with it also the correlator of the fluctuating force are enhanced by repulsive electron-electron interactions. For $K\to 1$ the effective dynamics Eq. (2.57) reproduce the non-interacting result of Ref. [Bustos-Marún et al., 2013].

The steady state velocity of the motor follows from the equation of motion (2.57) $\dot{\vartheta}=K\,eV$. Since the pumped charge in Eq. (2.50) is the only charge transported through the system, we can directly calculate the current I as pumped charge per unit time

$$I=\frac{e\dot{\vartheta}}{2\pi}=\frac{Ke^2}{2\pi\hbar}V\,, \tag{2.60}$$

where we reinserted $\hbar$ to bring the current in the usual form in terms of the *dc* conductance. We can use this current at steady state to define the *dc* conductance of the motor $g_M=Ke^2/h$, which takes the value of an infinite, ideal LL [Kane and Fisher, 1992].

We use these results to investigate the efficiency η of the interacting Thouless motor, which we define as the ratio between useful output power and input power [Fernández-Alcázar et al., 2015]

$$\eta = \frac{P_{out} - P_{diss}}{P_{in}} \,. \tag{2.61}$$

The useful power in the numerator is the work per cycle done by the mean force in Eq. (2.57) $P_{out} = eV/\tau$ (τ the cycle period) minus the power dissipated due to friction $P_{diss} = \dot{\vartheta}^2/2\pi K$. The electrical input power provided by the bias $P_{in} = IV$ is determined by the pumped current Eq. (2.60), which yields the efficiency

$$\eta = 1 - \frac{\dot{\vartheta}}{eV\,K} \,. \tag{2.62}$$

Thus for a given frequency, repulsive electron-electron interactions $K < 1$ decrease the efficiency of the Thouless motor as a consequence of the friction enhancement.

2.4.3 Friction and energy current in an infinite Luttinger liquid

It is interesting to obtain a more explicit description of the friction coefficient γ. To this end, we compute the energy current carried by the LL for the time-dependent boundary condition $\phi(0,t) = -\vartheta(t)/2$. The solution of ϕ under this time-dependent constraint is shown in Appendix A.1 Eq. (A.14) and takes, under assumption of a steady velocity, the form

$$\phi(x,t) = \frac{-\dot{\vartheta}}{2}\left(t - \frac{|x|}{v_c}\right) . \tag{2.63}$$

To see how this solution carries the dissipated energy away from the motor, we investigate the energy current density j^E corresponding to this solution. j^E can be derived from the Heisenberg equation of motion for the energy density

$$\rho^E = \frac{v_c}{2\pi}\left[\frac{1}{K}\left(\partial_x\phi(x)\right)^2 + K\left(\partial_x\theta(x)\right)^2\right] , \tag{2.64}$$

which yields

$$\partial_t\rho^E = i\left[H, \rho^E\right] = -\frac{v_c^2}{2\pi}\partial_x\left\{\partial_x\theta(x), \partial_x\phi(x)\right\} , \tag{2.65}$$

where we used the commutation relations of the bosonic fields introduced above in Sec. 2.1 and $\{.,.\}$ denotes the anticommutator. From here we can directly deduce the energy current via the continuity equation

$$\partial_t\rho^E = -\nabla j^E \tag{2.66}$$

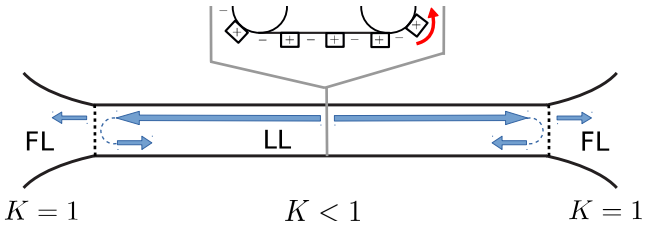

Figure 2.5: Connecting FL leads causes backscattering of plasmons at the FL-LL boundary.

which leads to

$$j^E = \frac{v_c^2}{2\pi} \{\partial_x \theta(x), \partial_x \phi(x)\} \,. \tag{2.67}$$

Since the gradient of θ if fully determined by the time dependence of ϕ, i.e. $\partial_t \phi(x,t) = i\,[H, \phi(x,t)] = -v_c K \partial_x \theta(x)$, we can write down the energy current corresponding to the solution Eq. (2.63)

$$j^E = \frac{\dot{\vartheta}^2}{4\pi K} \mathrm{sgn}(x) \,. \tag{2.68}$$

Thus we can see that the dissipated power

$$-P_{diss} = \gamma \dot{\vartheta}^2 = j^E(x > 0) - j^E(x < 0) \tag{2.69}$$

is evenly split between the two sides and sent to $x = \pm\infty$.

2.4.4 Contact to Fermi liquid leads

In the previous section we assumed an infinite LL which leads to enhanced dissipation due to repulsive electron-electron interactions and the motor conductance of an ideal infinite LL at steady state. It is well known that if a quantum wire containing a LL is attached to FL leads, the normal *dc* conductance of the wire is determined by the interactions in the attached leads and takes the value of an ideal non-interacting channel $g = e^2/h$ [Maslov and Stone, 1995]. In this section we investigate, whether by attaching FL leads also the dissipation of the Thouless motor at steady velocity is reduced to the non-interacting value, reproducing the non-interacting motor conductance $g_M = e^2/h$.

The connection to FL leads generates backscattering of plasmons at the FL-LL boundary, which includes memory into the effective equation of motion of the motor and results in reduced non-interacting dissipation at steady velocity, cf. Fig. 2.5. The transition between LL and FL can be modeled as a change of the interaction parameter $K \to 1$ and the charge velocity $v_c \to v_F$ [Maslov and Stone, 1995; Karzig et al., 2011]. We consider that the LL is connected to

FL reservoirs at $|x| = D/2$, which yields in the ϕ-representation of the LL Eq. (2.19)

$$S_0 = \int d\mathbf{r} \frac{1}{2\pi} \left[\frac{(\partial_\tau \phi)^2}{K(x)\, v_c(x)} + \frac{v_c(x)\, (\partial_x \phi)^2}{K(x)} \right], \tag{2.70}$$

with

$$K(x) = \begin{cases} 1 & |x| \geq D/2 \\ K & |x| < D/2 \end{cases} \quad v_c(x) = \begin{cases} v_F & |x| \geq D/2 \\ v_c & |x| < D/2\,. \end{cases} \tag{2.71}$$

We obtain the effective action of the motor by integrating out the LL under the constraint $\phi(0,t) = -\vartheta(t)/2$, as previously but now with attached FL leads. The procedure amounts to solving the saddle point equation for the ϕ-field in the presence of the appropriate boundary conditions for ϕ and $\partial_x \phi$, and is shown in Appendix A.1. We find the effective action

$$S[\vartheta]_{\text{eff}} = \sum_n \frac{M(\omega_n)}{4\pi K} |\omega_n|\, |\vartheta_n|^2 - \int_0^\beta d\tau \frac{eV}{2\pi} \vartheta\,. \tag{2.72}$$

with

$$M(\omega_n) = \left(1 + 2 \sum_{n=1}^{\infty} \mathrm{e}^{-n|\omega_n|\mathcal{T}} r_p^n \right), \tag{2.73}$$

where $\mathcal{T} = D/v_c$ is the travel time of the plasmons from $x = 0$ to the FL-LL boundary and back and $r_p = \frac{K-1}{K+1}$ is the plasmon reflection amplitude.

To obtain the real time dynamics we analytically continue to the Keldysh contour analogous to the infinite LL case above, where the kernels now take the form

$$K^{R(A)}(\omega) = \frac{\pm i\omega}{2\pi K} \left(1 + 2 \sum_{n=1}^{\infty} \mathrm{e}^{\pm n i \omega \mathcal{T}} r_p^n \right), \tag{2.74}$$

and $K^K(\omega) = \left(K^R(\omega) - K^A(\omega) \right) \coth(\omega/2T)$. Fourier transforming to real time shows that the plasmon scattering at the LL-FL boundary leads to a coupling of the quantum field to earlier classical velocities at multiples of the travel time $\mathcal{T}$

$$\begin{aligned} S_{\text{diss}} = S_{qq} - \int dt\, \frac{2\vartheta^q(t)}{2\pi K} \\ \times \left(\dot{\vartheta}^{cl}(t) + 2 \sum_{n=1}^{\infty} \dot{\vartheta}^{cl}(t - n\mathcal{T}) r_p^n \right). \end{aligned} \tag{2.75}$$

Here

$$S_{qq} = \int dt dt'\, K^K(t - t') \vartheta^q(t) \vartheta^q(t') \tag{2.76}$$

is the part of the dissipative action quadratic in the quantum fields. In contrast to the infinite LL case above, the Keldysh kernel

$$K^K(t) = \frac{iT^2}{K}\left[\sum_{n=-\infty}^{\infty} \frac{1}{\cosh\left(\pi T\left[t+n\mathcal{T}\right]\right)^2} r_p^{|n|}\right] \tag{2.77}$$

leads to a nonlocal coupling of the quantum fields also in the high temperature limit, resulting in non-local correlations of the fluctuating force in time. As before we combine the dissipative action with the free part and the bias induced mean force and decouple the quantum fields via a Hubbard-Stratonovich transformation, which yields the nonlocal classical saddle point equation

$$\begin{aligned}\mathcal{I}\ddot{\vartheta}^{cl}(t) = \frac{eV}{2\pi} + \xi(t) \\ -\frac{1}{2\pi K}\left[\dot{\vartheta}^{cl}(t) + 2\sum_{n=1}^{\infty}\dot{\vartheta}^{cl}(t-n\mathcal{T})r_p^n\right].\end{aligned} \tag{2.78}$$

The correlator of the fluctuating force is determined by

$$\langle\xi(t)\xi(t')\rangle = \frac{T^2}{2K}\left[\sum_{n=-\infty}^{\infty} \frac{1}{\cosh\left(\pi T\left[t-t'+n\mathcal{T}\right]\right)^2} r_p^{|n|}\right] \tag{2.79}$$

which reduces in the high temperature limit to finite correlations at all multiples of the travel time $\mathcal{T}$

$$\langle\xi(t)\xi(t')\rangle \simeq \frac{2T}{2\pi K}\left[\sum_{n=-\infty}^{\infty}\delta(t-t'+n\mathcal{T})\, r_p^{|n|}\right]. \tag{2.80}$$

Since $r_p < 0$, the non-local couplings to the velocity, i.e. the contribution $\propto r_p^n$ in Eq. (2.78) caused by multiple plasmon reflections at the FL-LL boundary and $x = 0$, have an alternating sign and a decaying amplitude $\propto |r_p|^n$. Hence this force damps the motion for all even multiples of the travel time and boosts the motion for all odd ones, if we assume the velocity does not change sign. How much energy gets dissipated in this process depends on the trajectory of ϑ.

At constant velocity, the effective dynamics described by Eq. (2.78) leads to reduced dissipation and an enhanced velocity $\dot{\vartheta} = eV$. This results in more pumped charge per unit time

$$I = \frac{e\dot{\vartheta}}{2\pi} = \frac{e^2}{2\pi\hbar}V\,, \tag{2.81}$$

and hence the enhanced *dc* motor conductance of an ideal *non-interacting* channel, where we again reinserted $\hbar$. Therefore, analogous to the *dc* conductance of an ideal LL channel in contact to FL reservoirs [Maslov and Stone, 1995], also the *dc motor conductance* is governed by the interactions in the attached reservoirs. Thereby also the efficiency of the Thouless motor is increased to the non-interacting value $K \to 1$ in Eq. (2.62).

2.4.5 Friction and energy current with attached Fermi liquid leads

To see explicitly how the energy current is modified by plasmon reflections at the LL-FL boundary, we analyze the solution for ϕ under the constraint $\phi(0,t) = -\vartheta(t)/2$ and the connection to FL leads. We analyze the dissipation for different trajectories by considering two limiting cases: The behavior at constant velocity $\vartheta(t) = \dot{\vartheta}t$, and the case of a sudden step $\vartheta(t) = \vartheta_0\Theta(t)$. With the expression for the energy current derived above Eq. (2.67), we can directly use the solution for ϕ given in the Appendix Eq. (A.25) to calculate the energy current in these cases.

For a sudden step, the gradient and time derivative of ϕ determining the energy current are strongly peaked δ-functions that can not interfere with each other. That leads to a situation, in which after integrating in time over all multiple scattering events all the energy of the initial excitation is released into the FL reservoirs. Thus, the total dissipated energy $E_{diss} = \int dt[j^E(x>0) - j^E(x<0)]$ is determined by the initial plasmon excitation and takes the value of an infinite LL

$$E_{diss} = \frac{\tau\overline{\dot{\vartheta}^2}}{2\pi K}\,. \tag{2.82}$$

Here $\int dt\dot{\vartheta}(t)^2 = \tau\overline{\dot{\vartheta}^2}$ determines the dissipation caused by the initial plasmon excitation and τ is the step duration.

In contrast to that, at steady velocity the reflected plasmons Eq. (A.25) interfere with each other, leading to a constant gradient $\partial_x\phi = K\dot{\vartheta}\,\mathrm{sgn}(x)/(2v_c)$ and time derivative $\partial_t\phi = -\dot{\vartheta}$ in the inside region $|x| < D/2$. This yields the reduced energy current

$$j^E = \frac{\dot{\vartheta}^2}{4\pi}\mathrm{sgn}(x)\,, \tag{2.83}$$

which corresponds to the dissipated power with the reduced *non-interacting* friction $\gamma = (2\pi)^{-1}$

$$-P_{diss} = \frac{1}{2\pi}\dot{\vartheta}^2 = j^E(x>0) - j^E(x<0)\,. \tag{2.84}$$

Therefore we can see that interference of the reflected plasmons (cf. Fig. 2.5) leads to a decreased energy current at steady state and thus prevents the system from releasing all the energy to the attached Fermi liquid leads.

2.5 Translation to magnetic system

The counter-propagating states of a single QSH edge (cf. Fig 2.1) can be described as a Luttinger liquid analogous to the spinless quantum wire introduced

in Sec. 2.1 [Wu et al., 2006]. The bosonization of the helical channels is obtained from Eqs. (2.13) and (2.14) by replacing $\psi_R \to \psi_{R,\uparrow}$ and $\psi_L \to \psi_{L,\downarrow}$, while the Hamiltonian in terms of the bosonic fields Eq. (2.10) remains unchanged. The Zeeman coupling to the nanomagnet

$$H_M = -\frac{J_0}{2}\int \mathrm{d}x \Psi^\dagger \vec{\sigma}\Psi \cdot \mathbf{M} \tag{2.85}$$

leads to back-scattering of the helical channels whenever there is a component of $\mathbf{M}$ in the x-y-plane, where $\vec{\sigma}$ is the vector of Pauli matrices that acts on $\Psi = (\psi_{R,\uparrow}, \psi_{L,\downarrow})^T$. Assuming a strong easy-plane anisotropy in the x-y-plane, we can parametrize the magnetization as $M_x = M\cos[\vartheta_M]$ and $M_y = M\sin[\vartheta_M]$, which leads to a sine-Gordon term for the Zeeman coupling

$$\begin{aligned} S_M =& -\frac{J_0 M}{2\pi\lambda}\int d\mathbf{r}\ (\cos[\vartheta_M]\cos(2k_F x + 2\phi(x)) - \sin[\vartheta_M]\sin(2k_F x + 2\phi(x))) \\ =& -\frac{J_0 M}{2\pi\lambda}\int d\mathbf{r}\ \cos(2\phi(x) + 2k_F x + \vartheta_M)\ . \end{aligned} \tag{2.86}$$

Here k_F measures the distance from the Dirac point $k = 0$ at which the system is operated. Thus, the coupling of the nanomagnet to the helical edge states takes the same form as the coupling of the sliding periodic potential to the spinless LL in the quantum wire Eq. (2.21), enabling us to directly translate the results of Sec. 2.3 and 2.4 to the magnetic case. For $K < 2$ the ϕ-field gets locked to $\phi(x) = n\pi - k_F x - \vartheta_M/2$, which corresponds to ferromagnetic order of the spin density

$$\vec{s} = \frac{1}{2}(\psi^\dagger_{R,\uparrow}, \psi^\dagger_{L,\downarrow})\,\vec{\sigma}\begin{pmatrix} \psi_{R,\uparrow} \\ \psi_{L,\downarrow} \end{pmatrix} \tag{2.87}$$

in phase with the in-plane magnetization of the nanomagnet

$$s_x(x) = \frac{1}{2\pi\lambda}\cos(\vartheta_M) \quad s_y(x) = \frac{1}{2\pi\lambda}\sin(\vartheta_M)\ . \tag{2.88}$$

A full precession of the magnetization leads to quantized charge pumping of one electron per cycle in Eq. (2.50). Quantum fluctuations around the ferromagnetically ordered state lead to an interaction dependent downward scaling of the effective strength of the Zeeman coupling J, which results in an effective gap size for the lowest available modes

$$\Delta_M = \left(\frac{2J_0 M K\, v_c}{(2\pi v_c \lambda^{-1})^K\,\lambda}\right)^{1/(2-K)}\ . \tag{2.89}$$

This formula reproduces the gap $\Delta_{\text{non-int.}} = J_0 M$ for non-interacting helical edge modes and shows the strong enhancement of the magnetically induced gap by repulsive electron-electron interactions, cf. Eq. (2.37). The noninteracting QSH edge remains insulating as long as the chemical potential remains within

the gap that is opened by the magnet around the Dirac point $k = 0$. Section 2.3.4 shows that interactions also make the magnetic system more robust against variations of the chemical potential and demonstrates that it remains gapped as long as $|\mu|$ is smaller than $\mu_c = 2\Delta_M/(\pi K)$, cf. Eq. (2.46).

In the case of a high easy-plane anisotropy energy $DM_z^2/2$ ($D > 0$), the Landau-Lifshitz-Gilbert equation governing the time evolution of the magnetization can be reduced to an equation of motion for the angle of the in-plane magnetization ϑ_M, in which the inverse anisotropy constant acts as an effective moment of inertia $\mathcal{I} = D^{-1}$ [Bode et al., 2012a; Meng et al., 2014; Arrachea and von Oppen, 2015]. We show the explicit derivation of this equation of motion in a short section, which can be skipped by readers uninterested in technical details.

2.5.1 Technical section: Derivation of the equation of motion for a nanomagnet with strong easy-plane anisotropy

We assume a nanomagnet with strong easy-plane anisotropy, with an associated potential $U = DM_z^2/2$ ($D > 0$). For simplicity, we use units in which the magnetization $\mathbf{M}$ has units of angular momentum. The equation of motion for the magnetization can be directly derived from the Heisenberg equation of motion for each component of the magnetization [Bode et al., 2012a]

$$\begin{aligned} \dot{M}_j &= i\,[H, M_j] && (2.90)\\ &= -\frac{D}{2}\epsilon_{zjk}\,(M_z M_k + M_k M_z)\,, && (2.91) \end{aligned}$$

where we used that the components of $\mathbf{M}$ commute like angular momenta

$$[M_i, M_j] = i\epsilon_{ijk} M_k\,. \tag{2.92}$$

Combining the components of $\mathbf{M}$, this leads to the free precession

$$\dot{\mathbf{M}} = -DM_z\,\mathbf{M}\times\mathbf{e}_z = -\partial_{\mathbf{M}} U\,, \tag{2.93}$$

where $\partial_{\mathbf{M}} = \sum_i \mathbf{e}_i \partial_{M_i}$.

The coupling of the nanomagnet to electronic degrees of freedom induces a back-action on the magnetization, analogous to the adiabatic reaction forces for translational degrees of freedom [Bode et al., 2011, 2012b; Thomas et al., 2012]. Assuming that the many-body Hamiltonian of the electronic system $\mathcal{H}$ depends on $\mathbf{M}$, we can repeat the derivation of the equation of motion above and obtain a Landau-Lifshitz-Gilbert (LLG) equation

$$\dot{\mathbf{M}} = \mathbf{M}\times(-DM_z\,\mathbf{e}_z + \mathbf{B}_{el} + \delta\mathbf{B})\,. \tag{2.94}$$

The back-action of the electronic degrees of freedom on the slowly changing magnetization takes the form

$$\mathbf{B}_{el} = \langle -\partial_{\mathbf{M}} \mathcal{H} \rangle_{\mathbf{M}(t)} = \mathbf{B}_0 - \gamma\left(\mathbf{M}\right) \dot{\mathbf{M}}\,, \tag{2.95}$$

with an additional fluctuating Langevin torque $\delta\mathbf{B}$, which is determined by the fluctuations of $-\partial_{\mathbf{M}}\mathcal{H}$. Here, $\mathbf{B}_0$ yields a spintransfer torque and corresponds to the Born-Oppenheimer part of the current induced forces on translational degrees of freedom, while $\gamma\left(\mathbf{M}\right)$ accounts for the first order corrections in $\dot{\mathbf{M}}$ and yields a damping torque.

In the case of a strong easy-plane anisotropy, the magnetization lies almost in plane and we can use cylindrical coordinates $\mathbf{M} \simeq M_\rho \mathbf{e}_\rho + M_z \mathbf{e}_z$ and $\dot{\mathbf{M}} \simeq M_\rho \dot{\vartheta}_M \mathbf{e}_\vartheta + \dot{M}_z \mathbf{e}_z$, where ϑ_M is the in-plane angle of the magnetization and M_ρ is the in-plane projection of $\mathbf{M}$. $\mathbf{e}_\rho$, $\mathbf{e}_\vartheta$ and $\mathbf{e}_z$ are the unit-vectors in radial, polar and z-direction. The small z-component M_z determines whether the magnetization precesses above or below the easy plane and controls the direction of the precession. Hence, it has to be kept in the equation of motion when it is multiplied with the large anisotropy constant D.

Due to the magnetization being almost in plane, the coupling to the helical edge can be assumed to occur only via the angle of the in-plane magnetization ϑ_M in Eq. (2.86). Hence the induced effective magnetic field $\mathbf{B}_{el} = \langle -\partial_{\mathbf{M}} \mathcal{H} \rangle_{\mathbf{M}(t)}$ and also its fluctuations point in $\mathbf{e}_\vartheta$-direction. Thereby the coupling of $\mathbf{M}$ to the helical edge leads to a torque $T\mathbf{e}_z$ driving the system out of its equilibrium position in the easy plane, a damping torque $-\gamma\dot{\vartheta}_M \mathbf{e}_z$ damping it back, and a Langevin torque $\xi\mathbf{e}_z$ [Meng et al., 2014; Arrachea and von Oppen, 2015]. We can approximate the equation of motion in Eq. (2.94) as

$$M_\rho \dot{\vartheta}_M \mathbf{e}_\vartheta + \dot{M}_z \mathbf{e}_z \simeq M_\rho D M_z \mathbf{e}_\vartheta + \left(T - \gamma\dot{\vartheta}_M + \xi\right)\mathbf{e}_z\,. \tag{2.96}$$

Thus, we get for the $\mathbf{e}_z$-component

$$\dot{M}_z = \left(T - \gamma\dot{\vartheta}_M + \xi\right) \tag{2.97}$$

and for the $\mathbf{e}_\vartheta$-component

$$\frac{\dot{\vartheta}_M}{D} = M_z\,. \tag{2.98}$$

Inserting M_z into the e_z-component of the LLG Eq. (2.97) leads to the equation of motion for the angle of the in-plane magnetization ϑ_M

$$\frac{\ddot{\vartheta}_M}{D} = T - \gamma\dot{\vartheta}_M + \xi\,. \tag{2.99}$$

This analysis shows that for strong easy-plane anisotropy, the LLG equation for the magnetization dynamics can be reduced to a Langevin equation for the angle

of the in-plane magnetization, in which the inverse anisotropy strength D^{-1} acts as an effective moment of inertia for the rotational degree of freedom ϑ_M. The derivation of T, γ and the correlator of the fluctuating torque is analogous to the calculation for the rotational degree of freedom in Sec. (2.4).

2.5.2 Reduced dynamics in the magnetic system

With this we can readily translate the results for the effective dynamics Sec. 2.4 to the magnetic case, replacing $\vartheta \to \vartheta_M$ and $\mathcal{I} \to D^{-1}$. Thus, in the case of an infinite helical liquid, one obtains

$$\frac{\ddot{\vartheta}_M^{cl}(t)}{D} = \frac{eV}{2\pi} - \frac{1}{2\pi K}\dot{\vartheta}_M^{cl}(t) + \xi(t)\,. \tag{2.100}$$

The dissipation is enhanced by repulsive interactions, leading to a reduced current and reduced motor conductance $g_M = Ke^2/h$ compared to the non-interacting case in Eq. (2.60). When assuming contact of the helical edge to Fermi liquid reservoirs as done in Sec. 2.4.4, the plasmon back-scattering at the transition between helical liquid and reservoirs leads to an effective equation of motion including memory in Eq. (2.78) and the reduced dissipation of a non-interacting helical liquid at steady state.

2.6 Conclusion

We investigated the effect of electron-electron interactions on the working principle of a quantum motor that is based on a 1d Thouless pump operating in reverse. Repulsive interactions, which gain importance due to the reduced dimensionality of the system, were shown to enhance the energy gap opened by the coupling to the periodic potential. Thereby interactions also increase the robustness of the system against variations of the chemical potential and increase the velocity range in which the system evolves adiabatically, allowing for an operation of the motor at higher speed. Therefore electron-electron interactions support the working principle of the motor. While for infinite LLs the friction is enhanced by repulsive electron-electron interactions, the connection to FL reservoirs and the resulting plasmon reflections lead to an effective equation of motion including memory and the decreased non-interacting dissipation at steady velocity. By that the effective motor conductance at steady state is determined by the attached non-interacting reservoirs analogous to the *dc* conductance in an ideal LL. We showed that the model of a nanomagnet with strong easy-plane anisotropy coupled to the helical edge of a QSH system can be readily mapped to the Thouless motor, leading to a possibly experimentally more feasible realization of the developed model.

3 Quantum thermodynamics of the resonant level model

In the aim of investigating the thermodynamic relations of electronic nanomachines, we consider the simplest possible example for such a device. We show in a thorough analysis how to derive the thermodynamic relations in the presence of strong hybridization with the surrounding bath. This chapter is based on Ref. [Bruch et al., 2016].

The simplest toy model for an electronic nanomachine is the driven resonant level model, which describes a single spinless electronic level (say, of a quantum dot) coupled to one or more leads described as free-electron metals. This system has long been studied as the simplest model for conducting nanoscopic junctions involving molecular or quantum dot bridges. When the resonant level energy and/or the level-lead coupling are driven by an external agent such as a gate voltage, it becomes a model for a quantum nanoengine, for which the thermodynamic relations be investigated. An outstanding issue is to derive a consistent formulation for the non-equilibrium thermodynamics of such strongly coupled systems. This requires proper accounting of energy conservation as well a proper definition of entropy that will lead to entropy production consistent with the second law of thermodynamics. In particular, the entropy production is the central element in deriving efficiencies for various energy-conversion processes and characterizes the irreversibility of the process. It is thus an essential aspect of the non-equilibrium thermodynamics of nanoscale devices [Esposito et al., 2010; Deffner and Lutz, 2011]. Our goal is to formulate a consistent non-equilibrium thermodynamic theory that will hold beyond the quasi-static limit in which the system remains in equilibrium and strictly follows the driving adiabatically.

Finding a consistent thermodynamic description of the driven resonant level model is non-trivial.[Ludovico et al., 2014; Esposito et al., 2015b] First, the level-lead coupling itself has to be accounted for. Second, the strong hybridization of the dot level with the lead electronic states makes it necessary to develop an

energy-resolved (or quantum) description of the dynamic processes, which goes beyond the kinetic (master-equation) schemes and stochastic approaches that are usually derived in the weak-coupling (or classical) limit.

Esposito et al.[Esposito et al., 2015b] pointed out these difficulties and, addressing the general case (i.e., including the driving in both the level energy and the level-lead coupling), formulated the basic laws of thermodynamics in a manner which includes the effects of irreversible driving through a modified spectral density. While satisfying the laws of thermodynamics, this formulation does not yield the known equilibrium forms of these thermodynamic functions in the quasistatic limit, already in the wide band limit and for time-independent level-lead coupling.

Here we present an alternative formulation of the non-equilibrium thermodynamics of the driven resonant level model, albeit for the more restricted case where the driving affects only the level energy. In developing a consistent thermodynamic description of this model, we are guided by several basic requirements: The thermodynamic functions must (i) reduce to the correct quasistatic (equilibrium) limit, (ii) fulfill particle and energy conservation at each order, (iii) predict a positive entropy production reflecting the irreversibility of the transformations, and (iv) correctly connect to the forces experienced by the driving (see Refs. [Bode et al., 2011] and [Bode et al., 2012b] for a general discussion and calculations of these forces). In departure from attempts to address the thermodynamic functions of the dot itself, which are marred by the need for a proper partitioning of the dot-lead coupling between the various subsystems, [Ludovico et al., 2014; Esposito et al., 2015b,a] we focus on the changes in the thermodynamic properties of the overall system (dot and lead) which result from local changes in parameters (i.e., the energy of the resonant level in the present context). This circumvents the need to address the contribution of the system-bath coupling to the thermodynamic functions of the dot, and instead defines the 'system' as that part of the 'world' which is influenced by the dynamics of the externally driven resonant level. We will henceforth refer to this part of the overall system as the extended resonant level.[1]

This chapter is organized as follows. In Sec. 3.1, we introduce the resonant level model. Section 3.2 contains a derivation of the equilibrium thermodynamics of the extended resonant level from the grand potential. Section 3.3 extends these thermodynamic functions to finite driving speed. This is done on the basis of non-equilibrium Green's functions within the gradient expansion, which we introduce in the technical section 3.3.1. To derive the non-equilibrium form of the thermodynamic functions of interest, we start with their representations in terms of quasistatic expectation values of operators, obtained in Sec. 3.2, and expand these to linear order in the driving speed with the help of the developed non-equilibrium Green's functions. In Sec. 3.4, we show that for weak level-lead coupling, our theory approaches the expected classical Master equation

[1]Note that, as we work in the grand canonical ensemble framework, the metal lead in our 'world' is assumed to be weakly open to an equilibrium bath of given temperature and electronic chemical potential.

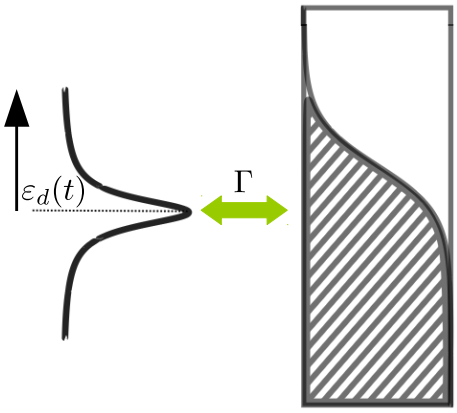

Figure 3.1: The driven resonant level model under consideration: strong coupling of the time-dependent single electronic level to a free electron metal leads to broadening given by the escape rate Γ. If Γ is comparable to or larger than the temperature T, which determines the width of the distribution function of the electrons in the metal depicted on the right, an energy resolved (i.e. quantum) description of the dynamic processes becomes necessary. We aim at describing the thermodynamic changes when the level is moved linearly by an external agent in this strong coupling regime.

limit. We conclude in Sec. 3.5. We have relegated most explicit calculations to separated technical sections and a series of appendices in order not to break the flow of the main arguments.

3.1 Model

We consider a single localized electronic level coupled to a free electron metal at temperature T and chemical potential μ. The Hamiltonian of the full system is

$$H = H_D + H_V + H_B \,, \tag{3.1}$$

where H_D, H_B, and H_V denote the Hamiltonians of the dot,

$$H_D = \varepsilon_d(t) d^\dagger d \,, \tag{3.2}$$

of the metal lead,

$$H_B = \sum_k \varepsilon_k c_k^\dagger c_k \,, \tag{3.3}$$

and of the lead-dot coupling,

$$H_V = \sum_k \left(V_k d^\dagger c_k + \text{h.c.} \right) \,. \tag{3.4}$$

Here, d annihilates an electron in the dot level, c_k an electron with momentum k and energy ε_k in the lead, and V_k denotes the coupling strength between dot level and lead.

The dot energy $\varepsilon_d(t)$ is driven by an external force. Our goal is to elucidate the effect of this driving on the thermodynamic properties of the system. We limit ourselves to the simplest situation of a single driven dot level, a single macroscopic lead, and the wide band approximation. (Alternative coupling models, see, e.g. Ref. [Ajisaka et al., 2012], can be considered.) Apart from the driving, the lead is assumed to be in thermal equilibrium characterized by a temperature T and an electronic chemical potential μ. In the wide band approximation the retarded dot self-energy

$$\Sigma^R(\varepsilon) = \lim_{\eta\to 0} \sum_k \frac{|V_k|^2}{\varepsilon - \varepsilon_k + i\eta} = -\frac{i}{2}\Gamma \tag{3.5}$$

can be taken as purely imaginary and energy independent for energies ε well within the bandwidth of the lead and vanishes for energies outside the band (see Appendix B.1). It is furthermore proportional to the decay rate of the dot electrons into the lead $\Gamma = 2\pi \sum_k |V_k|^2 \delta(\varepsilon - \varepsilon_k)$. Consequently, the spectral function associated with the dot's electronic state is a Lorentzian of width Γ centered at ε_d,

$$A(\varepsilon) = \frac{\Gamma}{(\varepsilon - \varepsilon_d)^2 + (\Gamma/2)^2}\,. \tag{3.6}$$

The broadening necessitates an energy resolved description of the electronic response to changes in the level energy and is responsible for the quantum nature of the problem. In Sec. 3.4 we show that our quantum results reduce to their classical counterparts in the limit $\Gamma \ll T$. As already mentioned, strong hybridization of dot and lead results in a reaction of the lead to changes in the level energy. This makes the definition of thermodynamic quantities associated with the driven subsystem alone a difficult task. We overcome this problem by considering as the driven system the entire part of the 'world' that is affected by changes in the dot level, as shown in the next section.

3.2 Equilibrium Thermodynamics

When $\varepsilon_d(t)$ moves infinitely slowly, the change induced by the driving is quasistatic and reversible.[2] The system stays in equilibrium at all times and follows the change in ε_d adiabatically. The desired thermodynamic functions can then be calculated from equilibrium thermodynamics. We do this in the grand canonical framework, where our 'full' system (i.e., dot and lead) is coupled to a reservoir that controls its temperature $T = \beta^{-1}$ and chemical potential μ. In

[2]The velocity of the level is measured by $\dot{\varepsilon}_d/\Gamma$ and in the strong coupling regime the corrections to the equilibrium occupation f given in Eq. (3.46) need to be small at each energy yielding the adiabaticity condition $\dot{\varepsilon}_d/\Gamma \ll T$.

the free electron model, the grand partition function Ξ and the grand potential $\Omega = -T \ln \Xi$ can be evaluated exactly, yielding

$$\Omega_{\text{tot}} = -T \int \frac{d\varepsilon}{2\pi} \rho(\varepsilon) \ln \left(1 + e^{-\beta(\varepsilon - \mu)}\right) , \tag{3.7}$$

where the label 'tot' stands for this being the grand potential of the total system. We emphasize that the total system comprises everything that is described by the Hamiltonians (3.2)-(3.4), namely the dot, the lead, and their coupling. In Eq. (3.7), $\rho(\varepsilon)$ is the density of states of the system as given by the trace of the spectral function,

$$\rho(\varepsilon) = \sum_n A_{nn}(\varepsilon) . \tag{3.8}$$

Here, $A_{nn}(\varepsilon) = -2 \operatorname{Im} G^R_{nn}(\varepsilon)$ with the retarded Green's function

$$G^R_{nn'}(t, t') = -i\Theta(t - t') \left\langle \left\{ c_n(t), c^\dagger_{n'}(t') \right\} \right\rangle . \tag{3.9}$$

The index n enumerates all single-particle states (lead and dot). For better comparison with the recent work of Ref. [Esposito et al., 2015b], we present the calculation of the density of states beyond the wide band limit in a small technical interlude, which can be skipped by readers uninterested in technical details.

3.2.1 Technical interlude: density of states

In the following we calculate the part of the density of states that changes when the dot level is moved, which in turn determines the relevant thermodynamic quantities of the extended resonant level. This derivation is presented without using the wide band limit to achieve better comparison with the recent work of Ref. [Esposito et al., 2015b]. This density of states is given by the trace of the spectral function $\rho(\varepsilon) = \sum_n A_{nn}(\varepsilon)$, where $A_{nn}(\varepsilon) = -2\,\mathrm{Im}\,G^R_{nn}(\varepsilon)$. In the basis of uncoupled dot (d) and lead free electron states (k) this gives

$$\rho(\varepsilon) = A_{dd}(\varepsilon) + \sum_k A_{kk}(\varepsilon)\,. \tag{3.10}$$

The spectral function of the dot electrons in the presence of the coupling takes the well known form

$$A_{dd}(\varepsilon) = \frac{-2\,\mathrm{Im}\,\Sigma^R(\varepsilon)}{(\varepsilon - \varepsilon_d - \mathrm{Re}\,\Sigma^R(\varepsilon))^2 + (\mathrm{Im}\,\Sigma^R(\varepsilon))^2} \tag{3.11}$$

where $\Sigma^R(\varepsilon) = \sum_k |V_k|^2 g^R_k(\varepsilon)$ is the retarded self energy of the dot state due to its coupling to the leads and $g^R_k(\varepsilon)$ is the retarded Green's function of a free lead electron in state k. Due to the strong coupling of the dot to the lead electrons, also the density of states of the surrounding responds upon changes in the dot level. To calculate A_{kk} we start from the Dyson equation for $G^R_{kk}(\varepsilon)$

$$G^R_{kk}(\varepsilon) = g^R_k(\varepsilon) + \left(g^R_k(\varepsilon)\right)^2 |V_k|^2 G^R_{dd}(\varepsilon)\,. \tag{3.12}$$

Summing over k and using $\Sigma^R(\varepsilon) = \sum_k |V_k|^2 g^R_k(\varepsilon)$ we can write the second term on the right of Eq. (3.12) in terms of the retarded self energy, leading to the total density of states

$$\rho(\varepsilon) = A_{dd}(\varepsilon)\left(1 - \frac{d}{d\varepsilon}\,\mathrm{Re}\,\Sigma^R(\varepsilon)\right) + 2\,\mathrm{Re}\,G^R_{dd}(\varepsilon)\frac{d}{d\varepsilon}\,\mathrm{Im}\,\Sigma^R(\varepsilon) + \nu(\varepsilon)\,, \tag{3.13}$$

where $\nu(\varepsilon) = -2\sum_k \mathrm{Im}\,g^R_k(\varepsilon)$ is the density of states of the free metal.

The total density of states

$$\rho(\varepsilon) = A_{dd}(\varepsilon)\left(1 - \frac{d}{d\varepsilon}\,\mathrm{Re}\,\Sigma^R(\varepsilon)\right) + 2\,\mathrm{Re}\,G^R_{dd}(\varepsilon)\frac{d}{d\varepsilon}\,\mathrm{Im}\,\Sigma^R(\varepsilon) + \nu(\varepsilon)\,, \tag{3.14}$$

determines the grand potential and its ε_d-dependent part arises from the first three of the four terms in Eq. (3.14). In the wide band limit, the second and third terms on the right hand side of Eq. (3.14) vanish, and the ε_d-dependent part of the density of states ρ_{ε_d} is given by the spectral function $A(\varepsilon)$, Eq. (3.6). In the general (non-wide-band) case, the ε_d-dependent part of the density of states is similar to the modified spectral function proposed in Ref. [Esposito et al., 2015b], with the difference that the energy derivative in the third term is taken

of the imaginary part of the self energy, while Esposito et al. have a contribution $-2\,\mathrm{Im}\,\Sigma^R \partial_\varepsilon\,\mathrm{Re}\,G^R_{dd}(\varepsilon)$ to their modified spectral function. This leads to different thermodynamic functions calculated with the help of the density of states, also in the wide band limit. We refer to the ε_d-dependent part of the system as the extended resonant level, since it accounts for the change of the surrounding in response to changing the level energy.

We now use the ε_d-dependent part of the density of states $\rho_{\varepsilon_d}(\varepsilon) = A(\varepsilon)$ to calculate the ε_d-dependent contribution to the grand potential Ω, which in turn yields the corresponding ε_d-dependent contributions to all the thermodynamic functions of the system. In particular, we calculate the entropy $S^{(0)}$, the internal energy $E^{(0)}$, and the particle number $N^{(0)}$ of the extended resonant level in equilibrium, i.e., for a frozen dot level, and show how they evolve when the dot level is changed quasistatically by an external force. We use superscripts on the thermodynamic functions to indicate to which order in the level velocity $\dot{\varepsilon}_d$ they are calculated. Furthermore we show how these quantities can be represented, in the model considered, as quasistatic expectation values of operators. This observation provides a convenient route for extending the quasistatic thermodynamic quantities to non-equilibrium, i.e., to situations where the dot level is moved at finite speed (see Sec. 3.3).

In the following, the notation Ω, $S^{(0)}$, $E^{(0)}$, $N^{(0)}$ and the corresponding names grand potential, entropy, energy, and particle number always refer to the ε_d-dependent parts of these functions. The grand potential takes the form

$$\Omega = -T \int \frac{d\varepsilon}{2\pi} A \ln\left(1 + e^{-\beta(\varepsilon-\mu)}\right) . \tag{3.15}$$

Here and in the following, we omit energy arguments for better readability. The particle number, entropy and energy are given by

$$N^{(0)} = -\frac{\partial\Omega}{\partial\mu} = \int \frac{d\varepsilon}{2\pi} A\, f\,, \tag{3.16}$$

$$\begin{aligned} S^{(0)} &= -\frac{\partial\Omega}{\partial T} \\ &= \int \frac{d\varepsilon}{2\pi} A \left[\beta\,(\varepsilon-\mu)\, f + \ln\left(1 + \mathrm{e}^{-\beta(\varepsilon-\mu)}\right)\right] \\ &= \int \frac{d\varepsilon}{2\pi} A \left[-f \ln f - (1-f)\ln(1-f)\right] , \end{aligned} \tag{3.17}$$

and

$$E^{(0)} = \Omega + \mu N^{(0)} + T S^{(0)} = \int \frac{d\varepsilon}{2\pi} \varepsilon A\, f\,, \tag{3.18}$$

where f is the Fermi-Dirac distribution. In the wide band limit, the grand potential as well as the internal energy depend on the bandwidth D and diverge in the limit $D \to \infty$. However, this only affects the reference point from which the grand potential and the internal energy are measured. Here, we are interested in the thermodynamic relations between *changes* in these quantities as the dot

level ϵ_d varies. These changes converge to bandwidth-independent values in the limit of an infinite bandwidth (see the detailed discussion in App. B.1).

Equation (3.16) implies that, in the wide band limit, the ε_d-dependent part of the equilibrium particle number $N^{(0)}$ is given by the quasistatic dot occupation $N^{(0)} = \left\langle d^\dagger(t)d(t)\right\rangle^{(0)}$, namely the equilibrium occupation for the instantaneous value of ε_d . The contribution to the energy, Eq. (3.18), explicitly shows that the coupling to the environment affects the energy cost associated with changes of the bare dot energy ε_d, as it cannot be represented as an expectation value of H_D only. Equation (3.17) is the energy resolved version of the Gibbs entropy of a single fermionic level with equilibrium occupation probability f, weighted by the spectral function of the dot electrons. For $T \to 0$, the term in square brackets in Eq. (3.17) for $S^{(0)}$ tends to zero for $\varepsilon \neq \mu$ and to $\ln 2$ for $\varepsilon = \mu$, reflecting the degeneracy at the Fermi edge. Integrating over energy leads to a vanishing equilibrium entropy $S^{(0)}$ of the extended resonant level for $T \to 0$.

It is important to note that the equilibrium energy of the extended resonant level, namely the ε_d-dependent part of the total (dot plus lead) internal energy, can be expressed as a sum of contributions from the different terms in the Hamiltonian (3.1). In particular, as shown in App. B.3, the part of the internal energy $E^{(0)}$ given by Eq. (3.18) can be represented by the quasistatic expectation value $E^{(0)} = \langle H_D\rangle^{(0)} + \frac{1}{2}\langle H_V\rangle^{(0)}$. This appears to indicate that, in the model considered, half the energy associated with the coupling H_V can be attributed to the extended resonant level. This interpretation, however, is an oversimplification as may be realized from the following: Calculating the ε_d-dependent part of the averages of H_D, H_V, and H_B from the grand potential, Eq. (3.15), we obtain $\langle H_B\rangle_{\varepsilon_d} = -\int \frac{d\varepsilon}{2\pi}\,(\varepsilon-\varepsilon_d)\;A\,f$, $\langle H_V\rangle_{\varepsilon_d} = 2\int \frac{d\varepsilon}{2\pi}(\varepsilon-\varepsilon_d)A\,f$, and $\langle H_D\rangle_{\varepsilon_d} = \varepsilon_d\int \frac{d\varepsilon}{2\pi}A\,f$ (see App. B.3). It is interesting to note that not only $\langle H_V\rangle$ but also $\langle H_B\rangle$ has an ε_d-dependent part and together with $\langle H_D\rangle$ they add up to $E^{(0)}$, Eq. (3.18). In fact, the contributions of H_V and H_B add to $\langle H_B\rangle_{\varepsilon_d} + \langle H_V\rangle_{\varepsilon_d} = \frac{1}{2}\langle H_V\rangle^{(0)}$, which shows the intricate physical origin of the symmetric splitting.

An apparent symmetric splitting of the coupling energy in the wide band limit of the resonant level model between an effective driven system $H_D + \frac{1}{2}H_V$ and an effective bath $H_B + \frac{1}{2}H_V$ was also found in the case of periodic driving.[Ludovico et al., 2014] It should be emphasized that this separation, namely assigning parts of the calculated thermodynamic functions to the different subsystems is not needed in the present analysis of the equilibrium thermodynamics. We allude to it both because it has been considered in recent discussions [Ludovico et al., 2014] and because it can help building intuition about the system behavior. Furthermore it serves as a convenient starting point for the Green's function based calculation of the internal energy when the level moves at finite velocity.

Next, we consider the evolution of the thermodynamic functions when changing the dot level quasistatically. In particular, we examine the different contributions to the reversible energy change $dE^{(0)}$, the reversible work $dW^{(0)}$, the heat $dQ^{(0)}$, and the chemical work $\mu\, dN^{(0)}$. These satisfy energy conservation as

expressed by the first law,

$$dE^{(0)} = dW^{(0)} + dQ^{(0)} + \mu\, dN^{(0)}\,, \tag{3.19}$$

when applied to the extended resonant level. Note that this equation relates properties of the full system (dot + lead). But because the individual terms result from changes in the bare dot energy ε_d, they are often referred to as changes in the corresponding dot property.

The reversible work is given by the change in the grand potential upon changing the level energy, $dW^{(0)} = d\varepsilon_d\, \partial_{\varepsilon_d}\Omega$. Expressed as an equation for the power $\dot{W}^{(1)}$, this takes the form

$$\dot{W}^{(1)} = \dot{\varepsilon}_d N^{(0)}\left(\varepsilon_d\right) = \dot{\varepsilon}_d \left\langle d^\dagger(t) d(t)\right\rangle^{(0)}\,. \tag{3.20}$$

It is frequently the case that the time dependence of $\varepsilon_d\left(t\right)$ reflects the dynamics of some external coordinate, $\varepsilon_d\left(t\right) = M x_d\left(t\right)$ with a coupling parameter M. The quantity $F = -M\left\langle d^\dagger(t) d(t)\right\rangle^{(0)}$ is then the quasistatic force needed to change the level energy. General expressions for such forces were obtained in the context of adiabatic reaction forces.[Bode et al., 2011, 2012b]

The quasistatic heat leaving or entering the system is calculated from $dQ^{(0)} = T d\varepsilon_d\, \partial_{\varepsilon_d} S^{(0)}$, with $S^{(0)}$ given by Eq. (3.17). By noting that $A(\varepsilon)$ depends only on $(\varepsilon - \varepsilon_d)$ and integrating by parts, the corresponding quasistatic heat current takes the form

$$\dot{Q}^{(1)} = T\dot{\varepsilon}_d \frac{\partial S^{(0)}}{\partial \varepsilon_d} = \dot{\varepsilon}_d \int \frac{d\varepsilon}{2\pi}\left(\varepsilon - \mu\right) A \partial_\varepsilon f. \tag{3.21}$$

With $N^{(0)}$ in Eq. (3.16), the quasistatic particle current $\dot{N}^{(1)} = \dot{\varepsilon}_d \partial_{\varepsilon_d} N^{(0)}$ is given by

$$\dot{N}^{(1)} = \dot{\varepsilon}_d \int \frac{d\varepsilon}{2\pi} A \partial_\varepsilon f\,. \tag{3.22}$$

The quasistatic change in the system's energy associated with the change in ε_d is given by

$$\dot{E}^{(1)} = \dot{\varepsilon}_d \frac{\partial E^{(0)}}{\partial \varepsilon_d} = \dot{\varepsilon}_d \int \frac{d\varepsilon}{2\pi} \varepsilon \frac{\partial A}{\partial \varepsilon_d} f \tag{3.23}$$

and is easily seen to indeed satisfy the first law, Eq. (3.19), since $\dot{E}^{(1)} = \dot{W}^{(1)} + \dot{Q}^{(1)} + \mu\, \dot{N}^{(1)}$. Note that the quasistatic power $\dot{W}^{(1)}$, the currents $\dot{N}^{(1)}$ and $\dot{Q}^{(1)}$, and the rate of energy change $\dot{E}^{(1)}$ are *linear* in the driving speed, as indicated by the superscript.

We end our discussion of quasistatic (equilibrium) processes with several comments:

(a) The integrand of $\dot{N}^{(1)}$ can be understood as an energy resolved particle current $J^{(1)}(\varepsilon) = \dot{\varepsilon}_d A \partial_\varepsilon f$ and the right hand side of Eq. (3.21) can be expressed in terms of the same current

$$\dot{Q}^{(1)} = \int \frac{d\varepsilon}{2\pi} J^{(1)}(\varepsilon)\left(\varepsilon - \mu\right)\,. \tag{3.24}$$

Consequently, $J_Q^{(1)}(\varepsilon) = J^{(1)}(\varepsilon)(\varepsilon - \mu)$ can be identified as the energy resolved heat current, providing physical insight into the nature of this current. It is important to note that identifying the integrand of an energy integral such as the particle current $\dot{N}^{(1)}$ in Eq. (3.22) as an energy resolved current is open to ambiguity. Other expressions could also be chosen following integration by parts. Considering the particle and heat currents together serves to resolve this ambiguity.

(b) For quasistatic processes, we could calculate the particle, energy, and heat currents without assigning these variables to expectation values of the dot operators themselves. Especially the quasistatic heat current, Eq. (3.21), was obtained without relying on any specific forms for the energetic properties of the dot itself. In particular the symmetric splitting of the coupling Hamiltonian between dot and lead, discussed above, was not used. It can, however, also be calculated from expectation values using the symmetric splitting into effective bath and system introduced above. Indeed, we show in App. B.4 that to lowest order in the level speed, the adiabatic heat current $\dot{Q}^{(1)}$ given in Eq. (3.21) is reproduced by the change of the energy of the effective bath $H_B + \frac{1}{2}H_V$ minus the chemical contribution of the particle flow,

$$\dot{Q}^{(1)} = -\frac{d}{dt}\left\langle H_B + \frac{1}{2}H_V \right\rangle^{(0)} - \mu \frac{d}{dt} N^{(0)} \,. \tag{3.25}$$

Eq. (3.25) confirms, for the present model and the wide band limit, the consistency of the symmetric splitting of the coupling Hamiltonian H_V into an effective bath and an effective driven system. This will serve as a convenient starting point for the calculation of the heat current at finite level speed. Note, however, that for more general models (e.g., beyond the wide band approximation and with variations in the level-lead coupling), the possibility to express the change in thermodynamic variables in terms of expectation values of 'system operators' is an open problem and subject to several difficulties.[Esposito et al., 2015a]

(c) In the quasistatic process, the entropy change $\dot{S}^{(1)} = \dot{\varepsilon}_d \, \partial_{\varepsilon_d} S^{(0)}$ is given by the corresponding heat current, $\dot{Q}^{(1)} = T\dot{S}^{(1)}$, indicating that no entropy is produced. This is not the case when the level moves at finite speed and dissipation sets in, as discussed in the next section.

We have described the equilibrium thermodynamics of the resonant level model and calculated the reversible change of the thermodynamic quantities in the wide band limit. We represented all thermodynamic quantities of the extended resonant level as quasistatic expectation values of operators. Next we extend our discussion to the non-adiabatic regime and consider the effect of moving the dot level energy at a small, but finite speed.

3.3 Non-equilibrium Thermodynamics

In this section, we consider the changes in thermodynamic quantities when the dot level moves at finite speed. For this non-equilibrium process we cannot use the equilibrium grand potential as a starting point. Instead, we extend our quasistatic results to finite speed processes by expanding the expectation values of the operators associated with the thermodynamic variables in powers of the level velocity, using the non-equilibrium Green's function approach together with the gradient expansion in the Wigner representation. Our theory should follow three guidelines: First, all non-equilibrium quantities should converge to their equilibrium forms, obtained in the previous section, in the limit of vanishing speed. Second, higher order corrections should satisfy conservation of energy and particle number at the corresponding order. Third, the non-equilibrium entropy of the extended resonant level should lead to positive entropy production characterizing the irreversibility of the process. Note that the corrections obtained below are of different orders in the level speed. The corrections to the equilibrium values of the thermodynamic variables themselves are linear in $\dot{\varepsilon}_d$, while the correction to their fluxes are quadratic. The corresponding order is again indicated by the superscript assigned to the different variables. We also assume a linear motion of the dot level, $\ddot{\varepsilon}_d = 0$.

We briefly introduce the non-equilibrium Green's functions formalism underlying this chapter in the following technical section, which can be skipped by readers either familiar with the topic or uninterested in technical details.

3.3.1 Technical section: Non-equilibrium Green's functions

This section gives a brief introduction into the non-equilibrium Green's functions formalism to provide the technical foundation underlying the present chapter. Since a detailed derivation of all necessary quantities is beyond the scope of this work, we refer the interested reader to the book by [Haug and Jauho, 1996], from which we benefited a lot throughout our work.

We want to describe the time evolution of the electronic system under a time-dependent drive: a genuine non-equilibrium problem. The central objects in this effort are electronic expectation values of the kind $\langle d^\dagger(t)d(t')\rangle$, where d is an electronic annihilation operator (e.g. of the single level). The goal is to capture the time evolution of these expectation values under the time-dependent drive (here the gate voltage) and a perturbation (here the coupling to the surrounding metallic bath).

In the effort of calculating the expectation values, one usually constructs a time-evolution to refer to the state of the system in the distant past $t = -\infty$ in absence of the perturbation, which is assumed to be known. From there the perturbation is adiabatically switched on, which forms the technical basis to calculate the desired expectation values in a perturbation theory. In equilibrium,

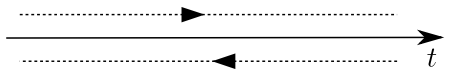

Figure 3.2: Time contour for the time evolution in the contour ordered non-equilibrium Green's function.

the only time dependence is the one of the adiabatic switch-on and the perturbation theory can be founded on the assumption that the system goes back to the initial state, when the perturbation is adiabatically turned off again. In contrast, in non-equilibrium systems this assumption is not satisfied, since there is an actual time-dependence additionally to the adiabatic switch-on of the perturbation. This necessitates the introduction of a more complex time-contour along which we consider the evolution of system from the distant past, where the perturbation was absent, to the present, where both time-dependent drive and perturbation act on the system, and back to the distant past again where the perturbation is switched off. The central object for this theory is the contour ordered Green's function

$$G(t,t') = -i\left\langle T_C\left[d(t)d^\dagger(t')\right]\right\rangle \tag{3.26}$$

describing the expectation value calculated with the time evolution along the described contour, where T_C is the time ordering operator on the contour (that ensures that the operator with times that are passed first on the contour appears to the right). Depending whether t and t' are on the forward (C_1) or backward (C_2) part of the contour, this Green's function contains four different functions for times along a single time axis

$$G(t,t') = \begin{cases} -i\left\langle T\left[d(t)d^\dagger(t')\right]\right\rangle & t,t' \in C_1 \\ i\left\langle d^\dagger(t')d(t)\right\rangle = G^<(t,t') & t \in C_2, t' \in C_1 \\ -i\left\langle d(t)d^\dagger(t')\right\rangle = G^>(t,t') & t \in C_1, t' \in C_2 \\ -i\left\langle \tilde{T}\left[d(t)d^\dagger(t')\right]\right\rangle & t,t' \in C_2 \end{cases}, \tag{3.27}$$

where T is the normal time-ordering operator and $\tilde{T}$ is the anti-time ordering operator. These Green's functions can be combined to build the retarded and advanced Green's function, which will be needed for our later analysis

$$G^R(t,t') = \Theta(t-t')\left[G^>(t,t') - G^<(t,t')\right] = -i\Theta(t-t')\left\langle\left\{d(t), d^\dagger(t')\right\}\right\rangle \tag{3.28}$$

$$G^A(t,t') = \Theta(t'-t)\left[G^<(t,t') - G^>(t,t')\right] = i\Theta(t'-t)\left\langle\left\{d(t), d^\dagger(t')\right\}\right\rangle, \tag{3.29}$$

where $\{..,..\}$ denotes the anti-commutator. Our central object of interest in the following will be the lesser Green's function $G^<$ that determines the occupation of the single level when evaluated at equal times.

The central appeal of introducing the contour ordered Green's function is that its perturbation theory takes the same form as for equilibrium Green's functions. One can thus capture the effect of the perturbation in terms of a self energy Σ in a Dyson equation for the contour ordered Green's function

$$G(t,t') = g(t,t') + \int_C dt_1 \int_C dt_2 g(t,t_1)\Sigma(t_1,t_2)G(t_2,t')\,, \tag{3.30}$$

where g is the Green's function in absence of the perturbation and all time integrals occur along the contour. All that is left to do is to relate the contour ordered Green's function to our quantity of interest: the lesser component, which is needed to calculate system properties such as occupation and energy.

The rules of analytical continuation from the contour to the desired lesser component are also known as Langreth rule, and take the form

$$C = \int_C AB \to C^< = \int_t \left[A^R B^< + A^< B^A\right]\,, \tag{3.31}$$

$$D = \int_C ABC \to D^< = \int_t \left[A^R B^R C^< + A^R B^< C^A + A^< B^A C^A\right]\,, \tag{3.32}$$

where we omitted the explicit time labels and convolutions along the contour ($\int_C$) or the real axis ($\int_t$) are implicit. With this rather technical introduction we build the foundation to calculate the evolution of the desired system properties under time-dependent drives.

We obtain the desired lesser component from the Dyson equation Eq. 3.30 with the rules of analytical continuation 3.32

$$G^< = g^< + g^R\Sigma^R G^< + g^R\Sigma^< G^A + g^<\Sigma^A G^A \tag{3.33}$$

$$= g^<\left(1+\Sigma^A G^A\right) + \left(g^R\right)\Sigma^< G^A + g^R\Sigma^R G^<\,. \tag{3.34}$$

Reinserting $G^<$ yields

$$G^< = \left(1+g^R\Sigma^R\right)g^<\left(1+\Sigma^A G^A\right) + \left(g^R + g^R\Sigma^R g^R\right)\Sigma^< G^A + g^R\Sigma^R G^<\,. \tag{3.35}$$

With the Dyson equation for the retarded component

$$G^R = g^R + g^R\Sigma^R G^R\,, \tag{3.36}$$

we can see that the first bracket resembles $\left(1+G^R\Sigma^R\right)$ upon further iteration, while the term in the third bracket resembles G^R. This yields upon repeated iteration

$$G^< = \left[1+G^r\Sigma^r\right]g^<\left[1+\Sigma^a G^a\right] + G^r\Sigma^< G^a\,. \tag{3.37}$$

For non-interacting electrons we can write $\left[1+G^R\Sigma^R\right]g^< = G^R\left(g^R\right)^{-1}g^< = 0$ and thereby neglect the initial occupation of the dot at $t=-\infty$ and the transient dynamics induced by the adiabatic switch on of the coupling between level and metallic bath. This yields the desired form of the lesser component [Jauho et al., 1994]

$$G^<(t,t') = \int dt_1 dt_2 G^R(t,t_1)\Sigma^<(t_1,t_2)\,G^A(t_2,t')\,, \tag{3.38}$$

where $\Sigma^<$ is the lesser component of the self energy.

Now we have everything at hand to evaluate the necessary elements of the non-equilibrium Green's functions for the driven resonant level model. We utilize the gradient expansion to take advantage of the model assumption that the driving speed is slow relative to the electronic relaxation rates.

We start by deriving the form of the retarded dot Green's function at finite speed. The equation of motion for the retarded Green's function can be written in the form

$$\delta(t-t') = \int dt_1 G^R(t,t_1)\left[i\partial_{t_1}\delta(t_1-t') - \varepsilon_d(t_1)\delta(t_1-t') - \Sigma^R(t_1-t')\right]\,, \tag{3.39}$$

with the retarded self energy $\Sigma^R(t,t') = \sum_k |V_k|^2 g_k^R(t,t')$ induced by the coupling to the electrons in the lead. To perform an adiabatic expansion it is beneficial to switch to a description in terms of Wigner transforms

$$G(\varepsilon,t) = \int d\tau\, G(t_1,t_2)\, e^{i\varepsilon\tau}\,, \tag{3.40}$$

where $t=\frac{t_1+t_2}{2}$ and $\tau = t_1-t_2$ and the corresponding inverse transform. Using that the Wigner transform of a convolution can be written as

$$\int C(t_1,t_3)\,D(t_3,t_2)\,dt_3 = \int \frac{d\varepsilon}{2\pi} e^{-i\varepsilon\tau} C(\varepsilon,t) * D(\varepsilon,t) \tag{3.41}$$

with $C(\varepsilon,t)*D(\varepsilon,t) = C(\varepsilon,t)\exp\left[\frac{i}{2}\left(\overleftarrow{\partial}_\varepsilon\,\vec{\partial}_t - \overleftarrow{\partial}_t\,\vec{\partial}_\varepsilon\right)\right]D(\varepsilon,t)$, we take the Wigner transform of Eq. (3.39) and expand the exponential up to first order to obtain

$$1 \;=\; G^R(\varepsilon,t)\left[\varepsilon - \varepsilon_d(t) + \frac{1}{2}i\Gamma\right] + \frac{i}{2}\left[\partial_\varepsilon G^R(\varepsilon,t)\left[-\dot{\varepsilon}_d(t)\right] - \partial_t G^R(\varepsilon,t)\right] \tag{3.42}$$

where we used the wide band limit $\Sigma^R = -\frac{1}{2}i\Gamma$. Thus the retarded Green's function of the dot electrons is, up to first order in the velocity, given by the frozen form $G^R(\varepsilon,t) = (\varepsilon - \varepsilon_d(t) + i\frac{\Gamma}{2})^{-1}$. An analogous calculation gives for the advanced Green's function $G^A(t,t') = i\Theta(t'-t)\left\langle\left\{d(t),d^\dagger(t')\right\}\right\rangle$ the Wigner transform $G^A(\varepsilon,t) = (\varepsilon-\varepsilon_d(t)-i\frac{\Gamma}{2})^{-1}$.

Now we can use the form of the lesser Green's function derived above in Eq. (3.38), take again the Wigner transform of this convolution and expand it up

to first order in the velocity. We obtain at the different orders

$$G^{<(0)}(\varepsilon,t) = G^R\Sigma^<G^A\,, \tag{3.43}$$

$$G^{<(1)}(\varepsilon,t) = \frac{i}{2}\left(\partial_\varepsilon G^R\partial_t\Sigma^< - \partial_t G^R\partial_\varepsilon\Sigma^<\right)G^A + \frac{i}{2}\left[\partial_\varepsilon\left(G^R\Sigma^<\right)\partial_t G^A - \partial_t\left(G^R\Sigma^<\right)\partial_\varepsilon G^A\right]\,. \tag{3.44}$$

Using $\partial_t G^{R/A} = -\dot\varepsilon_d\partial_\varepsilon G^{R/A}$, $\Sigma^<(\varepsilon) = if\,(\varepsilon)\,\Gamma$ and $\partial_\varepsilon G^R\,G^A - G^R\partial_\varepsilon G^A = i\frac{A^2}{\Gamma}$ this yields

$$G^<(\varepsilon,t) = iA\,f - i\frac{\dot\varepsilon_d}{2}\partial_\varepsilon f\,A^2\,. \tag{3.45}$$

3.3.2 Induced non-equilibrium thermodynamics

We use the results of the Green's functions calculation above to explore the induced non-equilibrium effects in the thermodynamic functions of the resonant level.

Particle number. We extend the calculation of the particle number of the resonant level to finite speed by expanding the lesser Green's function $\left\langle d^\dagger(t)d(t)\right\rangle = -iG^<_{dd}(t,t)$ to linear order in the level speed, as shown above. Alternatively, the effect of the level speed on the dot occupation can be expressed through a non-equilibrium distribution function ϕ (as done in Ref. [Esposito et al., 2015b]), which is related to the Wigner transform of the lesser Green's function via $G^< = iA\phi$. The equation of motion for ϕ and its solution are given in App. B.2, and the final result for the non-equilibrium distribution ϕ is

$$\phi = f - \frac{\dot\varepsilon_d}{2}\partial_\varepsilon f A\,. \tag{3.46}$$

Both approaches are equivalent and lead to $G^< = iA\left(f - \frac{\dot\varepsilon_d}{2}\partial_\varepsilon f\,A\right)$ and therefore to a correction to the particle number linear in the velocity,

$$N^{(1)} = -\frac{\dot\varepsilon_d}{2}\int\frac{d\varepsilon}{2\pi}\partial_\varepsilon f\,A^2\,. \tag{3.47}$$

This correction in the particle number accounts for the fact that the dot population lags behind the equilibrium value since electrons are not exchanged fast enough with the leads. The time derivative of Eq. (3.47) now yields the correction $\dot N^{(2)} = \frac{d}{dt}N^{(1)}$ to the quasistatic current, $\dot N^{(1)}$, that takes the form

$$\dot N^{(2)} = -\frac{\dot\varepsilon_d^2}{2}\int\frac{d\varepsilon}{2\pi}\partial_\varepsilon^2 f\,A^2\,. \tag{3.48}$$

One might be tempted to identify the integrand of $\dot N^{(2)}$ as the second order correction to the energy resolved particle current. However, this cannot be done unambiguously because other expressions can be obtained after integration by

parts. As before, more information can be obtained by considering the particle and heat currents together as further discussed below.

Work. The quasistatic work per unit time $\dot{W}^{(1)} = \dot{\varepsilon}_d N^{(0)}$ can be extended to finite level speed with the correction to the dot occupation $N^{(1)}$, Eq. (3.47). With this we readily obtain the extra power that the external driving has to provide for moving the level at finite speed by multiplying $N^{(1)}$, Eq. (3.47), by the level speed

$$\dot{W}^{(2)} = -\frac{\dot{\varepsilon}_d^2}{2} \int \frac{d\varepsilon}{2\pi} \partial_\varepsilon f \, A^2 \,. \tag{3.49}$$

$\dot{W}^{(2)}$ thus corresponds to the power dissipated by driving the system at finite speed. When considering the time dependence of $\varepsilon_d(t)$ as reflecting the dynamics of some external coordinate, $\varepsilon_d(t) = M x_d(t)$, the dissipated power is caused by a friction force acting on the external coordinate $F_{\text{fric}} = -M N^{(1)} = -\gamma \dot{x}_d$. This yields the friction coefficient

$$\gamma = -\frac{M^2}{2} \int \frac{d\varepsilon}{2\pi} \partial_\varepsilon f \, A^2 \,. \tag{3.50}$$

The same expression for the friction in the resonant level model was found in Ref. [Bode et al., 2012b].

Internal energy. We showed above that the equilibrium internal energy of the extended resonant level can be represented as the quasistatic expectation value $E^{(0)} = \langle H_D \rangle^{(0)} + \frac{1}{2} \langle H_V \rangle^{(0)}$. Expanding the expectation values to first order in the velocity (see App. B.3), we obtain the first order correction to the internal energy,

$$E^{(1)} = \frac{-\dot{\varepsilon}_d}{2} \int \frac{d\varepsilon}{2\pi} \varepsilon \partial_\varepsilon f A^2 \,. \tag{3.51}$$

Heat flux. Taking the next order correction to the expression of the quasistatic heat flux, Eq. (3.25), in terms of the energy change in the effective bath and the chemical contribution (shown in App. B.4) gives the correction to the heat flux that originates from moving the level at finite speed,

$$\dot{Q}^{(2)} = -\frac{\dot{\varepsilon}_d^2}{2} \int \frac{d\varepsilon}{2\pi} (\varepsilon - \mu) \, \partial_\varepsilon^2 f \, A^2 \,. \tag{3.52}$$

As in the case of the quasistatic heat current, the integrand of the correction $\dot{Q}^{(2)}$ can be understood as heat $(\varepsilon - \mu)$ carried into the lead by the energy resolved particle current $J^{(2)}(\varepsilon)$, $\dot{Q}^{(2)} = \int \frac{d\varepsilon}{2\pi} (\varepsilon - \mu) J^{(2)}(\varepsilon)$. The energy resolved particle current $J^{(2)}(\varepsilon)$ in turn is the properly chosen integrand in $\dot{N}^{(2)} = \int \frac{d\varepsilon}{2\pi} J^{(2)}(\varepsilon)$ as given by Eq. (3.48). This unambiguously defines the second order correction to the energy resolved particle current as $J^{(2)} = -\frac{\dot{\varepsilon}_d^2}{2} \partial_\varepsilon^2 f \, A^2$.

Consistency checks. The consistency of our thermodynamic description should be examined by its behavior in the quasistatic limit, by satisfying particle conservation, and by its adherence to the first law (energy conservation). Furthermore

the entropy, discussed below, should give a consistent second law. Indeed, our expressions go over to the equilibrium (quasistatic) limit by construction, and taking the time derivative of the first order correction to the internal energy $E^{(1)}$, Eq. (3.51), shows (see App. B.3) that also the expressions for the first order corrections of particle number, internal energy, work, and heat satisfy the first law $\dot{E}^{(2)} = \dot{W}^{(2)} + \dot{Q}^{(2)} + \mu\,\dot{N}^{(2)}$.

As an additional check, we show in the following that the corrections to work, heat, and particle number exhibit the correct behavior under transformations between equilibrium points, corresponding to a path-independent change of internal energy and particle number. To this end, we consider a path between two points that essentially represent a system in equilibrium, namely the dot level ε_d moving from a position far below μ, where it is completely occupied, at time t_1 to a position far above μ, where it is completely empty, at time t_2. The change of the particle number associated with this transformation is thus path-independent, requiring that the non-equilibrium correction $\dot{N}^{(2)}$ in Eq. (3.48) vanishes when integrated along this path

$$\Delta N^{(2)} = \int_{t_1}^{t_2} dt \dot{N}^{(2)} = 0\,. \tag{3.53}$$

We show in App. B.5 that this is indeed the case. Furthermore, also the change in internal energy ΔE cannot depend on the path and must therefore be given by its adiabatic value, i.e., as an integral over time of $\dot{E}^{(1)}$ in Eq. (3.23). This must hold although the instantaneous value of $E = E^{(0)} + E^{(1)}$ is velocity dependent, cp., Eq. (3.51). Thus, the extra work exerted for moving the level along this path at finite speed needs to appear as additional heat given to the leads,

$$\int_{t_1}^{t_2} dt \dot{W}^{(2)} = -\int_{t_1}^{t_2} dt \dot{Q}^{(2)}\,. \tag{3.54}$$

We show in App. B.6 that this equality is indeed satisfied by the second order quantities Eqs. (3.49) and (3.52).

Entropy. In addition to the consistency checks discussed above, the non-equilibrium correction to the entropy should comply with the second law of thermodynamics. A consideration of this issue requires a proper definition of the non-equilibrium entropy. In Sec. 3.2 we showed that the equilibrium entropy S_0 of the extended resonant level (cp., Eq. (3.17)) is an integral over the energy resolved version of the Gibbs entropy of a single fermionic level with equilibrium occupation probability f. In order to extend this result to finite level speeds, we follow Esposito et al.,[Esposito et al., 2015b] and use Eq. (3.17) as an ansatz for the non-equilibrium entropy after replacing the equilibrium distribution f by its non-equilibrium counterpart ϕ given in Eq. (3.46),

$$S = \int \frac{d\varepsilon}{2\pi} A\left(-\phi \ln \phi - [1-\phi] \ln [1-\phi]\right)\,. \tag{3.55}$$

Note that in contrast to Esposito et al.,[Esposito et al., 2015b] we define the non-equilibrium entropy with the standard broadened spectral function $A(\varepsilon)$ of the

dot electrons. Consequently, our form of the non-equilibrium entropy smoothly connects to the equilibrium limit $S^{(0)}$ given in Eq. (3.17) above. Expanding Eq. (3.55) up to first order in $\dot{\varepsilon}_d$ leads to the form $S = S^{(0)} + S^{(1)}$, where $S^{(0)}$ is the equilibrium entropy Eq. (3.17) and $S^{(1)}$ is the first order correction,

$$S^{(1)} = \frac{-\dot{\varepsilon}_d}{2} \int \frac{d\varepsilon}{2\pi} \left(\frac{\varepsilon - \mu}{T} \right) \partial_\varepsilon f A^2 \,. \tag{3.56}$$

From Eq. (3.56) the correction to the entropy evolution (quadratic in the velocity) is given by

$$\dot{S}^{(2)} = \frac{\dot{\varepsilon}_d^2}{2T} \int \frac{d\varepsilon}{2\pi} \left(\varepsilon - \mu \right) \partial_\varepsilon f \, \partial_\varepsilon A^2 \,. \tag{3.57}$$

While the change of the equilibrium entropy $\dot{S}_0 = \dot{\varepsilon}_d \, \partial_{\varepsilon_d} S_0$ is solely given by the corresponding heat current, $\dot{Q}_0 = T\dot{S}_0$, the second order correction $\frac{dS}{dt}^{(2)}$ cannot be written only in terms of the heat current $\dot{Q}^{(2)}/T$ in Eq. (3.52). We identify the remaining entropy change as the entropy production $\dot{\mathcal{S}}^{(2)}$,

$$\frac{dS}{dt}^{(2)} = \frac{\dot{Q}}{T}^{(2)} + \dot{\mathcal{S}}^{(2)} \,. \tag{3.58}$$

The entropy production can be related to the dissipated power, Eq. (3.49),

$$\dot{\mathcal{S}}^{(2)} = \frac{\dot{W}^{(2)}}{T} \geq 0 \,. \tag{3.59}$$

Therefore the non-equilibrium entropy defined above obeys the second law of thermodynamics and the entropy production vanishes for quasistatic driving. Furthermore, the entropy production calculated for finite driving speeds is properly related to the dissipated power. We have thus found, for this model, a consistent extension of quantum thermodynamics to this non-equilibrium situation.

3.4 Classical limit

Here we show that the energy resolved thermodynamic quantities obtained above reduce to their classical equivalents in the limit $\Gamma \ll T$. Thus, the quantum thermodynamics framework developed here is consistent with the familiar classical limit in which the dot level is well described by a Pauli master equation. The latter takes the form of a rate equation for the occupation probability of the resonant level p,

$$\frac{dp}{dt} = -\Gamma \left[1 - f(\varepsilon_d) \right] p + \Gamma f(\varepsilon_d) \left[1 - p \right] \,. \tag{3.60}$$

We first consider the thermodynamic implications of this dynamics. To this end, we solve Eq. (3.60) to linear order in the velocity in terms of a static solution $f(\varepsilon_d)$ plus a velocity dependent correction,

$$p = N^{(0)} + N^{(1)} = f(\varepsilon_d) - \frac{\dot{\varepsilon}_d f'(\varepsilon_d)}{\Gamma} \,, \tag{3.61}$$

with $f'(\varepsilon_d) = \partial_\varepsilon f|_{\varepsilon_d}$. As in the strongly coupled quantum system considered above, the power that the external driving needs to provide is set by the dot occupation $\dot{W} = \dot{\varepsilon}_d N$. Eq. (3.61) then directly yields the power up to second order as $\dot{W}^{(1)} + \dot{W}^{(2)} = \dot{\varepsilon}_d p$. In this weak coupling case, the ε_d-dependent part of the thermodynamic properties of the overall system are well represented by those that are usually assigned to the dot itself. This leads directly to the classical internal energy, $E = \varepsilon_d N$, up to first order in the velocity

$$E^{(0)} + E^{(1)} = \varepsilon_d \left(f(\varepsilon_d) - \frac{\dot{\varepsilon}_d f'(\varepsilon_d)}{\Gamma} \right) , \tag{3.62}$$

and to the heat flux between the dot and its environment, $\dot{Q} = (\varepsilon_d - \mu)\, \dot{N}$, up to second order in the velocity

$$\dot{Q}^{(1)} + \dot{Q}^{(2)} = (\varepsilon_d - \mu) \left(\dot{\varepsilon}_d f'\left(\varepsilon_d\right) - \frac{\dot{\varepsilon}_d^2}{\Gamma} f''(\varepsilon_d) \right) . \tag{3.63}$$

Finally, the ε_d-dependent part of the entropy in this weak coupling limit is again given by the dot entropy itself. Assuming the latter is given by the Gibbs form

$$S = -\left(p \ln p + (1-p) \ln\left(1-p\right)\right) , \tag{3.64}$$

one obtains

$$\dot{S}^{(1)} = \frac{\dot{Q}^{(1)}}{T} \quad \text{and} \quad \dot{S}^{(2)} = \frac{\dot{Q}^{(2)}}{T} + \frac{\dot{W}^{(2)}}{T} , \tag{3.65}$$

where $\dot{W}^{(2)} = -\frac{\dot{\varepsilon}_d^2}{\Gamma} f'(\varepsilon_d)$.

This weak coupling thermodynamics can be directly reproduced from the thermodynamic quantities of the resonant level model derived in Secs. 3.2 and 3.3 by taking the limit $\Gamma \ll T$. In this limit, the spectral function A becomes strongly peaked around ε_d so that we can neglect the variation of the Fermi distribution within the broadened level and, in case the thermodynamic function contains the spectral function A to the first power, replace it by a δ-function, $A \to \delta(\varepsilon - \varepsilon_d)$. Expressions that contain higher powers of A have to be handled more carefully by performing the integral over the spectral functions explicitly. Thus, for example, Eq. (3.52) leads to

$$\begin{aligned} \dot{Q}^{(2)} &= -\int \frac{d\varepsilon}{2\pi} (\varepsilon - \mu) \frac{\dot{\varepsilon}_d^2}{2} \partial_\varepsilon^2 f\, A^2 \\ &\to -(\varepsilon_d - \mu) \frac{\dot{\varepsilon}_d^2}{2} f''(\varepsilon_d, \mu)\, \frac{2}{\Gamma} , \end{aligned} \tag{3.66}$$

which is identical to the quadratic contribution in Eq. (3.63). It is readily realized that the weak coupling limit of all the thermodynamic quantities in Secs. 3.2 and 3.3 are identical to the expressions Eqs. (3.61)-(3.65) derived form the rate equation (3.60).

3.5 Conclusion

We have developed a consistent non-equilibrium quantum thermodynamics of the driven resonant level model where the effects of the driving are evaluated within the framework of non-equilibrium Green's functions and the gradient expansion. Our construction is consistent with the first and second laws of thermodynamics and with particle conservation. The problem of taking proper account of the strong system-bath coupling was circumvented by considering the extended resonant level – the part of the overall system, or the 'world', that is affected by local changes in the level energy. The method developed here of representing these equilibrium thermodynamic functions by quasistatic expectation values of operators and subsequently extending the model to finite level speed with the help of the non-equilibrium Green's functions formalism can provide a guideline for future thermodynamic treatments of strongly coupled quantum systems. It should be kept in mind, however, that our model was restricted to a particular kind of driving – a time-dependent level energy – and our calculations were done in the wide band limit. Extending our treatment to more general situations may require further theoretical considerations, with some difficulties already pointed out in Ref. [Esposito et al., 2015a]. Another interesting problem is the inclusion of interactions of the dot electron with the electrons in the lead. Some thermodynamic properties have been been studied including these interactions, in particular the specific heat and susceptibility in the context of Kondo systems [Tsvelick and Wiegmann, 1983] and the ohmic two-state system.[Nghiem et al., 2016; Weiss, 2008] However, an inclusion of interactions into the full thermodynamic description of the driven level remains an open issue.

4 The extended resonant level model: Energy fluctuations and behavior beyond the wide band limit

In this chapter, we study the limitations of the approach developed above in Chapter 3. As discussed above, an interesting observation about this model is that when the metal is described in the wide band approximation, the ε_d-dependent part of the energy can be identified as the energy of an effective subsystem characterized by the Hamiltonian

$$H_{\text{eff}} = H_D + \frac{1}{2} H_V . \tag{4.1}$$

This observation was made for the average of the internal energy. It leaves open the question whether H_{eff} has an intrinsic fundamental meaning as the subsystem Hamiltonian, or is it only $\langle H_{\text{eff}} \rangle$ that happens to yield the ε_d-dependent part of the energy for this model. It is also interesting to explore the possibility that such a (not necessarily symmetric) splitting may lead to a consistent thermodynamic theory in more general situations. At first we study the equilibrium energy distribution of the extended resonant level and compare this with the predictions made with the symmetric splitting of the interaction term. We find that even in the simple case of a single resonant level interacting with a wide band bath, the effective system Hamiltonian describes only the average of the internal energy, but fails to recover higher moments of the equilibrium energy distribution. In a second step we show that beyond the wide band limit, any splitting of the coupling Hamiltonian already fails to reproduce the mean internal energy.

4.1 Fluctuations of the internal energy

We can compute the second moment of the energy distribution and therefore calculate the fluctuations with respect to its mean value, by introducing a rescaling parameter λ in the Hamiltonian

$$H(\lambda) = \lambda(H_D + H_V + H_B), \tag{4.2}$$

with the consequent rescaling of the partition function $\Xi(\lambda) = \mathrm{tr}\{e^{-\beta(\lambda H - \mu N)}\}$ and grand potential $\Omega(\lambda) = -\beta^{-1} \ln \Xi(\lambda)$. As illustrated in Appendix C.1, rescaling the Hamiltonian amounts to rescaling of the spectral function A of the dot electrons, which represents the ϵ_d-dependent part of the total density of states in the wide band limit, see Sec. 3.2.1. The energy fluctuation for the extended resonant level is obtained by differentiation of the grand potential

$$\langle H^2 \rangle - \langle H \rangle^2 = -\frac{1}{\beta} \frac{\partial^2}{\partial \lambda^2} \Omega \Big|_{\lambda=1}, \tag{4.3}$$

which can be computed with the help of the relation

$$\frac{\partial}{\partial \lambda} A = -\Gamma \frac{\partial}{\partial \varepsilon} \mathrm{Re} G^R - \varepsilon_d \frac{\partial}{\partial \varepsilon} A. \tag{4.4}$$

Taking into account only the ε_d-dependent part of the grand potential

$$\Omega = -T \int \frac{d\varepsilon}{2\pi} A(\varepsilon) \ln(1 + e^{-\beta(\varepsilon - \mu)}), \tag{4.5}$$

we obtain the variance of the internal energy of the extended resonant level model

$$\langle H^2 \rangle - \langle H \rangle^2 = \int \frac{d\varepsilon}{2\pi} \varepsilon^2 A(\varepsilon) f(\varepsilon)(1 - f(\varepsilon)). \tag{4.6}$$

In a similar fashion, one can determine the energy fluctuations for a subsystems associated with a part of the Hamiltonian. To this end we use the rescaled Hamiltonian

$$H(\lambda_D, \lambda_B, \lambda_V) = \lambda_D H_D + \lambda_B H_B + \lambda_V H_V. \tag{4.7}$$

This readily yields the different variances from the scaled grand potential

$$-\frac{1}{\beta} \frac{\partial^2}{\partial \lambda_i^2} \Omega \Big|_{\lambda \to 1} = \langle H_i^2 \rangle - \langle H_i \rangle^2. \tag{4.8}$$

The parameters in the spectral function of the dot electrons A

$$A(\varepsilon, \varepsilon_d, \Gamma) = \frac{\Gamma}{(\varepsilon - \varepsilon_d)^2 + (\Gamma/2)^2} \tag{4.9}$$

change accordingly, i.e. $A(\varepsilon, \varepsilon_d, \Gamma) \to A(\varepsilon, \lambda_D \varepsilon_d, \lambda_B^{-1}\lambda_V^2\Gamma)$ (see Appendix C.1). Direct computation yields

$$\frac{\partial}{\partial \lambda_D} A = -\varepsilon_d \frac{\partial}{\partial \varepsilon} A, \tag{4.10}$$

$$\frac{\partial}{\partial \lambda_B} A = \lambda_B^{-2}\lambda_V^2 \Gamma \frac{\partial}{\partial \varepsilon} \mathrm{Re} G^R, \tag{4.11}$$

$$\frac{\partial}{\partial \lambda_V} A = -2\lambda_B^{-1}\lambda_V \Gamma \frac{\partial}{\partial \varepsilon} \mathrm{Re} G^R. \tag{4.12}$$

As discussed above in Chapter 3, the average thermodynamic properties of the extended resonant level subsystem can be accounted for in this model by assigning to it the effective Hamiltonian H_{eff} defined in Eq. (4.1), corresponding to a symmetric splitting of the interaction Hamiltonian between system and environment. Next we check if fluctuations in the energy derived from H_{eff} are equivalent to those given by Eq. (4.6) as far as their dependence on ε_d is concerned. To this end, we adopt a rescaling of the form

$$H(\lambda_{\mathrm{eff}}, \lambda_B, \lambda_V') = \lambda_{\mathrm{eff}} H_{\mathrm{eff}} + \lambda_B H_B + (1/2)\lambda_V' H_V. \tag{4.13}$$

Comparing to the rescaling in Eq. (4.7), one finds that the parameters in the spectral function change as $A(\varepsilon, \varepsilon_d, \Gamma) \to A(\varepsilon, \lambda_{\mathrm{eff}}\varepsilon_d, \lambda_B^{-1}([\lambda_{\mathrm{eff}} + \lambda_V']/2)^2\Gamma)$, see Appendix C.1. In addition, we obtain from Eqs. (4.10)-(4.12) the following identity

$$\frac{\partial A}{\partial \lambda_{\mathrm{eff}}} = -\lambda_B^{-1}\Gamma \frac{(\lambda_{\mathrm{eff}} + \lambda_V')}{2} \frac{\partial}{\partial \varepsilon} \mathrm{Re} G^R - \varepsilon_d \frac{\partial A}{\partial \varepsilon}\,. \tag{4.14}$$

With Eq. (4.8), this yields the energy variance of the effective Hamiltonian

$$\langle (H_{\mathrm{eff}})^2 \rangle - \langle H_{\mathrm{eff}} \rangle^2 = \int \frac{d\varepsilon}{2\pi} \varepsilon^2 A(\varepsilon) f(\varepsilon)(1 - f(\varepsilon)) - \frac{1}{2\beta} \int \frac{d\varepsilon}{2\pi} (\varepsilon - \varepsilon_d) A(\varepsilon) f(\varepsilon). \tag{4.15}$$

If the Hamiltonian H_{eff} of Eq. (4.1) was a consistent choice for the extended resonant level Hamiltonian, the ε_d-dependence of Eqs. (4.6) and (4.15) (i.e. their derivatives with respect to ε_d) should have been the same. Writing the difference between the Eq. (4.6) and Eq. (4.15) as a function of the level energy

$$g_2(\varepsilon_d) = \frac{1}{2\beta} \int \frac{d\varepsilon}{2\pi} (\varepsilon - \varepsilon_d) A(\varepsilon) f(\varepsilon), \tag{4.16}$$

and calculating its derivative with respect to ε_d[1]

$$\frac{\partial g_2(\varepsilon_d)}{\partial \varepsilon_d} = \frac{1}{2} \int \frac{d\varepsilon}{2\pi} (\varepsilon_d - \varepsilon) A(\varepsilon) f(\varepsilon)(1 - f(\varepsilon)), \tag{4.17}$$

[1]The derivative is taken in order to focus on the part of this difference that is associated with the extended resonant level and to discard parts that are independent of ε_d and thus irrelevant for the description of the extended resonant level. The derivative would be zero if the presence of the dot had the same effect on the fluctuations described by Eqs. (4.6) and (4.15)

we find that the effective Hamiltonian H_{eff} predicts a different behavior in the fluctuations upon changes in local parameters of the extended resonant level.

The discrepancy between the thermodynamic energy distribution of the extended resonant level, as described by the grand potential Eq. (4.5), and the one of the effective Hamiltonian Eq. (4.1), appears also in higher moments of the energy distribution. For example, the dependence on ε_d of the third moment (skewness) for the extended resonant level can be calculated using the rescaling for the Hamiltonian in Eq. (4.2) and by differentiation respect to λ of the rescaled grand potential

$$\left\langle (H - \langle H \rangle)^3 \right\rangle = \frac{1}{\beta^2} \frac{\partial^3 \Omega}{\partial \lambda^3}\bigg|_{\lambda \to 1},$$

and in terms of the ε_d-dependent part of the grand potential in Eq. (4.5)

$$\left\langle (H - \langle H \rangle)^3 \right\rangle = \int \frac{d\varepsilon}{2\pi} \varepsilon^3 A(\varepsilon) f(\varepsilon)(1 - f(\varepsilon))(1 - 2f(\varepsilon)). \tag{4.18}$$

This result can be compared to that obtained from the third moment of the energy distribution associated with the effective dot Hamiltonian Eq. (4.1). The latter is obtained using the rescaling for the Hamiltonian in Eq. (4.13) and by differentiation respect to λ_{eff}

$$\begin{aligned} \left\langle \left(H_{\text{eff}} - \langle H_{\text{eff}} \rangle\right)^3 \right\rangle &= \frac{1}{\beta^2} \frac{\partial^3 \Omega}{\partial \lambda_{\text{eff}}^3}\bigg|_{\lambda \to 1} \\ &= \int \frac{d\varepsilon}{2\pi} \varepsilon^3 A(\varepsilon) f(\varepsilon)(1 - f(\varepsilon))(1 - 2f(\varepsilon)) \\ &\quad - \frac{3}{2\beta} \int \frac{d\varepsilon}{2\pi} \varepsilon(\varepsilon - \varepsilon_d) A(\varepsilon) f(\varepsilon)(1 - f(\varepsilon)). \end{aligned} \tag{4.19}$$

Once again, direct comparison between Eqs. (4.18) and (4.19) demonstrates that the effective Hamiltonian H_{eff} does not predict the energy distribution of the extended resonant level correctly. In fact, the difference $g_3(\varepsilon_d)$ of the third moment of the energy of the extended resonant level and the one of the effective Hamiltonian and its derivative respect to ε_d

$$g_3(\varepsilon) = \frac{3}{2\beta} \int \frac{d\varepsilon}{2\pi} \varepsilon(\varepsilon - \varepsilon_d) A(\varepsilon) f(\varepsilon)(1 - f(\varepsilon)) \tag{4.20}$$

$$\begin{aligned} \frac{\partial}{\partial \varepsilon_d} g_3(\varepsilon) =& \frac{3}{2\beta} \int \frac{d\varepsilon}{2\pi} (\varepsilon - \varepsilon_d) A(\varepsilon) f(\varepsilon)(1 - f(\varepsilon)) \\ & - \frac{3}{2} \int \frac{d\varepsilon}{2\pi} \varepsilon(\varepsilon - \varepsilon_d) A(\varepsilon) f(\varepsilon)(1 - f(\varepsilon))(1 - 2f(\varepsilon)), \end{aligned} \tag{4.21}$$

reveal that upon driving in the level energy, the ε_d-dependent part of the skewness is incorrectly predicted by H_{eff}.

4.2 Energy splitting beyond the wide band limit

The effective Hamiltonian in Eq. (4.1) was found above in Chapter 3 to correctly represent the dependence of the average system energy on ε_d in the wide band approximation. We now consider the extended resonant level model when this approximation regarding the bath is relaxed. In this case the retarded self energy of the dot electrons becomes a complex function of the energy, with a finite real part (Lamb shift Λ) and an energy-dependent imaginary part, which is the energy-dependent decay rate Γ. The ε_d-dependent part of the grand potential reads

$$\tilde{\Omega} = -\frac{1}{\beta}\int \frac{d\varepsilon}{2\pi}\rho_{\varepsilon_d}(\varepsilon)\ln(1+e^{-\beta(\varepsilon-\mu)})\,, \tag{4.22}$$

with $\rho_{\varepsilon_d}(\varepsilon)$

$$\rho_{\varepsilon_d}(\varepsilon) = \tilde{A}(\varepsilon)(1-\partial_\varepsilon\Lambda(\varepsilon)) - \mathrm{Re}G^R\partial_\varepsilon\Gamma(\varepsilon), \tag{4.23}$$

setting the form of the complete equilibrium thermodynamics of the extended resonant level, see Sec. 3.2.1. Here $\tilde{A}$ is the spectral function of the dot electrons beyond the wide band limit

$$\tilde{A}(\varepsilon) = \frac{\Gamma(\varepsilon)}{(\varepsilon-\varepsilon_d-\Lambda(\varepsilon))^2+(\Gamma(\varepsilon)/2)^2}\,. \tag{4.24}$$

In particular, the ε_d-dependent part of the internal energy E can be calculated from $\tilde{\Omega}$ as follows

$$E = \left(\frac{\partial}{\partial\beta} - \frac{\mu}{\beta}\frac{\partial}{\partial\mu}\right)\beta\tilde{\Omega} = \int\frac{d\varepsilon}{2\pi}\varepsilon\rho_{\varepsilon_d}(\varepsilon)f(\varepsilon)\,. \tag{4.25}$$

The important observation (see Appendix C.2)

$$\frac{\partial}{\partial\varepsilon_d}\rho_{\varepsilon_d}(\varepsilon) = -\frac{\partial}{\partial\varepsilon}\tilde{A}(\varepsilon), \tag{4.26}$$

has the consequence that the quasistatic work

$$dW = d\varepsilon_d\frac{\partial}{\partial\varepsilon_d}\tilde{\Omega} = d\varepsilon_d\int\frac{d\varepsilon}{2\pi}\tilde{A}(\varepsilon)f(\varepsilon), \tag{4.27}$$

connects correctly to the force experienced by external driving also beyond the wide band limit. That can be seen by considering that the time-dependent dot level is associated with some external coordinate, in which case the quasistatic work is the work done by the external coordinate against the quasistatic part of the adiabatic reaction forces generated by the coupling to the electronic system [Bode et al., 2011, 2012b].

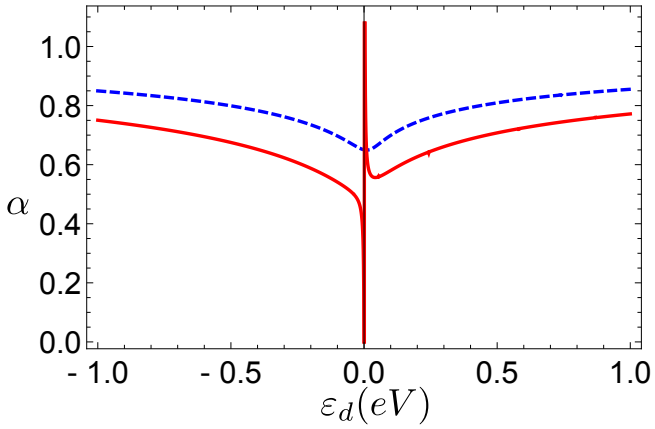

Figure 4.1: Splitting factors α_1 (blue, dashed) and α_2 (red, solid) defined in Eqs. (4.28) and (4.30) respectively, as a function of the energy level ε_d for a resonant level with Lorentizian decay rate Γ and the corresponding Lamb shift (Eqs. (4.33) and (4.34)). Parameters for this model are: $\Gamma_o = 0.1eV$, $\mu = 0$, $W = 0.5eV$, $E_B = 0.2eV$, $T = 10K$.

Next we address the question whether beyond the wide band limit a splitting of the interaction Hamiltonian between effective bath and effective system can properly account for the internal energy of the extended resonant level. If some consistent, not necessarily symmetric, splitting exists, then we can reproduce this energy as expectation value of the effective Hamiltonian $\langle H_D + \alpha_1 H_V\rangle = E$. Using Eq. (4.25) for E and solving for α_1 yields

$$\alpha_1 = \frac{\int \frac{d\varepsilon}{2\pi}\varepsilon\rho_{\varepsilon_d}(\varepsilon)f(\varepsilon) - \langle H_D\rangle}{\langle H_V\rangle}\,, \tag{4.28}$$

where the resulting α_1 should be constant (ε_d-independent). Alternatively, the validity of the splitting would be implied by a weaker criterion—that the dependence on ε_d of the averaged effective Hamiltonian and of E (Eq. (4.25)) are the same. This implies

$$\frac{\partial}{\partial\varepsilon_d}\langle H_D\rangle + \alpha_2\frac{\partial}{\partial\varepsilon_d}\langle H_V\rangle = \frac{\partial}{\partial\varepsilon_d}E. \tag{4.29}$$

This leads to

$$\alpha_2 = \frac{\frac{\partial}{\partial\varepsilon_d}\int \frac{d\varepsilon}{2\pi}\varepsilon\rho_{\varepsilon_d}(\varepsilon)f(\varepsilon) - \frac{\partial}{\partial\varepsilon_d}\langle H_D\rangle}{\frac{\partial}{\partial\varepsilon_d}\langle H_V\rangle}. \tag{4.30}$$

Note that the attempt to reproduce the quasistatic heat current leaving the extended resonant level via the energy flow into the effective bath $H_B + (1-\alpha_2)H_V$ leads to the same equation for α_2 Eq. (4.30). Again, if splitting works, the resulting α_2 would be a constant, independent of ε_d. The expectation values

of H_D and H_V can be either calculated from the grand potential $\tilde{\Omega}$ as described in Appendix C.2 and C.3 respectively, or directly by computing $\langle H_D \rangle$ and $\langle H_V \rangle$ within the Green function formalism. They take the form

$$\langle H_D \rangle = \varepsilon_d \int \frac{d\varepsilon}{2\pi} \tilde{A}(\varepsilon) f(\varepsilon), \tag{4.31}$$

$$\langle H_V \rangle = 2 \int \frac{d\varepsilon}{2\pi} (\varepsilon - \varepsilon_d) \tilde{A}(\varepsilon) f(\varepsilon). \tag{4.32}$$

In the wide band limit, $\rho_{\varepsilon_d}(\varepsilon) \to A(\varepsilon)$ and $\tilde{A}(\varepsilon) \to A(\varepsilon)$ leads to $\alpha_1 \to 1/2$ in Eq. (4.28), independent of local parameters. Figure 4.1 shows the splitting factors α_1 and α_2 calculated from Eqs. (4.28) and (4.30) plotted against ε_d, for a model with a Lorentzian form of the decay rate and the corresponding Lamb shift

$$\Gamma(\varepsilon) = \Gamma_o \frac{W^2}{W^2 + (\varepsilon - E_B)^2}, \tag{4.33}$$

$$\Lambda(\varepsilon) = \frac{\Gamma_o}{2} \frac{W(\varepsilon - E_B)}{W^2 + (\varepsilon - E_B)^2}, \tag{4.34}$$

where W and E_B are the width and the center of the band, respectively, and Γ_o is the decay rate at the center of the band. Clearly, the symmetric splitting fails to predict the ε_d-dependence of the system energy. Moreover, the fact that the calculated splitting parameters depend on the dot level ε_d implies that there does not exist a splitting factor that can be used to write an effective dot Hamiltonian in the general non-wide-band model.

4.3 Conclusion

For the resonant level model, splitting the system-bath interaction symmetrically and taking Eq. (4.1) to represent the system Hamiltonian has been useful in analyzing the average thermodynamic properties in the wide band approximation, as shown above in Chapter 3. The present analysis indicates that this symmetric splitting does not reflect any fundamental physics and fails when considering higher moments of the energy distribution even in the wide band limit. In particular, we observe that the width and the asymmetry of the distribution are not reproduced with the split Hamiltonian.

The equilibrium thermodynamics for the strongly coupled resonant level model can be extended to situations beyond the wide band limit based on the equilibrium grand potential as shown above. However, a simple representation of the internal energy of the extended resonant level in terms of the expectation value of an effective system Hamiltonian that splits the coupling Hamiltonian between system and bath does not generally exist. With that also an extension to finite velocity transformations with the help of the nonequilibrium Green's functions formalism, analogous to Chapter 3, is impossible. Hence the approach

developed above in Chapter 3 is strongly limited and does not provide a general tool to treat the thermodynamics of nanoelectronic machines.

5 Landauer-Büttiker approach to strongly coupled quantum thermodynamics and inside-outside duality of entropy evolution

We showed in Chapter 4 that the approach to strongly coupled thermodynamics developed in Chapter 3 is limited to the resonant level model in the wide band limit. To treat more general electronic nanomachines, we develop a new approach that is not afflicted by these limitations and instead provides full thermodynamic description, applicable to arbitrary non-interacting electron systems. This formalism is based on the Landauer-Büttiker theory of quantum transport and describes the evolution of the thermodynamic functions from an *outside* persepective. A key advantage of this approach is that it naturally avoids the system-bath distinction, the central problem in the Green's functions approach above and the strong coupling regime in general [Hänggi et al., 2008; Campisi et al., 2009; Hilt and Lutz, 2009; Esposito et al., 2010; Gallego et al., 2014; Strasberg et al., 2016; Perarnau-Llobet et al., 2016, 2017]. Moreover, it reproduces the results for the resonant level model presented above in Chapter 3.

To introduce the Landauer-Büttiker approach to strongly coupled quantum thermodynamics we at first take a step back: In an elementary thermodynamic transformation, an external agent performs work on a system by changing its Hamiltonian, constituting a single "stroke" of a quantum engine. For electronic nanomachines, this is achieved by changing the potential in a finite region which is coupled to electronic reservoirs. This type of machine can for instance be realized by a quantum dot connected to leads and subject to a time-dependent gate potential. If the gate potential is changed slowly, the coupling to the reservoir ensures thermal equilibrium at all times and the transformation occurs quasistatically. We assume that the total system consisting of dot and lead(s) is weakly coupled to an auxiliary bath, so that we can neglect the associated

coupling Hamiltonian in the description. This bath sets the temperature T and chemical potential μ of the system. Under quasistatic transformations, the density operator is at all times given by the grand-canonical equilibrium form

$$\rho_{eq} = \frac{\mathrm{e}^{-\beta(H-\mu N)}}{Z} \,, \tag{5.1}$$

where $\beta = T^{-1}$ and H is the total Hamiltonian of the system including dot and lead(s). The change of the von-Neumann entropy

$$\mathbf{S}[\rho] = -\mathrm{Tr}\left(\rho \ln \rho\right) \,, \tag{5.2}$$

associated with the equilibrium state of the system is proportional to the heat $dQ = T d\mathbf{S}$ released into the bath

$$d\mathbf{S}\left[\rho_t\right] = -\mathrm{Tr}\left(d\rho \ln \rho_{eq}\right) \tag{5.3}$$

$$= \frac{1}{T}\mathrm{Tr}\left(d\rho \left[\hat{H} - \mu N\right]\right) = \frac{dQ}{T} \tag{5.4}$$

where we used $\mathrm{Tr}\left(d\rho\right) = 0$. For a more extensive discussion of the connection between thermodynamics and quantum statistical mechanics we refer to the book by Balian [Balian, 2007].

This should be contrasted with the entropy evolution of a closed quantum system. Its purely unitary time evolution implies that the von-Neumann entropy remains unchanged at all times, since $\mathbf{S}$ is constant under any unitary dynamics, specifically under unitary dynamics determined by the von-Neumann equation, which describes the time evolution of closed systems

$$\frac{d\rho}{dt} = -i\left[H, \rho\right] \,. \tag{5.5}$$

This yields a vanishing time derivative of the associated von-Neumann entropy

$$\frac{d}{dt}\mathbf{S}[\rho] = \mathrm{Tr}\left(\frac{d\rho}{dt}\left(\ln \rho + 1\right)\right) \tag{5.6}$$

$$= i\mathrm{Tr}\left(H\left[\rho, \ln \rho\right]\right) \,, \tag{5.7}$$

since $\left[\rho, \ln \rho\right] = 0$.

Here we want to discuss the entropy evolution of simple electronic nanomachines, which combine fully coherent quantum dynamics with contact to baths and can involve strong coupling between system and reservoir. In this problem, quantum effects such as coherences, hybridization, and entanglement are expected to become important.

Such electronic nanomachines effectively constitute setups of mesoscopic physics which are elegantly described by the Landauer-Büttiker formalism. This framework combines coupling to equilibrium reservoirs and fully coherent quantum

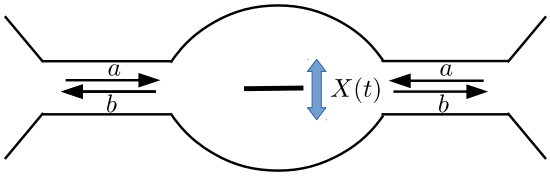

Figure 5.1: The scattering potential in the central region, e.g. a quantum dot, gets slowly changed by an external parameter $X(t)$. This leads to a net heat and entropy current in the leads, which are subject of this paper.

dynamics. One considers a scattering region connected to ideal leads, as depicted in Fig. 5.1, where non-interacting electrons propagate freely and under fully coherent quantum dynamics. Relaxation is accounted for by connecting the leads to electronic reservoirs at well defined temperatures and chemical potentials, which determine the distribution of incident electrons. This allows one to calculate quantities such as energy or particle currents in the leads by accounting for in- and outgoing electrons. With energy and particle conservation, these currents permit one to deduce the change of energy and particle number in the scattering region from an *outside perspective,* while above in Chapter 3, we described the thermodynamic transformations of the system from an *inside perspective*, i.e., in terms of the thermodynamic variables of the single level. Since the von-Neumann entropy $\mathbf{S}$ is conserved under coherent unitary dynamics, also the change of entropy in the scattering region can also be inferred from the entropy currents carried by the scattered electrons. The subsequent relaxation processes in the bath are complicated and require electron-electron interactions. This relaxation, however, is external to the Landauer-Büttiker formalism: The reservoirs are macroscopic and retain their equilibrium distribution, such that excitations entering a reservoir never return.

In the past the Landauer-Büttiker approach has been used intensively to study, among others, electron pumping [Brouwer, 1998], heat transport and current noise [Büttiker, 1992; Moskalets and Büttiker, 2002, 2004a; Avron et al., 2001], and entanglement creation [Beenakker et al., 2003; Samuelsson et al., 2004]. Here we extend the formalism to describe the entropy evolution generated by time-dependent potentials. In an adiabatic expansion around the quasistatic equilibrium it provides a detailed understanding of the connection between entropy and heat currents. Combined with the forces experienced by the driving [Bode et al., 2011, 2012b; Thomas et al., 2012], which determine the work, this provides a full thermodynamic description from an *outside* perspective.

In the following technical section we introduce the Landauer-Büttiker formalism, which can be skipped by readers familiar with it.

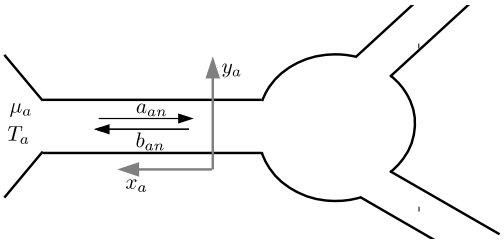

Figure 5.2: The scattering setup: a scattering region is attached to one or several ideal leads, which are connected to equilibrium reservoirs.

5.1 Technical section: introduction to scattering theory

We briefly introduce the most important aspects of scattering theory needed for the present work. Since a derivation of all the needed properties is beyond the scope of this thesis, we refer the interested reader to the work of Büttiker, e.g. Ref. [Büttiker, 1992], and the book by Moskalets [Moskalets, 2012].

We consider a scattering region in contact to ideal leads, in which the electrons can propagate freely and fully phase coherent. The leads are moreover connected to macroscopic equilibrium reservoirs, which set the distribution of the incoming electrons. The motion in the leads is unbound in longitudinal and confined in transverse direction, such that far away from the scatterer the wave function of a scattering state m in lead a is given by a plane wave in longitudinal direction x_a and a transverse wave function function $\phi_m(\mathbf{y}_a)$ in the orthogonal directions $\mathbf{y}_a$, see Fig. 5.2. The different transverse wave functions describe different scattering channels. Therefore, the wave function in channel m and lead a reads far away from the scatterer

$$\psi_{am}^{in(out)}(\epsilon, \mathbf{r}) = \frac{1}{\sqrt{v(\epsilon)}} \mathrm{e}^{\mp i k_{am}(\epsilon) x_a} \phi_m(\mathbf{y}_a)\,, \tag{5.8}$$

where $v_{am}(\epsilon) = \partial\epsilon/\partial k_{am} = k_{am}(\epsilon)/m$ is the group velocity. The corresponding eigenenergies are

$$\epsilon = \epsilon_{am} + \frac{k^2}{2m}\,, \tag{5.9}$$

where ϵ_{am} is the eigenenergy of the transverse wave function, which sets the threshold energy needed to populate the scattering channel. The longitudinal wavevector $k_{am}(\epsilon)$ is fixed by the total energy of the scattering state $k_{am}(\epsilon) = 2m\sqrt{\epsilon - \epsilon_{am}}$. We normalize the states to carry unit flux in the longitudinal direction, from which follows directly the orthogonality relation

$$\langle \psi_{an}^{in}(\epsilon') | \psi_{bm}^{in}(\epsilon) \rangle = 2\pi\delta(E - E')\delta_{ab}\delta_{mn}\,. \tag{5.10}$$

An incident wave typically causes reflected waves in all channels n of lead a, and and transmitted waves in all channels of all other attached leads. Introducing the operators a (b) that annihilate an electron in the incoming (outgoing) channel, we can write the fermionic field operators as

$$\hat{\psi}(\mathbf{r},t) = \sum_{am} \int \frac{d\epsilon}{2\pi} \left[\psi^{in}_{am}(\epsilon,\mathbf{r}) \hat{a}_{am}(\epsilon) + \psi^{out}_{am}(\epsilon,\mathbf{r}) \hat{b}_{am}(\epsilon) \right] e^{-i\epsilon t} \,, \tag{5.11}$$

with the anti-commutation relations

$$\left\{ a^\dagger_{am}(\epsilon), a_{bn}(\epsilon') \right\} = \left\{ b^\dagger_{am}(\epsilon), b_{bn}(\epsilon') \right\} = 2\pi \delta_{ab} \delta_{mn} \delta(\epsilon - \epsilon') \,. \tag{5.12}$$

While the reservoirs determine the distribution of the incoming uncorrelated equilibrium channels

$$\langle a^\dagger_{am}(\epsilon) a_{bn}(\epsilon') \rangle = \delta_{ab} \delta_{mn} f_a(\epsilon) 2\pi \delta(\epsilon - \epsilon') \,, \tag{5.13}$$

the subsequent scattering event mixes incoming states and thereby redistributes the electrons between the outgoing scattering channels. This is captured by the exact scattering matrix of the time-dependent problem $\mathcal{S}$

$$\begin{pmatrix} b_{11}(\epsilon) \\ ... \\ b_{Nn}(\epsilon) \end{pmatrix} = \int \frac{d\epsilon'}{2\pi} \mathcal{S}(\epsilon,\epsilon') \begin{pmatrix} a_{11}(\epsilon') \\ ... \\ a_{Nn}(\epsilon') \end{pmatrix} . \tag{5.14}$$

On this basis we derive the particle current in the lead, to investigate the currents generated in the scattering event. The general form of the current density operator follows immediately from the continuity of the equation of the particle density

$$\partial_t \left(\hat{\psi}^\dagger \hat{\psi} \right) + \nabla \cdot \mathbf{j} = 0 \,. \tag{5.15}$$

With the Heisenberg equation of motion this yields

$$\partial_t \left(\hat{\psi}^\dagger \hat{\psi} \right) = \frac{1}{i} \left[\hat{\psi}^\dagger H \hat{\psi} - H \hat{\psi}^\dagger \hat{\psi} \right] \tag{5.16}$$

$$= \nabla \left(\frac{-1}{2mi} \left[\hat{\psi}^\dagger \nabla \hat{\psi} - \nabla \hat{\psi}^\dagger \hat{\psi} \right] \right) . \tag{5.17}$$

Hence, the current operator takes the form

$$\hat{\mathbf{j}} = \frac{1}{2mi} \left[\psi^\dagger \nabla \psi - \nabla \psi^\dagger \psi \right] \,. \tag{5.18}$$

Using the fermionic field operator in terms of in- and outgoing scattering states in Eq. 5.11, we can calculate the particle current operator $\hat{I}^N_a = \int d\mathbf{y}_a \, \hat{j}_{x_a}(\epsilon,\mathbf{r})$

through any cross-section of lead a far away from the scatterer. Since the transverse wave functions are orthonormal $\int d\mathbf{y}\phi_m(y)\phi_n^*(y) = \delta_{mn}$, only operators of the same scattering channel contribute and we obtain

$$\hat{I}_a^N(t,x_a) = \frac{1}{2mi}\sum_m \int\int \frac{d\epsilon_1}{2\pi}\frac{d\epsilon_2}{2\pi}\frac{\mathrm{e}^{i(\epsilon_1-\epsilon_2)t}}{\sqrt{v_{am}(\epsilon_1)v_{am}(\epsilon_2)}}\int dy_a^2|\phi_m(y_a)|^2$$
$$\times\left\{\partial_x\left[a_{am}^\dagger(\epsilon_1)\mathrm{e}^{-ik_{am}(\epsilon_1)x_a}+b_{am}^\dagger(\epsilon_1)\mathrm{e}^{ik_{am}(\epsilon_1)x_a}\right]\left(a_{am}(\epsilon_2)\mathrm{e}^{ik_{am}(\epsilon_2)x_a}+b_{am}(\epsilon_2)\mathrm{e}^{-ik_{am}(\epsilon_2)x_a}\right)\right.$$
$$\left.-\left[a_{am}^\dagger(\epsilon_1)\mathrm{e}^{-ik_{am}(\epsilon_1)x_a}+b_{am}^\dagger(\epsilon_1)\mathrm{e}^{ik_{am}(\epsilon_1)x_a}\right]\partial_x\left(a_{am}(\epsilon_2)\mathrm{e}^{ik_{am}(\epsilon_2)x_a}+b_{am}(\epsilon_2)\mathrm{e}^{-ik_{am}(\epsilon_2)x_a}\right)\right\}.$$

With this at hand, we calculate the expectation value of the current in lead a. Assuming a slowly changing scattering potential and small bias voltages, the contributing energies are restricted to $|\epsilon_1-\epsilon_2| \ll \epsilon_1 \sim E_F$, where E_F is the Fermi energy. Under this condition, we can approximate $v_{am}(\epsilon_1)\approx v_{am}(\epsilon_2)$ and $k_{am}(\epsilon_1)\approx k_{am}(\epsilon_2)$[1], which yields the current

$$\langle\hat{I}_a^N(t,x)\rangle = \sum_m\int\int\frac{d\epsilon_1}{2\pi}\frac{d\epsilon_2}{2\pi}\,\mathrm{e}^{i(\epsilon_1-\epsilon_2)t}\,\langle b_{am}^\dagger(\epsilon_1)b_{am}(\epsilon_2)-a_{am}^\dagger(\epsilon_1)a_{am}(\epsilon_2)\rangle\ , \tag{5.19}$$

where we used $v_{am}(\epsilon_1) = k_{am}(\epsilon_1)/m$.

To make use of the assumption of a slowly changing potential, we write the current in the Wigner representation by going to sum and difference energies $\tilde{\epsilon} = \epsilon_2-\epsilon_1$ and $\epsilon = (\epsilon_1+\epsilon_2)/2$, which leads to the particle current

$$\begin{aligned} I_a^N(t) = \langle\hat{I}_a(t,x)\rangle &= \sum_{\alpha\in a}\int\int\frac{d\epsilon}{2\pi}\frac{d\tilde{\epsilon}}{2\pi}\,\mathrm{e}^{-i\tilde{\epsilon}t}\,\langle b_\alpha^\dagger(\epsilon-\frac{\tilde{\epsilon}}{2})b_\alpha(\epsilon+\frac{\tilde{\epsilon}}{2})-a_\alpha^\dagger(\epsilon-\frac{\tilde{\epsilon}}{2})a_\alpha(\epsilon+\frac{\tilde{\epsilon}}{2})\rangle \\ &= \sum_{\alpha\in a}\int\frac{d\epsilon}{2\pi}\left[\phi_{\alpha\alpha}^{out}(\epsilon,t)-\phi_{\alpha\alpha}^{in}(\epsilon,t)\right]\ , \end{aligned} \tag{5.20}$$

where we combined channel and lead index for notational simplicity, so that the sum goes over all scattering channels in lead a. The distribution matrix ϕ is a Wigner transform

$$\phi_{\alpha\beta}^{out}(t,\epsilon) = \int\frac{d\tilde{\epsilon}}{2\pi}e^{-i\tilde{\epsilon}t}\,\langle b_\beta^\dagger\left(\epsilon-\frac{\tilde{\epsilon}}{2}\right)b_\alpha\left(\epsilon+\frac{\tilde{\epsilon}}{2}\right)\rangle\ , \tag{5.21}$$

which can be expanded in powers of velocity, analogous to the lesser Green's function above in Sec. 3.3.1.

[1] With $\epsilon_1-\epsilon_2=\omega$, the corrections from the wavevector mismatch are of order ω/v_F, while the pre-factor $v(\epsilon_2)^{-1/2}$ gives corrections of order ω/E_F.

The same procedure can be repeated for the energy current. Using that the scattering states are free states deep in the lead (up to the constant threshold energy needed to populate the channel), we can use the kinetic energy density

$$\hat{\epsilon}_{kin} = \psi^\dagger(\mathbf{r}) \left(-\frac{1}{2m} \nabla^2 \right) \psi(\mathbf{r}) \tag{5.22}$$

to derive the energy current density from a continuity equation with the same steps as above

$$\hat{\mathbf{j}}^E = \frac{-1}{i\,(2m)^2} \left[\psi^\dagger \nabla^3 \psi - \nabla \psi^\dagger \nabla^3 \psi \right] . \tag{5.23}$$

Using the same approximations as above this yields the energy current through lead a

$$I_a^E(t) = \langle \hat{I}_\alpha^E(t,x) \rangle = \sum_{\alpha \in a} \int \frac{d\epsilon}{2\pi} \epsilon \left[\phi_{\alpha\alpha}^{out}(\epsilon,t) - \phi_{\alpha\alpha}^{in}(\epsilon,t) \right] . \tag{5.24}$$

With this we have everything at hand to calculate the heat current in the leads induced by the time-dependent scattering potential and to connect it to the entropy carried by the scattering states.

5.2 Entropy current carried by scattering states

The heat current $I_a^Q = I_a^E - \mu_a I_a^N$ carried by the electrons in lead a is the combination of particle current I_a^N into the corresponding reservoir with chemical potential μ_a and the energy current I_a^E. Thus, with Eqs. (5.20) and (5.24), we can express the total heat current in terms of the diagonal elements of the distribution matrix, i.e. the slowly changing occupations of the scattering channels

$$I_{tot}^Q(t) = \int_{-\infty}^{\infty} \frac{d\epsilon}{2\pi} (\epsilon - \mu) \mathrm{tr}_c \left\{ \phi^{out}(t,\epsilon) - \phi^{in}(\epsilon) \right\} , \tag{5.25}$$

where the trace runs over channel and lead space. Here, for simplicity we assume the same chemical potential μ in all reservoirs.

In quasistatic equilibrium the heat Q and entropy $\mathbf{S}$ are directly connected via $dQ = T d\mathbf{S}$, which implies the same relation for the associated currents carried by the scattering states

$$I^{S(1)} = \frac{I^{Q(1)}}{T} , \tag{5.26}$$

where the superscripts counts the order of velocity and quasistatic currents are of first order. However, in general out-of-equilibrium situations this is not

necessarily the case. In terms of the thermodynamic changes of a subsystem, the second law states that the entropy change of the subsystem is greater than the heat absorbed from the reservoir $\dot{\mathbf{S}} \geq \dot{Q}/T$, marking the onset of dissipation and irreversibility. This suggests also a deviation in the relation between entropy and heat *currents* carried by the scattering states from the relation $I^Q = T\, I^S$. However, in the quasistatic limit the developed entropy current needs to go back to the known equilibrium form Eq. 5.26.

To obtain the general entropy current, we begin by considering the entropy of a single incoming channel. For a given energy the channel can be either occupied or empty, according to $f_\alpha(\epsilon)$, and contributes with

$$\sigma\left[f_\alpha(\epsilon)\right] = -f_\alpha(\epsilon)\ln\left[f_\alpha(\epsilon)\right] - (1-f_\alpha(\epsilon))\ln\left[1-f_\alpha(\epsilon)\right] \tag{5.27}$$

to the system entropy. By analogy with the particle current, Eq. (5.20), we write the incoming entropy current as

$$I_\alpha^{S\,\mathrm{in}} = \int_{-\infty}^{\infty} \frac{d\epsilon}{2\pi}\,\sigma\left[f_\alpha(\epsilon)\right]\,. \tag{5.28}$$

Hence, as expected [Pendry, 1983], each of the incoming channels carries an entropy current of $\pi T/6$ towards the scattering region.

Scattering redistributes the electrons between the outgoing channels, thereby modifying the entropy flow into the leads. The scattering-induced correlations between outgoing scattering states [Moskalets and Büttiker, 2002, 2004a] are encoded in the non-diagonal distribution matrix $\phi^{\mathrm{out}}_{\alpha\beta}(t,\epsilon)$ for the outgoing electrons. As we show below, the natural extension of Eq. (5.28) reads

$$I^{S\,\mathrm{in(out)}}(t) = \int_{-\infty}^{\infty} \frac{d\epsilon}{2\pi}\,\mathrm{tr}_c\left\{\sigma[\phi^{\mathrm{in(out)}}(t,\epsilon)]\right\}\,. \tag{5.29}$$

Here σ Eq. (5.27)is a matrix-valued function of the distribution matrix $\phi^{\mathrm{in(out)}}$ and thereby depends on its off-diagonal elements.

To motivate Eq. (5.29) we derive the non-interacting fermionic density matrix for a given distribution matrix $\bar{\phi}_{\alpha\beta} = \mathrm{Tr}[\rho c^\dagger_\beta c_\alpha]$. In the scattering setup the incoming operators describe particles of an equilibrium reservoir and the outgoing operators are linear functions of the incoming ones, cf. Eq. (5.14). Hence, all averages can be calculated via Wick's theorem and the single-particle correlations described by ϕ fully determine all expectation values.

Our derivation exploits the maximum entropy principle that yields the most general density matrix given certain single-particle correlations [Jaynes, 1957]. (We obtain the same result following the approach of Ref. [Peschel, 2003].) The Lagrangian for maximizing the von-Neumann entropy under the constraints $\mathrm{Tr}\rho = 1$ and $\bar{\phi}_{\alpha\beta} = \mathrm{Tr}[\rho c^\dagger_\beta c_\alpha]$ reads

$$\begin{aligned}\mathcal{L} = &-\mathrm{Tr}\left[\rho\ln\rho\right] + \sum_{\alpha\beta}\lambda_{\alpha\beta}\left(\mathrm{Tr}\left[\rho c^\dagger_\beta c_\alpha\right] - \bar{\phi}_{\alpha\beta}\right)\\ &-\gamma\left(\mathrm{Tr}\rho - 1\right)\,,\end{aligned} \tag{5.30}$$

where Tr denotes the many-particle trace over all possible occupations and γ as well as the λ's are Lagrange multipliers. It is convenient to diagonalize the Hermitian matrix $\bar{\phi}$ and introduce a rotated basis, namely

$$\bar{\phi} = U\Lambda U^\dagger \quad \text{and} \quad c_\alpha = \sum_c U_{\alpha c} d_c \,, \tag{5.31}$$

where U is a unitary matrix and $\Lambda_{\alpha\beta} = \Lambda_\alpha \delta_{\alpha\beta}$ is diagonal containing the real eigenvalues of $\bar{\phi}$. In the rotated basis the Lagrangian $\mathcal{L}$ allows us to maximize the von-Neumann entropy with the given constraints. This yields the density matrix

$$\rho = \prod_\alpha (1 - \Lambda_\alpha) \left(\frac{\Lambda_\alpha}{1 - \Lambda_\alpha} \right)^{\hat{n}_\alpha} \,, \tag{5.32}$$

where $\hat{n}_\alpha$ is the occupation of mode α in the rotated basis. We calculate the entropy $\boldsymbol{S}$ of this density matrix by summing over all possible occupations in the rotated basis,

$$\boldsymbol{S} = \sum_\alpha \sigma[\Lambda_\alpha] = \mathrm{tr}\left(\sigma[\Lambda]\right) \,, \tag{5.33}$$

where the sum over the diagonal elements of Λ is included through the single-particle trace tr. Finally, rotating back to the original basis, $\Lambda = U^\dagger \bar{\phi} U$, we find the entropy in terms of the distribution matrix $\bar{\phi}$,

$$\boldsymbol{S} = \mathrm{tr}\left(\sigma[\bar{\phi}]\right) \,. \tag{5.34}$$

For a slowly changing scattering potential, we associate the entropy with the time-dependent distribution matrix $\phi_{\alpha\beta}(t, \epsilon)$ of the scattering states in Eq. (5.21), for which the single-particle trace represents an integral over energy and a trace tr_c over channel and lead indices.

By combing in- and outgoing entropy currents we write the total entropy current into the leads as

$$I^S_{\mathrm{tot}}(t) = \int_{-\infty}^{\infty} \frac{d\epsilon}{2\pi} \, \mathrm{tr}_c \left\{ \sigma[\phi^{\mathrm{out}}(t, \epsilon)] - \sigma[\phi^{\mathrm{in}}(\epsilon)] \right\} \,. \tag{5.35}$$

In the case of a static scatterer between two biased reservoirs at zero temperature, the entropy current can be used to quantify the entanglement of outgoing electron-hole pairs created in a tunneling event. Indeed, we verify that an immediate generalization of Eq. (5.35) reproduces the quantum mutual information between outgoing scattering channels on the left and right as obtained in Ref. [Beenakker et al., 2003]. This we show explicitly in the following interlude.

5.3 Interlude: Entanglement creation and entropy current

The developed form of the entropy current carried by the scattering states allows us to quantify the the correlations between different scattering channels created

in the scattering event. If we regard the case of two attached leads (L and R), we can measure the correlations created by the scattering event in terms of the quantum mutual information between outgoing channels to the left and right

$$\mathcal{I}(L:R) = \boldsymbol{S}_L + \boldsymbol{S}_R - \boldsymbol{S}_{\rm tot}\,, \tag{5.36}$$

where $\boldsymbol{S}_{L/R}$ is the von-Neumann entropy of the reduced density matrix of the left (right) lead and $\boldsymbol{S}_{\rm tot}$ is the total entropy of the outgoing states, including correlations between L and R. In the case of a pure state of the composite system $S_{\rm tot} = 0$, and $\mathcal{I}(L:R)$ reduces to twice the entanglement entropy $\mathcal{F} = S_L = S_R$ created in the scattering event.

The reduced density matrix and the corresponding entropy of the outgoing states in the left and right lead can be obtained by a method developed by Peschel [Peschel, 2003, 2012], which takes the form of the argument presented in the main text above, but confined to the subspace of interest. This results in the entropy of the reduced density matrix of subsystem A

$$\boldsymbol{S}_A = {\rm tr}_c\left(\sigma[\phi^A]\right)\,. \tag{5.37}$$

where ϕ^A is the submatrix of the full distribution matrix ϕ, defined on subspace A only. Applied to outgoing scattering states analogous to the derivation in the main text, we obtain from Eq. (5.36) a mutual information current

$$I^{MI} = I^S_{{\rm red},L} + I^S_{{\rm red},R} - I^{S,{\rm out}}_{\rm tot}\,, \tag{5.38}$$

as a measure of the correlations created per unit time. Here

$$I^{S,{\rm out}}_{\rm tot} = \int_{-\infty}^{\infty}\frac{d\epsilon}{2\pi}\,{\rm tr}_c\left\{\sigma[\phi^{\rm out}(t,\epsilon)]\right\}\,, \tag{5.39}$$

is the outgoing component of the total entropy current Eq. (5.35). The entropy current corresponding to the reduced density matrix of the electrons in the left (right) lead $I^S_{{\rm red},L(R)}$ takes the form

$$I^S_{{\rm red},L(R)} = \int_{-\infty}^{\infty}\frac{d\epsilon}{2\pi}\,{\rm tr}_c\left\{\sigma[\phi^{{\rm out},L(R)}(t,\epsilon)]\right\}\,, \tag{5.40}$$

with $\phi^{{\rm out},L(R)}$ being the submatrix of the distribution matrix $\phi^{\rm out}$ defined on the left (right) subspace only.

The simplest case to which we can apply this developed formalism is the case of a static scatterer between two reservoirs at zero temperature with an applied bias voltage, which was investigated as a device to create entangled electron-hole pairs in Ref. [Beenakker et al., 2003]. Considering two channels on each side (the authors of Ref. [Beenakker et al., 2003] consider a quantum Hall setup, in which the two channels can either represent two spin channels within the same Landau level or two different Landau levels), the scattering matrix,

$$S = \begin{pmatrix} r & t' \\ t & r' \end{pmatrix}\,, \tag{5.41}$$

is a 4×4 matrix, with the 2×2 submatrices r,r', t, t' describing the reflection and transmission from the left or right respectively. Here we neglect the energy dependence of the scattering matrix in the bias window and drop the energy labels for better readability.

For a static scatterer, the outgoing distribution matrix can be obtained by a simplified version of Eq. (D.6)

$$\phi^{\text{out}}(\epsilon) = S\,\phi^{\text{in}}(\epsilon)\,S^{\dagger}\,. \tag{5.42}$$

Hence in the static case ϕ^{out} is obtained from ϕ^{in} by a unitary transformation given by the frozen scattering matrix S. At zero temperature, the incoming electrons are either fully occupied or empty at each energy $f_L = \Theta(\mu + eV - \epsilon)$ and $f_R = \Theta(\mu - \epsilon)$, and hence carry no entropy

$$I^{S\,\text{in}}_{\text{tot}} = \int_{-\infty}^{\infty} \frac{d\epsilon}{2\pi}\,\text{tr}_c\left\{\sigma[\phi^{\text{in}}(\epsilon)]\right\} = 0\,. \tag{5.43}$$

ϕ^{out} in Eq. (5.42) then shows that full outgoing entropy current also vanishes

$$I^{S\,\text{out}}_{\text{tot}} = \int_{-\infty}^{\infty} \frac{d\epsilon}{2\pi}\,\text{tr}_c\left\{\sigma[\phi^{\text{out}}(\epsilon)]\right\} = 0\,, \tag{5.44}$$

since the unitary transformation with the frozen scattering matrix leaves the incoming pure states pure at each energy.

For the reduced entropy currents we calculate the outgoing distribution matrix from Eq. (5.42)

$$\phi^{\text{out}} = \Theta(\mu - \epsilon)\hat{I} + \Theta(\mu + eV - \epsilon)\Theta(\epsilon - \mu)\varrho\,, \tag{5.45}$$

with

$$\varrho = \begin{pmatrix} rr^{\dagger} & rt^{\dagger} \\ tr^{\dagger} & tt^{\dagger} \end{pmatrix}. \tag{5.46}$$

Inserting ϕ^{out} into the mutual information current Eq. (5.38) leads to

$$\begin{aligned} I^{MI} &= \frac{eV}{2\pi}\text{tr}_c\sigma\left[rr^{\dagger}\right] + \frac{eV}{2\pi}\text{tr}_c\sigma\left[tt^{\dagger}\right] && (5.47)\\ &= 2\frac{eV}{2\pi}\text{tr}_c\sigma\left[tt^{\dagger}\right] && (5.48)\\ &= 2\frac{eV}{2\pi}\left(\sigma(T_1) + \sigma(T_2)\right)\,, && (5.49) \end{aligned}$$

where $T_1, T_2 \in (0,1)$ are the eigenvalues of the transmission matrix product $t^{\dagger}t = \hat{I} - r^{\dagger}r$, which reproduces the entanglement entropy or entanglement of formation $\mathcal{F} = I^{MI}/2$ calculated in Ref. [Beenakker et al., 2003].

5.4 Entropy current induced by a dynamic scatterer

The entropy and heat currents generated by a slowly changing scattering potential $V[X(t)]$ are obtained by expanding the scattering matrix and the outgoing distribution matrix about the frozen configuration in powers of the velocity $\dot{X}$ [Bode et al., 2011, 2012b; Thomas et al., 2012, 2015]. Up to first order, the Wigner transform of the scattering matrix can be expressed in terms of the frozen scattering matrix S and its first order correction A, $\mathcal{S}(\epsilon, t) = S + \dot{X}A$. This expansion is well motivated in the regime where $X(t)$ changes on a characteristic time scale much longer than the electronic dwell time in the scattering region. Accordingly, we write ϕ^{out} as

$$\phi^{\text{out}} \simeq \hat{I}\, f + \phi^{\text{out}(1)} + \phi^{\text{out}(2)}\,, \tag{5.50}$$

where $\hat{I}$ is a unit matrix in channel and lead space and the superscript stands for the order in $\dot{X}$. (We omit time and energy labels for better readability.) Similarly, we expand $\sigma[\phi^{\text{out}}(\epsilon)]$ up to second order about the uncorrelated equilibrium

$$\begin{aligned}\sigma[\phi^{\text{out}}] \simeq \hat{I}\sigma\,[f] + \hat{I}\frac{d\sigma\,[f]}{df}\left(\phi^{\text{out}(1)} + \phi^{\text{out}(2)}\right) \\ + \frac{1}{2}\hat{I}\,\frac{d^2\sigma\,[f]}{df^2}\left(\phi^{\text{out}(1)}\right)^2\,.\end{aligned} \tag{5.51}$$

Note that the second order contribution proportional to $d^2\sigma\,[f]\,/df^2 = (T\partial_\epsilon f)^{-1}$ is always negative due to the concavity of σ. By inserting the above expression in Eq. (5.35) we obtain

$$\begin{aligned}I^S_{\text{tot}} = \int_{-\infty}^{\infty}\frac{d\epsilon}{2\pi}\,\text{tr}_c\Big\{\frac{\epsilon-\mu}{T}\left(\phi^{\text{out}(1)} + \phi^{\text{out}(2)}\right) \\ + \frac{1}{2T\partial_\epsilon f}\left(\phi^{\text{out}(1)}\right)^2\Big\}\,,\end{aligned} \tag{5.52}$$

where we have used that $\phi^{\text{in}} = \hat{I}\, f(\epsilon)$. By the same token, Eqs. (5.25) and (5.50) give

$$I^Q_{\text{tot}} = \int_{-\infty}^{\infty}\frac{d\epsilon}{2\pi}(\epsilon-\mu)\,\text{tr}_c\Big\{\phi^{\text{out}(1)} + \phi^{\text{out}(2)}\Big\}\,. \tag{5.53}$$

These expressions nicely elucidate the connection between heat and entropy currents, and the departure from $dQ = Td\boldsymbol{S}$ beyond the quasistatic limit. At first order in $\dot{X}$, corresponding to the quasistatic regime, the entropy current is entirely given by the heat current over temperature $I^{S(1)}_{\text{tot}} = I^{Q(1)}_{\text{tot}}/T$, i.e., the proposed form of the entropy current correctly connects to the quasistatic equilibrium. In contrast, at second order an additional negative correction appears

$$I^{S(2)}_{\text{tot}} = \frac{I^{Q(2)}_{\text{tot}}}{T} + \int_{-\infty}^{\infty}\frac{d\epsilon}{2\pi}\frac{1}{2T\partial_\epsilon f}\,\text{tr}_c\left\{\left(\phi^{\text{out}(1)}\right)^2\right\}\,. \tag{5.54}$$

Since $\mathrm{tr}_c\{(\phi^{\mathrm{out}(1)})^2\}$ contains all off-diagonal elements of $\phi^{\mathrm{out}(1)}$, it encodes the correlations created by the dynamic scatterer. These correlations determine by how much the entropy current in the leads is smaller than the corresponding heat current over temperature. This net inflow of entropy into the scattering region reflects the local dissipation-induced increase of entropy.

We calculate ϕ explicitly within the gradient expansion [Bode et al., 2011, 2012b; Thomas et al., 2012]. Assuming that $f_\alpha(\epsilon) = f(\epsilon)$, one writes $\phi^{\mathrm{out}(1)}$ in terms of the frozen scattering matrix S,

$$\phi^{\mathrm{out}(1)}(\epsilon, t) = i\dot{X}\partial_\epsilon f\, S\partial_X S^\dagger\,. \tag{5.55}$$

Inserting $\phi^{\mathrm{out}(1)}$ into the entropy current Eq. (5.54), we obtain the entropy current up to second order

$$I^S_{\mathrm{tot}} = \frac{I^Q_{\mathrm{tot}}}{T} - \frac{\dot{W}^{(2)}}{T}\,. \tag{5.56}$$

with

$$\dot{W}^{(2)} = -\frac{\dot{X}^2}{2}\int_{-\infty}^{\infty}\frac{d\epsilon}{2\pi}\partial_\epsilon f(\epsilon)\mathrm{tr}_c\left(\partial_X S^\dagger \partial_X S\right) \geq 0\,. \tag{5.57}$$

Remarkably, $\dot{W}^{(2)} = \gamma\dot{X}^2$ is exactly the dissipated power that the external agent pumps into the system as a result of the time-dependent system Hamiltonian. $\dot{W}^{(2)}$ was derived in Refs. [Bode et al., 2011, 2012b; Thomas et al., 2012] in terms of the friction coefficient γ of the back-action force that needs to be overcome by the external agent. Thus, from our *outside perspective,* dissipation leads to an inflow of entropy into the scattering region in addition to the heat-current contribution.

We are now ready to discuss the inside-outside duality of entropy evolution: We utilize the acquired knowledge about the entropy current (outside perspective) to draw conclusions about the evolution of the entropy $\boldsymbol{s}$ of the strongly coupled subsystem located in the scattering region (inside perspective). To calculate the thermodynamic functions of such a subsystem directly has proven problematic in the past due to difficulties in taking proper account of the coupling Hamiltonian and the presence of strong hybridization [Ludovico et al., 2014; Esposito et al., 2015b; Bruch et al., 2016; Ochoa et al., 2016]. These problems are naturally avoided within the Landauer-Büttiker formalism. Since this formalism considers fully coherent unitary dynamics in both the leads and the scattering region, the von-Neumann entropy associated with the scattering states is conserved in a scattering event. Hence, an additional inflow of entropy is reflected in an increased entropy $\boldsymbol{s}$ stored in the scattering region. As a result, the entropy is source-free

$$\frac{d\boldsymbol{s}}{dt} + I^S_{\mathrm{tot}} = 0\,. \tag{5.58}$$

We can use this continuity equation and Eq. (5.56) to infer the evolution of $\boldsymbol{s}$. Invoking energy and particle conservation, we identify $\dot{Q} = -I^Q_{\mathrm{tot}}$ as the heat leaving the scattering region from the inside perspective. Thus, the entropy

evolution can be expressed in terms of the thermodynamic functions of the (strongly) coupled subsystem as

$$\frac{d\boldsymbol{s}}{dt} = \frac{\dot{Q}}{T} + \frac{\dot{W}^{(2)}}{T} \,. \tag{5.59}$$

Therefore, dissipation leads to a local increase of entropy, which is provided by the scattered electrons. This constitutes the inside-outside duality of entropy evolution. Integrated over a full cyclic transformation of X, the entropy current needs to vanish, as it derives from a source-free thermodynamic state function, see Eq. (5.58). Averaged over a cycle, Eq. (5.56) thus implies that all extra energy pumped into the scattering region $\dot{W}^{(2)}$ eventually has to be released as heat into the leads

$$\overline{I^{Q(2)}_{\mathrm{tot}}} = \overline{\dot{W}^{(2)}} \,. \tag{5.60}$$

5.5 Application to the resonant level model: inside-outside duality

To emphasize the advantage of the outside approach over calculating the thermodynamic functions of a subsystem directly, we connect here to the thermodynamics of the resonant level model derived earlier from an *inside perspective*. This model consists of a single localized electronic level $H_D = \varepsilon_d(t) d^\dagger d$, which can be changed in time by an external agent. It is coupled to a free electron metal $H_B = \sum_k \epsilon_k c_k^\dagger c_k$ via a coupling Hamiltonian $H_V = \sum_k \left(V_k d^\dagger c_k + \mathrm{h.c.} \right)$ and was intensively studied in the past [Ludovico et al., 2014; Ochoa et al., 2016], with difficulties in Ref. [Esposito et al., 2015b] pointed out and overcome in Chapter 3.

The inside approach demands a splitting of the coupling Hamiltonian H_V between effective system and bath, which strongly limits its applicability to the resonant level model in the wide band limit of energy-independent hybridization, see Chapter 4. In contrast, the here developed outside approach yields the strong coupling thermodynamics for arbitrary non-interacting electron systems and furthermore reproduces the results for the resonant level. Deriving the distribution matrix ϕ for this model explicitly, we show order by order that both the heat current I^Q in Eq. (5.53) and the entropy current I^S_{tot} in Eq. (5.52) exactly reproduce the absorbed heat $\dot{Q} = -I^Q_{\mathrm{tot}}$ and entropy change $\dot{\boldsymbol{s}} = -I^S_{\mathrm{tot}}$ from the inside perspective in Chapter 3 (see Technical interlude below). Thereby we also explicitly confirm the inside-outside duality of entropy evolution: The dissipated power $\dot{W}^{(2)}$ was shown to lead to a local increase of entropy for the resonant level in Chapter 3, and we demonstrate here that this is reflected in an additional inflow of entropy I^S_{tot} carried by the scattering states, leaving the entropy source-free, Eq. (5.58).

We show the derivation of the resonant level model explicitly in a technical interlude that can be skipped by readers uninterested in technical details.

5.6 Technical interlude: Application to the resonant level model

Here we derive the distribution matrix ϕ for the resonant level model. In this case the scattering matrix can be reduced to a single element, the reflection coefficient, which can be obtained via the Mahaux-Weidenmueller formula Eq. (D.9)

$$S(\epsilon, t) = 1 - \frac{i\Gamma}{\epsilon - \epsilon_d(X) + i\Gamma/2}\,. \tag{5.61}$$

Here Γ is the decay rate of the dot electrons into the lead $\Gamma = 2\pi \sum_k |V_k|^2 \,\delta(\varepsilon - \varepsilon_k)$, and the A-matrix Eq. (D.10) vanishes [Bode et al., 2012b]. The distribution matrix ϕ only contains a single element describing the occupation of the in- and outgoing scattering channel. The first order and second order contribution Eqs. (5.55) and (D.18) take the form

$$\phi^{\mathrm{out}(1)}(\epsilon, t) = -\dot{X}\partial_\epsilon f \frac{\partial \epsilon_d}{\partial X} A_{dd}\,, \tag{5.62}$$

$$\phi^{\mathrm{out}(2)}(\epsilon, t) = \dot{X}^2 \frac{1}{2}\partial_\epsilon^2 f \left(\frac{\partial \epsilon_d}{\partial X}\right)^2 A_{dd}^2\,, \tag{5.63}$$

where $A_{dd} = \Gamma/\left([\epsilon - \epsilon_d(X)]^2 + \Gamma^2/4\right)$ is the spectral function of the dot electrons. With this we show that the heat current in the leads I^Q in Eq. (5.53) is identical to the heat that leaves the extended level from the inside perspective $\dot{Q}$ in Eqs. (3.21) and (3.52) order by order

$$I^{Q(1)} = -\dot{\epsilon}_d \int_{-\infty}^{\infty} \frac{d\epsilon}{2\pi}\,(\epsilon - \mu)\partial_\epsilon f A_{dd} = -\dot{Q}^{(1)}, \tag{5.64}$$

$$I^{Q(2)} = \frac{1}{2}\dot{\varepsilon}_d^2 \int_{-\infty}^{\infty} \frac{d\epsilon}{2\pi}\,(\epsilon - \mu)\partial_\epsilon^2 f A_{dd}^2 = -\dot{Q}^{(2)}\,, \tag{5.65}$$

where we wrote $\dot{X}\frac{\partial \epsilon_d}{\partial X} = \dot{\epsilon}_d$ to directly compare to the quantities in Chapter 3. The inside-outside duality of entropy evolution, Eq. (5.58), can be explicitly checked order by order by inserting ϕ^{out} Eqs. (5.62) and (5.63) into I^S_{tot} in Eq. (5.52) and comparing it to the change of the entropy $\boldsymbol{s}$ of the resonant level in Eqs. (3.21) and (3.57)

$$I^{S(1)} = -\dot{\epsilon}_d \int_{-\infty}^{\infty} \frac{d\epsilon}{2\pi}\,\frac{(\epsilon - \mu)}{T}\partial_\epsilon f A_{dd} = -\frac{d\boldsymbol{s}^{(1)}}{dt} \tag{5.66}$$

$$I^{S(2)} = \dot{\varepsilon}_d^2 \int_{-\infty}^{\infty} \frac{d\epsilon}{2\pi}\left\{\frac{(\epsilon - \mu)}{T}\frac{1}{2}\partial_\epsilon^2 f A_{dd}^2 + \frac{\partial_\epsilon f}{2T}A_{dd}^2\right\} = -\frac{d\boldsymbol{s}^{(2)}}{dt}\,. \tag{5.67}$$

Thereby we reproduced the results presented in Chapter 3 with the here developed outside perspective.

5.7 Conclusion

We developed a Landauer-Büttiker approach to entropy evolution in strongly coupled fermionic systems, which considers fully coherent quantum dynamics in combination with coupling to macroscopic equilibrium baths. This formalism naturally avoids the system-bath distinction and is applicable to arbitrary non-interacting electron systems. We showed that the entropy current generated by a dynamic scatterer depends on the correlations between different scattering channels, which are generated in the scattering event. At quasistatic order, the entropy current is just the heat current over temperature, while at next order the dissipation induced by the finite velocity transformation yields a net inflow of entropy into the scattering region. This inflow reflects the dissipation-induced local increase of entropy constituting the inside-outside duality of entropy evolution.

6 | Interlude: Fluctuation theorems

At small scales the thermodynamic quantities necessarily acquire strong fluctuations, as introduced in Section 1.3. These fluctuations can be very elegantly characterized by fluctuation theorems describing the probability distribution of the concerning thermodynamic quantities [Jarzynski, 1997; Crooks, 1999; Talkner et al., 2007; Jarzynski, 2011; Hänggi and Talkner, 2015]. In the following, we show the validity of the Jarzynsiki equality for non-interacting electron systems under slow driving. We start by a short introduction into work fluctuation theorems and demonstrate the validity of the Jaryzynski equality for slow transformations in Sec. 6.1.

Remarkably, thermodynamic inequalities such as the rule that the work W done on a path has be larger than the free energy difference ΔF between start and end point,

$$W \geq \Delta F \,, \tag{6.1}$$

can be turned into equalities for the distribution of the fluctuating thermodynamic quantities [Jarzynski, 2011]. Jarzynski showed that the distribution of the classical non-equilibrium work along a certain protocol is directly related to the free energy difference between start and end point,

$$\langle \mathrm{e}^{-\beta W} \rangle = \mathrm{e}^{-\beta \Delta F} \,, \tag{6.2}$$

where $\langle ... \rangle$ refers to averages over many realizations of the same protocol. Here the system is assumed to be initially in thermal equilibrium and ΔF is the free energy difference between initial equilibrium state and a hypothetical equilibrium state with the initial temperature and the parameters at the end of the protocol. Crooks later derived the slightly more general fluctuation theorem [Crooks, 1999]

$$\frac{P_F(W)}{P_R(-W)} = \exp\left(\frac{W - \Delta F}{T}\right) , \tag{6.3}$$

where $P_F(W)$ is the probability distribution of the non-equilibrium work along the forward protocol, and $P_R(-W)$ the distribution along the reversed protocol.

The Crooks relation immediately leads back to the Jarzynski equality Eq. 6.2 by solving Eq. (6.3) for $P_F(W)\exp(W/T)$ and integrating over W. The initial fluctuation theorems were derived for classical systems. Later, Campisi et al. [Campisi et al., 2009] generalized the Crooks relation to open quantum systems at arbitrary coupling strengths.

Both the Jarzynski and the Crooks relation Eqs. (6.8) and (6.3) relate the full non-equilibrium work distribution to the free energy difference. Expanding the exponential in the Jarzynsiki equality yields a relation for the cumulants of the work distribution. Starting from the Jarzynski equality Eq. (6.8),

$$\Delta F = -\frac{1}{\beta}\ln\langle \mathrm{e}^{-\beta W}\rangle \tag{6.4}$$

we can expand the right-hand side in terms of the cumulants of W, since $\ln\langle \mathrm{e}^{-\beta W}\rangle$ is the cumulant generating function of the random variable W [Jarzynski, 1997]. This yields

$$\ln\langle \mathrm{e}^{-\beta W}\rangle = \sum_{n=1}^{\infty}(-\beta)^n\,\frac{\omega_n}{n!} \tag{6.5}$$

where ω_n is the nth cumulant of the non-equilibrium work distribution.

For a Gaussian work distribution we hence obtain

$$\Delta F = -\frac{1}{\beta}\ln\langle \mathrm{e}^{-\beta w}\rangle \tag{6.6}$$

$$= \langle W\rangle - \beta\frac{\sigma_W^2}{2} \tag{6.7}$$

where $\sigma^2 = \langle W^2\rangle - \langle W\rangle^2$ is the variance (second cumulant) of the non-equilibrium work distribution. Since the difference between the non-equilibrium work and the equilibrium free energy difference is the dissipated work $\langle W\rangle - \Delta F = \langle W_{diss}\rangle$, this can be expressed as a fluctuation dissipation relation

$$\langle W_{diss}\rangle = \beta\frac{\sigma_W^2}{2}\,. \tag{6.8}$$

Below we show that for slow transformations this form of the Jarzynski equality is ensured by the fluctuation dissipation theorem of the adiabatic reaction forces [Bode et al., 2011, 2012b; Thomas et al., 2012, 2015].

6.1 Work fluctuations

To make the connection between the Jarzynski equality and the fluctuation dissipation theorem of the adiabatic reaction forces explicit, we again consider the setting of a quantum dot with energy levels changing slowly in time

due to the coupling to an external coordinate X, $H_D = \sum_{n,n'} d_n^\dagger h_{n,n'}(X) d_{n'}$, which is coupled to leads $H_L = \sum_\eta \epsilon_\eta c_\eta^\dagger c_\eta$ via a coupling Hamiltonian $H_T = \sum_{\eta,n} c_\eta^\dagger W_{\eta n} d_n + h.c.$. We define the operator of work done between two times under slow transformations as

$$W\left(t_1 t_2\right) = \int_{t_1}^{t_2} dt \frac{\partial H}{\partial t}\left(t\right) = \int_{t_1}^{t_2} dt \dot{X}(t) \sum_{nm} d_n^\dagger(t) \Lambda_{X,nm} d_m\left(t\right) , \tag{6.9}$$

where $\Lambda_X = \partial h(X)/\partial X$. Here, $-d^\dagger \Lambda_X d$ is the force operator of the coupling induced forces acting on the slow degree of freedom X. The coupling to the electronic degrees of freedom induces a mean force F, friction characterized by γ and an associated fluctuating force ξ [Bode et al., 2011, 2012b]

$$M\ddot{X} = F(t) - \gamma(t)\dot{X} + \xi(t) , \tag{6.10}$$

where the correlator of the fluctuating force on time scales long compared to electronic relaxation rates is in absence of a bias given by the fluctuation dissipation theorem

$$\langle \xi(t)\xi(t')\rangle = 2T\gamma(t)\delta(t-t') . \tag{6.11}$$

Due to fluctuations of the force, the resulting work done on a path is also a fluctuating quantity. To calculate its variance, we at first express the average work done by the external drive between t_1 and t_2 in terms of the lesser Green's function

$$\langle W\left(t_1, t_2\right)\rangle = \int_{t_1}^{t_2} dt \mathrm{Tr}\left[i\Lambda_X G^<\left(t,t\right)\right] . \tag{6.12}$$

The resulting variance $\sigma_W^2 = \left\langle W^2\right\rangle - \langle W\rangle^2$, with

$$\begin{aligned}\left\langle W\left(t_1 t_2\right)^2\right\rangle = &- \int_{t_1}^{t_2}\int_{t_1}^{t_2} dt dt' \dot{X}(t)\dot{X}(t') \\ &\times \sum_{nm,n',m'} \left\langle d_n^\dagger(t)\Lambda_{X,nm} d_m\left(t\right) d_{n'}^\dagger(t')\Lambda_{X,n'm'} d_{m'}\left(t'\right)\right\rangle ,\end{aligned} \tag{6.13}$$

can be expressed as trace over the lesser and greater dot Green's function

$$\sigma_W^2 = \int_{t_1}^{t_2}\int_{t_1}^{t_2} dt dt' \dot{X}(t)\dot{X}(t')\mathrm{Tr}\left[\Lambda_X G^>(t,t')\Lambda_X G^<(t,t')\right] . \tag{6.14}$$

The variance of the non-equilibrium work distribution is determined by the correlator of the fluctuating force

$$\hat{\xi}(t) = -d^\dagger(t)\Lambda_X d(t)\left\langle d^\dagger(t)\Lambda_X d(t)\right\rangle \tag{6.15}$$

$$\langle \hat{\xi}(t)\hat{\xi}(t')\rangle = \mathrm{Tr}\left[\Lambda_X G^>(t,t')\Lambda_X G^<(t',t)\right] , \tag{6.16}$$

so that

$$\sigma_W^2 = \int_{t_1}^{t_2}\int_{t_1}^{t_2} dt dt' \dot{X}(t)\dot{X}(t')\left\langle \hat{\xi}(t)\hat{\xi}(t')\right\rangle . \tag{6.17}$$

For the integral over a slow transformation, the contributions in σ_W^2 for which $t-t'$ is smaller than typical electronic relaxation times are negligible. With this we can write the lowest order work fluctuations in terms of the equal time noise correlator Eq. (6.11)

$$\sigma_W^2 \simeq \int_{t_1}^{t_2} dt \dot{X}(t)^2 \, 2T\,\gamma(t) = 2T\,\langle W_{diss}\rangle \,, \tag{6.18}$$

where we used that the dissipated work is the time integral over the dissipated power

$$\langle W_{diss}\rangle = \int_{t_1}^{t_2} dt\, \dot{X}(t)^2 \gamma(t)\,. \tag{6.19}$$

Hence, the Jarzynski equality for a Gaussian work distribution in Eq. 6.8 is automatically fulfilled by the fluctuation dissipation theorem of the adiabatic reaction forces at each point of the protocol. In a final technical interlude, we show how the delta-correlated noise follows from the energy dependence of the electronic Green's functions.

For slow transformations, the noise is delta-correlated on time scales much larger than typical electronic relaxation times, Eq. (6.11). To make that explicit, we express the noise correlator Eq. (6.16) in terms of the Wigner transforms and keep only terms to lowest order in $\dot{X}$

$$\begin{aligned} G^{>}(t,t')G^{<}(t,t') &= \int \frac{d\varepsilon}{2\pi} e^{-i\varepsilon\tau} G^{>(0)}(t,\epsilon) \int \frac{d\varepsilon'}{2\pi} e^{i\varepsilon'\tau} G^{<(0)}(t,\epsilon') \\ &= \int \frac{d\varepsilon}{2\pi} \int \frac{d\,\delta\epsilon}{2\pi} e^{i\delta\epsilon(t-t')} G^{>(0)}(t,\epsilon) G^{<(0)}(t,\epsilon+\delta\epsilon)\,, \end{aligned} \tag{6.20}$$

where we used $\delta\epsilon = \epsilon' - \epsilon$. Due to the oscillating factor only times and energies $|(t-t')\delta\epsilon| \ll 1$ contribute to the integral. For time scales long compared to the electronic ones $|t-t'| \gg \Gamma^{-1}$, where Γ is a typical electronic relaxation rate, the contribution of the integrals is restricted to $\delta\epsilon \ll \Gamma$. Since $\delta\epsilon \ll \Gamma$ is an energy scale on which the dot Green's functions barely change, we can approximate $G^{<(0)}(t,\epsilon+\delta\epsilon) \simeq G^{<(0)}(t,\epsilon)$ and obtain the noise correlator Eq. (6.16)

$$\begin{aligned} \langle \hat{\xi}(t)\hat{\xi}(t')\rangle &\simeq \int \frac{d\varepsilon}{2\pi} \mathrm{Tr}\left[\Lambda_X G^{>(0)}(t,\epsilon)\Lambda_X G^{<(0)}(t,\epsilon)\right] \int \frac{d\delta\epsilon}{2\pi} e^{i(\delta\epsilon)\tau} \\ &= D(t)\delta(t-t')\,. \end{aligned} \tag{6.21}$$

In absence of an electronic bias, the equal time noise correlator is determined by the fluctuation dissipation theorem $D(t) = 2\gamma(t)$ [Bode et al., 2011, 2012b], which yields Eq. (6.11).

7 | Conclusion and outlook

In this thesis we investigated how electron-electron interactions and strong system-bath coupling influence the working principles of electronic nanomachines.

First we derived the properties of an electronic quantum motor, in which the electron-electron interactions gain importance due to reduced dimensionality: a one-dimensional electron system coupled to a slowly changing mechanical or magnetic degree of freedom. This model is realized for instance in a quantum wire proximitized by a slowly sliding periodic potential and a QSH edge coupled to a precessing nanomagnet. In a fully field theoretic treatment, we derived how the coupling to the interacting electron system leads to directed motion. We demonstrated in an RG treatment that the repulsion between the electrons enhances the energy gap opened by the sliding periodic potential of the Thouless motor, and analogously the gap opened by the nanomagnet in the QSH edge. Thereby electron-electron interactions increase the robustness against variations of the chemical potential, allow for higher operating speeds, and protect the quantum motor against leakages, which would decrease its output power. On the other hand, the friction of the motor is enhanced by repulsive interactions for infinite one-dimensional electron systems. Nevertheless, a closer look shows that putting the system into contact with 3d electronic reservoirs, such as a battery to drive the motor, reduces the dissipation to the non-interacting value at steady velocity. This phenomenon is caused by plasmon reflection at the boundary of the 1d system, which feed part of the dissipated energy back into the motor degree of freedom. Thereby the motor exhibits the conductance of an ideal non-interacting channel at steady velocity, analogous to the *dc* conductance of a Luttinger liquid with attached Fermi liquid leads [Maslov and Stone, 1995].

In the second part we showed how to describe the thermodynamic transformations of electronic quantum machines in the strong coupling regime. To overcome the problems posed by the strong system-bath coupling, we at first thoroughly investigated the simplest possible case: the driven resonant level model. By considering everything which is influenced by local changes of the level as 'system', and everything that is not as 'bath', the equilibrium thermodynamics of this model could be derived from standard statistical mechanics. Going beyond the quasistatic equilibrium to treat finite velocity transformations

demands a representation of the thermodynamic quantities in terms of expectation values. For the resonant level model in the wide band limit, this leads to a symmetric splitting of the coupling Hamiltonian between system and bath. On this basis, the full characterization of the thermodynamic transformations to first order beyond the quasistatic equilibrium were derived, including a positive entropy production given by the dissipated power.

However, we subsequently found that the symmetric splitting of the coupling Hamiltonian is limited to the mean value of the internal energy and fails to correctly predict its fluctuations. And furthermore, moving away from the wide band limit entirely precludes a simple accounting for the coupling energy by dividing the Hamiltonian between system and bath, even for the mean value. To treat more general electronic nanomachines we hence developed an approach that is based on a formalism, which naturally avoids this system-bath distinction: the Landauer-Büttiker theory of quantum transport. Invoking energy, particle, and—due to the fully coherent quantum dynamics—also entropy conservation, we showed that the thermodynamic evolution of the strongly coupled subsystem can be inferred from the associated currents in the attached leads. In an expansion around the quasistatic equilibrium, we showed that the onset of dissipation leads to a local increase of entropy and a deviation from the equilibrium relation $dQ = TdS$. The developed approach provides an efficient tool to the theoretical treatment of electronic nanomachines, as it is applicable to arbitrary non-interacting electron systems under slow driving. In a last step, we demonstrated the validity of the Jarzynsiki equality in these systems.

An exciting next step would be to combine several strokes of a quantum engine, which we can now describe thermodynamically in the strong coupling regime, to a full cyclic transformation as in the Carnot heat engine in Sec. 1.3. Thereby one could follow the full thermodynamic evolution of a simple electronic quantum engine in the strong coupling regime. Furthermore, the effects of electron-electron interactions on the thermodynamic properties in the strong coupling regime pose an interesting direction of future research.

A | Appendices: An interacting adiabatic quantum motor

A.1 Effective action of the motor degree of freedom

In the following we derive the effective action of the motor degree of freedom ϑ that results from the coupling to the LL at the boundary of the periodic potential, given by the pinning condition $\phi(0,t) = -\vartheta(t)/2$. Since the coupling to an applied bias Eq. (2.51) $\propto \phi(0,\tau)$ is already given in terms of the field at $x = 0$ only, it is not affected by the integrating out procedure. We can directly impose the constraint $\phi(0,\tau) = -\vartheta(\tau)/2$ and obtain its contribution to the effective action of ϑ

$$S_{\text{bias}} = -\int_0^\beta d\tau \frac{eV}{2\pi}\vartheta(\tau)\,. \tag{A.1}$$

To obtain the dissipative part of the effective dynamics, we integrate out the fields of the LL under the constraint $\phi(0,\tau) = -\vartheta(\tau)/2$, which we implement via a functional delta function

$$\delta\left[\phi(0,\tau) + \frac{\vartheta(\tau)}{2}\right] = \int D[\kappa] \exp\left(-i\int_0^\beta d\tau\,\kappa(\tau)\left[\phi(0,\tau) + \frac{\vartheta(\tau)}{2}\right]\right), \tag{A.2}$$

where we introduced an additional real-valued field $\kappa(\tau)$. With that we can write effective action $S_{\text{diss}}[\vartheta]$ as

$$\exp(-S_{\text{diss}}[\vartheta]) = \int D[\phi]\,\delta\left[\phi(0,\tau) + \frac{\vartheta(\tau)}{2}\right]\exp\left(-S_0\right) = \int D[\phi]\,D[\kappa]\,\exp\left(-S\right)\,. \tag{A.3}$$

Using Eq. (A.2), the exponent $-S$ reads

$$S = \frac{1}{2\pi}\int dr\left[\frac{1}{K(x)\,v_c(x)}\left(\partial_\tau\phi\right)^2 + \frac{v_c(x)}{K(x)}\left(\partial_x\phi\right)^2\right] + i\int_0^\beta d\tau\,\kappa(\tau)\left(\phi(0,\tau)+\frac{\vartheta(\tau)}{2}\right), \tag{A.4}$$

where the space-dependent charge velocity and interaction parameter Eq. (2.71) model the contact to the FL leads. We find the effective action by solving the saddle point equations under a variation of ϕ and κ, which enables us to to take proper account of the boundary conditions at the intersections of FL and LL and the constraint $\phi(0,\tau) = -\vartheta(\tau)/2$. For that we write down the saddle point equation under a variation of ϕ

$$\frac{1}{\pi}\left(\frac{\omega_n^2}{K(x)\,v_c(x)} - \partial_x\frac{v_c(x)}{K(x)}\partial_x\right)\phi(x,\omega_n) \quad = \quad -i\kappa(\omega_n)\delta(x)\,. \tag{A.5}$$

We can solve this equation by writing the solutions for each region of constant v_c and K and solving for their coefficients by taking proper account of the boundary conditions as shown below. Inserting the implicit solution of the saddle point equation into the action (A.4) leads to

$$S \quad = \quad \frac{i}{2}\int d\tau\kappa(\tau)\phi(0,\tau) + i\int_0^\beta d\tau\,\kappa(\tau)\frac{\vartheta(\tau)}{2}\,, \tag{A.6}$$

where $\phi(0,\tau)$ is the solution of the saddle point equation. From there we can later obtain the saddle point equation for κ to reach the desired dissipative action of the motor.

Infinite Luttinger liquid We start with the infinite LL case. To find the explicit solution for $\phi(0,\tau)$ we write down the solution of Eq. (A.5) for $x > 0$ and $x < 0$

$$\phi(x,\omega_n) = \begin{cases}\beta \mathrm{e}^{\frac{|\omega_n|}{v_c}x} & x<0\\ \delta \mathrm{e}^{-\frac{|\omega_n|}{v_c}x} & 0<x\,,\end{cases} \tag{A.7}$$

where we directly omitted the part of the solution that grows for $x \to \pm\infty$. The appropriate boundary conditions follow from the saddle point equation Eq. (A.5) and are given by the continuity $\phi(x=0^+) = \phi(x=0^-)$, which directly gives $\beta = \delta$, and

$$\frac{v_c}{\pi K}\partial_x\phi(x,\omega_n)|_{x=0^-}^{x=0^+} \quad = \quad i\kappa(\omega_n) \tag{A.8}$$

$$\to \beta \quad = \quad -\frac{i\kappa(\omega_n)\pi K}{2|\omega_n|} = \phi(0,\omega_n)\,. \tag{A.9}$$

We use the solution for $\phi(0,\omega_n)$ and insert it into S Eq. (A.6)

$$S = \frac{1}{4}\sum_{\omega_n}\frac{|\kappa(\omega_n)|^2\pi K}{|\omega_n|} + i\sum_{\omega_n}\left(\kappa(\omega_n)\frac{\vartheta(-\omega_n)}{2}\right). \tag{A.10}$$

A variation of $\kappa(\omega_n)$ leads to the saddle point equation

$$\kappa(-\omega_n) = -i\frac{\vartheta(-\omega_n)|\omega_n|}{\pi K}\,. \tag{A.11}$$

Inserting κ Eq. (A.11) into the action Eq. (A.10) yields the dissipative action used in the main text Eq. (2.52)

$$S_{\rm diss}[\vartheta] = \sum_{\omega_n}\frac{|\omega_n|}{4\pi K}|\vartheta_n|^2\,. \tag{A.12}$$

Furthermore we can use the solution for $\kappa(-\omega_n)$ Eq. (A.11) to determine $\beta = -\vartheta(\omega_n)/2$ in Eq. (A.9) and write down the real space solution for ϕ

$$\phi(x,\omega_n) = \begin{cases} -\frac{\vartheta(\omega_n)}{2}\mathrm{e}^{\frac{|\omega_n|}{v_c}x} & x<0 \\ -\frac{\vartheta(\omega_n)}{2}\mathrm{e}^{-\frac{|\omega_n|}{v_c}x} & 0<x\,. \end{cases} \tag{A.13}$$

Analytical continuation to real frequencies $|\omega_n| \to -i\omega$ and taking the Fourier transform to real time leads to

$$\phi(x,t) = \begin{cases} -\frac{\vartheta\left(t+\frac{x}{v_c}\right)}{2} & x<0 \\ -\frac{\vartheta\left(t-\frac{x}{v_c}\right)}{2} & 0<x\,. \end{cases} \tag{A.14}$$

Thus, the boundary condition travels with $\pm v_c$ on the right (left) side.

Contact to Fermi liquid leads In the case of a finite LL in contact to FL leads, we need to write down the solution of the saddle point equation (A.5) in the various regions

$$\phi(x,\omega_n) = \begin{cases} A\mathrm{e}^{\frac{|\omega_n|}{v_F}x} & x<-D/2 \\ [\beta+\gamma/2]\,\mathrm{e}^{\frac{|\omega_n|}{v_c}x} + [\beta-\gamma/2]\,\mathrm{e}^{-\frac{|\omega_n|}{v_c}x} & -D/2<x<0 \\ [\delta+\epsilon/2]\,\mathrm{e}^{\frac{|\omega_n|}{v_c}x} + [\delta-\epsilon/2]\,\mathrm{e}^{-\frac{|\omega_n|}{v_c}x} & 0<x<D/2 \\ F\mathrm{e}^{-\frac{|\omega_n|}{v_F}x} & D/2<x\,, \end{cases} \tag{A.15}$$

where we again directly omitted the part of the solution that grows for $x \to \pm\infty$. Additionally to the boundary condition at $x=0$ Eq. (A.8) we get at $x=D/2$ an additional condition from the saddle point Eq. (A.5)

$$-\frac{1}{\pi}\frac{v_c(x)}{K(x)}\partial_x\phi(x,\omega_n)|_{x=0^-}^{x=0^+} = 0 \tag{A.16}$$

$$\frac{v_c}{K}\partial_x\phi\left(\frac{D}{2}^-,\omega_n\right) = v_F\partial_x\phi\left(\frac{D}{2}^+,\omega_n\right)\,, \tag{A.17}$$

where ϕ has to be continuous and the analogous condition at $x = -D/2$. Solving for the coefficient $\beta = \phi(0, \omega_n)/2$ leads to

$$\phi(0,\omega_n) = -\frac{i\kappa(\omega_n)\pi K}{2|\omega_n|\, M(\omega_n)} \tag{A.18}$$

$$\begin{aligned} M(\omega_n) &= \frac{\left(1+\frac{1}{K}\right)\mathrm{e}^{\frac{|\omega_n|D}{2v_c}} + \left(1-\frac{1}{K}\right)\mathrm{e}^{-\frac{|\omega_n|D}{2v_c}}}{\left(1+\frac{1}{K}\right)\mathrm{e}^{\frac{|\omega_n|D}{2v_c}} - \left(1-\frac{1}{K}\right)\mathrm{e}^{-\frac{|\omega_n|D}{2v_c}}} \\ &= \left(1 + 2\sum_{n=1}^{\infty} \mathrm{e}^{\frac{-n|\omega_n|D}{v_c}} \left[\frac{K-1}{K+1}\right]^n\right) \\ &= \left(1 + 2\sum_{n=1}^{\infty} \mathrm{e}^{-n|\omega_n|\mathcal{T}} r_p^n\right), \end{aligned} \tag{A.19}$$

where we used the plasmon or charge reflection amplitude $r_p = \frac{K-1}{K+1}$ and the travel time of the plasmons from x=0 to the FL-LL boundary and back $\mathcal{T} = D/v_c$. Using the explicit solution for $\phi(0,\tau)$ in Eq. (A.6) yields

$$S = \frac{1}{4}\sum_{\omega_n} \frac{\pi K}{|\omega_n|\, M(\omega_n)} |\kappa(\omega_n)|^2 + i\sum_{\omega_n}\left(\kappa(\omega_n)\frac{\vartheta(-\omega_n)}{2}\right). \tag{A.20}$$

A variation of $\kappa(\omega_n)$ leads to

$$\kappa(-\omega_n) \quad = \quad -i\frac{\vartheta(-\omega_n)|\omega_n|M(\omega_n)}{\pi K}, \tag{A.21}$$

which we insert into the action Eq. (A.20) to obtain the dissipative action used in the main text Eq. (2.72)

$$S_{\mathrm{diss}}[\vartheta] = \sum_{\omega_n} \frac{|\omega_n|\, M(\omega_n)}{4\pi K} |\vartheta_n|^2 . \tag{A.22}$$

Finally we use $\kappa(-\omega_n)$ Eq. (A.21) to obtain the solution of ϕ under the constraint $\phi(0,t) = -\vartheta(t)/2$. We focus here on the inner part $|x| < D/2$, since the outer parts do not provide any additional insight. Inserting $\kappa(-\omega_n)$ Eq. (A.21) into Eq. (A.18) and using the relations between the coefficients of ϕ Eq. (A.15) that we obtained from matching the boundary conditions, we get

$$\phi(x,\omega_n) = -\frac{\vartheta(\omega_n)}{4}\begin{cases} [1+M]\,\mathrm{e}^{\frac{|\omega_n|}{v_c}x} + [1-M]\,\mathrm{e}^{-\frac{|\omega_n|}{v_c}x} & -D/2 < x < 0 \\ [1-M]\,\mathrm{e}^{\frac{|\omega_n|}{v_c}x} + [1+M]\,\mathrm{e}^{-\frac{|\omega_n|}{v_c}x} & 0 < x < D/2 \end{cases} \tag{A.23}$$

$$= -\frac{\vartheta(\omega_n)}{4}\begin{cases} \left[2 + 2\sum_{n=1}^{\infty}\mathrm{e}^{-n|\omega_n|\mathcal{T}} r_p^n\right]\mathrm{e}^{\frac{|\omega_n|}{v_c}x} - 2\left[\sum_{n=1}^{\infty}\mathrm{e}^{-n|\omega_n|\mathcal{T}} r_p^n\right]\mathrm{e}^{-\frac{|\omega_n|}{v_c}x} \\ -2\sum_{n=1}^{\infty}\mathrm{e}^{-n|\omega_n|\mathcal{T}} r_p^n \mathrm{e}^{\frac{|\omega_n|}{v_c}x} + \left(2 + 2\sum_{n=1}^{\infty}\mathrm{e}^{-n|\omega_n|\mathcal{T}} r_p^n\right)\mathrm{e}^{-\frac{|\omega_n|}{v_c}x}, \end{cases} \tag{A.24}$$

where we used Eq. (A.19). Analytical continuation to real frequencies $|\omega_n| \to -i\omega$ and Fourier transformation to real times leads to

$$\phi(x,t) = -\frac{1}{2}\begin{cases} \vartheta\left(t+\frac{x}{v_c}\right) - \sum_{n=1}^{\infty}\vartheta\left(t-\frac{x}{v_c}-\mathcal{T}n\right)r_P^n + \sum_{n=1}^{\infty}\vartheta\left(t+\frac{x}{v_c}-\mathcal{T}n\right)r_P^n \\ \vartheta\left(t-\frac{x}{v_c}\right) - \sum_{n=1}^{\infty}\vartheta\left(t+\frac{x}{v_c}-\mathcal{T}n\right)r_P^n + \sum_{n=1}^{\infty}\vartheta\left(t-\frac{x}{v_c}-\mathcal{T}n\right)r_P^n \end{cases}, \tag{A.25}$$

where the upper line is again for $x \in [-D/2, 0]$ and the lower one for $x \in [0, D/2]$. Here we can see that additionally to the initial excitation that travels with $\pm v_c$ to the right (left) side, ϕ contains the field that gets reflected with amplitude $-r_p$ at the LL-FL boundary and is subsequently reflected with amplitude -1 at $x = 0$ and so on, which leads to the reduced uniform energy current Eq. (2.83) in the main text.

B | Appendices: Quantum thermodynamics of the resonant level model

B.1 Density of states in the wide band limit

In this work, we use the term wide band limit in the following sense: We consider a large bandwidth $2D$ in the lead with a constant product of coupling matrix element $|V_k|^2$ and lead density of states $\nu(\varepsilon)$,

$$\Gamma = 2\pi\nu(\varepsilon)|V(\varepsilon)|^2, \tag{B.1}$$

for energies ε within the bandwidth of the lead. This leads to the retarded dot self energy

$$\Sigma^R(\varepsilon) = \lim_{\eta\to 0}\sum_k \frac{|V_k|^2}{\varepsilon - \varepsilon_k + i\eta} = \frac{\Gamma}{2\pi}\ln|\frac{D+\varepsilon}{D-\varepsilon}| - i\frac{\Gamma}{2}\Theta\left(D - |\varepsilon|\right) , \tag{B.2}$$

where Θ is the Heaviside function.

For energies $\varepsilon \ll D$, we can approximate the real part as $\Sigma^R(\varepsilon) \simeq 2\varepsilon/D$, which gives small corrections to the quasiparticle weight, the level energy ε_d, and the level width Γ. Neglecting this contribution in the limit $D \to \infty$, we find the approximation used in the bulk of the paper.

Strictly speaking, this approximation leads to divergences. To see that these divergences do not lead to complications in our discussion of the thermodynamics, one needs to treat the wide band limit somewhat more carefully. From Eq.

(3.14) in the main text we obtain the density of states in the wide band limit

$$\rho(\varepsilon) = \frac{\Gamma\Theta(D-|\varepsilon|)}{\left(\varepsilon-\varepsilon_d-\frac{\Gamma}{2\pi}\ln|\frac{D+\varepsilon}{D-\varepsilon}|\right)^2+\left(\frac{1}{2}\Gamma\Theta(D-|\varepsilon|)\right)^2}\left(1-\frac{\Gamma}{2\pi}\frac{d}{d\varepsilon}\ln|\frac{D+\varepsilon}{D-\varepsilon}|\right) - \frac{\left(\varepsilon-\varepsilon_d-\frac{\Gamma}{2\pi}\ln|\frac{D+\varepsilon}{D-\varepsilon}|\right)}{\left(\varepsilon-\varepsilon_d-\frac{\Gamma}{2\pi}\ln|\frac{D+\varepsilon}{D-\varepsilon}|\right)^2+\left(\frac{1}{2}\Gamma\Theta(D-|\varepsilon|)\right)^2}\frac{d}{d\varepsilon}\Gamma\Theta(D-|\varepsilon|)+\nu(\varepsilon)\,. \tag{B.3}$$

The large but finite bandwidth of the lead reduces the energy interval in which the density of states takes finite values to $\varepsilon \in [-D, D]$. The energy dependence of the self energy that arises from the finite bandwidth leads to additional contributions to the density of states of the extended resonant level (the full density of states ρ minus the unperturbed density of states in the bath ν) for energies close to the band edge $\varepsilon \sim \pm D$. To calculate the influence of these additional terms on the thermodynamic quantities, we consider their contribution to the quasistatic energy $E^{(0)} = \Omega + \mu N^{(0)} + TS^{(0)}$ Eq. (3.18), the quantity with the largest contribution from the band edge. The correction to the internal energy δE_1 originating from the term $\propto \frac{d}{d\varepsilon}\Im\Sigma^R(\varepsilon)$ vanishes,

$$\delta E_1 = -\int\frac{d\epsilon}{2\pi}\epsilon f(\epsilon)\frac{\left(\varepsilon-\varepsilon_d-\frac{\Gamma}{2\pi}\ln|\frac{D+\epsilon}{D-\epsilon}|\right)}{\left(\varepsilon-\varepsilon_d-\frac{\Gamma}{2\pi}\ln|\frac{D+\epsilon}{D-\epsilon}|\right)^2+\left(\frac{1}{2}\Gamma\Theta(D-|\epsilon|)\right)^2}\frac{d}{d\varepsilon}\Gamma\Theta(D-|\epsilon|)=0\,. \tag{B.4}$$

The correction δE_2 from the term $\propto \frac{d}{d\varepsilon}\Re\Sigma^R(\varepsilon)$ takes the form

$$\delta E_2 = \int\frac{d\epsilon}{2\pi}\epsilon f(\epsilon)\frac{-\Gamma\Theta(D-|\epsilon|)}{\left(\varepsilon-\varepsilon_d-\frac{\Gamma}{2\pi}\ln|\frac{D+\epsilon}{D-\epsilon}|\right)^2+\left(\frac{1}{2}\Gamma\Theta(D-|\epsilon|)\right)^2}\frac{\Gamma}{2\pi}\frac{2D}{D^2-\epsilon^2}\,, \tag{B.5}$$

where we used $\frac{d}{d\varepsilon}\ln|\frac{D+\epsilon}{D-\epsilon}| = \frac{2D}{D^2-\epsilon^2}$. To estimate the correction from the band edge, consider the contribution from the upper edge $\varepsilon \sim D$. The divergence of $\frac{\Gamma}{2\pi}\ln|\frac{D+\epsilon}{D-\epsilon}|$ dominates the denominator when

$$D \lesssim \frac{\Gamma}{2\pi}\ln|\frac{D+\epsilon}{D-\epsilon}| \tag{B.6}$$

$$2D\mathrm{e}^{-D/\Gamma} \lesssim D-\epsilon. \tag{B.7}$$

Hence we can separate the energy integral in δE_2 into the two parts,

$$\delta E_2 \simeq \int^{D-2D\mathrm{e}^{-D/\Gamma}}\frac{d\epsilon}{2\pi}Df(D)\frac{-\Gamma}{D^2}\frac{\Gamma}{2\pi}\frac{2D}{2D(D-\epsilon)} + \int_{D-2D\mathrm{e}^{-D/\Gamma}}^{D}\frac{d\epsilon}{2\pi}Df(D)\frac{-\Gamma}{\left(\frac{\Gamma}{2\pi}\ln|\frac{D-\epsilon}{2D}|\right)^2}\frac{\Gamma}{2\pi}\frac{2D}{2D(D-\epsilon)}\,. \tag{B.8}$$

Estimating the integrals leads to

$$\delta E_2 \simeq -f(D)\frac{\Gamma}{(2\pi)^2} - \Gamma f(D)\,. \tag{B.9}$$

The contribution from the lower edge $\varepsilon \sim -D$ follows analogously and yields an analogous result with $f(D)$ replaced by $f(-D)$. Thus, the contribution to the density of states $\propto \frac{d}{d\varepsilon}\Re\Sigma^R(\varepsilon)$ gives a finite cutoff-dependent correction to the internal energy that does not vanish in the limit $D \to \infty$.

However, the thermodynamics actually relates changes in the thermodynamic state functions, and not the state functions themselves. We can similarly consider how these changes are affected by starting with a finite bandwidth. To be specific, consider the change of the internal energy upon moving the dot level $\frac{d}{d\epsilon_d}\delta E$. By analogy with the above, the contribution $\propto \frac{d}{d\varepsilon}\Im\Sigma^R(\varepsilon)$ yields

$$\frac{d}{d\epsilon_d}\delta E_2 = \int \frac{d\epsilon}{2\pi}\epsilon f(\epsilon)\frac{-2\Gamma\Theta\left(D-|\epsilon|\right)\left(\varepsilon-\varepsilon_d-\frac{\Gamma}{2\pi}\ln|\frac{D+\epsilon}{D-\epsilon}|\right)}{\left(\left(\varepsilon-\varepsilon_d-\frac{\Gamma}{2\pi}\ln|\frac{D+\epsilon}{D-\epsilon}|\right)^2+\left(\frac{1}{2}\Gamma\Theta\left(D-|\epsilon|\right)\right)^2\right)^2}\frac{\Gamma}{2\pi}\frac{2D}{D^2-\epsilon^2} \tag{B.10}$$

$$\simeq \frac{-2f(D)\Gamma}{(2\pi)^2 D} + \frac{4\pi\Gamma f(D)}{2D} \to 0 \text{ for } D\to\infty\,. \tag{B.11}$$

Hence for the *changes of the thermodynamic quantities*, the corrections associated with the energy dependence of the self energy vanish in the limit $D \to \infty$. The specific choice of the bandwidth D merely sets the reference point from which the grand potential Ω and the internal energy $E^{(0)}$ of the extended resonant level are being measured – all changes of thermodynamic quantities and non-equilibrium corrections are converging to cutoff-independent results in the limit $D \to \infty$. This leads to the wide band limit expression for the density of states of the extended resonant level in the limit of large D

$$\rho_{\varepsilon_d}(\varepsilon) = \frac{\Gamma}{(\varepsilon-\varepsilon_d)^2+(\Gamma/2)^2} \tag{B.12}$$

used in the main text, which leaves the dependence on D that sets the reference point of the internal energy $E^{(0)}$ and the grand potential Ω implicit.

B.2 An alternative derivation of the non-equilibrium Green's functions in terms of a quantum kinetic equation

Here we present an alternative derivation of the non-equilibrium properties of the dot electrons. Instead of deriving the lesser component of the non-equilibrium Green's function using the Langreth rule in the Keldysh integral

formulation, one can equivalently derive the non-equilibrium occupation of the level using the a quantum kinetic (Kadanoff-Baym or Quantum Boltzmann) equation in first order gradient approximation,[Haug and Jauho, 1996] as it is done in Ref. [Esposito et al., 2015b] and [Kita, 2010]. For the description of a single electronic level in contact to leads these approaches are equivalent and we explicitly show both here to clarify the connection of our work to Ref. [Esposito et al., 2015b]. For a single electronic level, the retarded Green's function of the dot electrons takes the frozen form $G^R(\varepsilon,t) = (\varepsilon - \varepsilon_d(t) + i\frac{\Gamma}{2})^{-1}$ when considering the gradient expansion of the Dyson equation up to second order. Thereby also the form of the spectral function $A(\varepsilon) = -2\,\mathrm{Im}\,G^R(\varepsilon)$ is set and all effects of the level speed up to linear order can be cast in a non-equilibrium distribution function ϕ, related to the lesser Green's function via $G^< = iA\phi$. The non-equilibrium distribution function of the dot electrons in contact to one lead satisfies the equation of motion [Kita, 2010]

$$\{G_0^{-1} - \mathrm{Re}\,\Sigma^R,\ A\phi\} - \{\Gamma f,\,\mathrm{Re}\,G^R\} = A\Gamma(f-\phi)\,, \tag{B.13}$$

where $\{C,\ D\} = \partial_\varepsilon C\,\partial_t D - \partial_t C\,\partial_\varepsilon D$ is the Poisson bracket and $G_0^{-1} = \varepsilon - \varepsilon_d(t)$. [1] Using the wide band limit we solve this equation for ϕ consistently up to linear in the velocity to obtain

$$\begin{aligned}\phi &= f - \dot{\varepsilon}_d\partial_\varepsilon f\left(\frac{1}{\Gamma} + \partial_\varepsilon\,\mathrm{Re}\,G^R\right)\\ &= f - \frac{\dot{\varepsilon}_d}{2}\partial_\varepsilon f A\,,\end{aligned} \tag{B.14}$$

which is identical to the solution above obtained via the Langreth rule for the lesser component of the Green's function Eq. (3.45).

B.3 Calculation of the internal energy

As mentioned in the main text, the internal energy of the extended resonant level model can be, at different orders i, represented as expectation value of the Hamiltonian of the effective system $H_D + \frac{1}{2}H_V$

$$E^{(i)} = \langle H_D\rangle^{(i)} + \frac{1}{2}\langle H_V\rangle^{(i)}\ . \tag{B.15}$$

To calculate $\langle H_V\rangle$ we write

$$\langle H_V\rangle = \sum_k \left(V_k\,\langle d^\dagger c_k\rangle + V_k^*\,\langle c_k^\dagger d\rangle\right) \tag{B.16}$$

$$= 2\sum_k \mathrm{Im}\,\left(V_k^* G^<_{d,k}(t,t)\right)\,, \tag{B.17}$$

[1] Eq. (B.13) differs from Eq. (4.19) in Ref. [Kita, 2010], used in Ref. [Esposito et al., 2015b], in the second Poisson bracket on the left, as our expression involves f rather than ϕ. We believe that our form is correct, but in any case both forms are equivalent up to the first order in velocity considered here and both lead to the same solution for ϕ Eq. (B.14).

with $G^<_{d,k}(t,t') = i\left\langle c_k^\dagger(t')d(t)\right\rangle$ and where we used $G^<_{d,k}(t,t) = -\left(G^<_{k,d}(t,t)\right)^*$. The equation of motion for the mixed Green's function $G^<_{d,k}$ and analytical continuation from the Keldysh contour to the lesser component leads to [Jauho et al., 1994]

$$\begin{aligned}\langle H_V\rangle &= 2\sum_k \mathrm{Im}\left(\int dt'|V_k|^2\left[G^R(t,t')g_k^<(t',t) + G^<(t,t')g_k^A(t',t)\right]\right)\\ &= 2\,\mathrm{Im}\left(\int dt'\left[G^R(t,t')\Sigma^<(t',t) + G^<(t,t')\Sigma^A(t',t)\right]\right). \qquad \text{(B.18)}\end{aligned}$$

Moving to the Wigner transform we obtain

$$\langle H_V\rangle = 2\,\mathrm{Im}\left(\int \frac{d\varepsilon}{2\pi}\left[G^R(\varepsilon,t) * \Sigma^<(\varepsilon) + G^<(\varepsilon,t) * \Sigma^A\right]\right). \qquad \text{(B.19)}$$

Note that $G^<(\varepsilon,t) * \Sigma^A = G^<(\varepsilon,t)\,\frac{1}{2}i\Gamma$ does not contribute, since it is purely real. This leads up to linear order in the velocity to

$$\langle H_V\rangle = 2\,\mathrm{Im}\left(\int \frac{d\varepsilon}{2\pi}\left[G^R(\varepsilon,t)if(\varepsilon)\Gamma - \frac{i}{2}\partial_t G^R(\varepsilon,t)i\partial_\varepsilon f(\varepsilon)\Gamma\right]\right). \qquad \text{(B.20)}$$

From the fact that G^R does not have a correction linear in the velocity it follows that the first term on the right contributes only in zero order, and yields the quasistatic coupling energy $\langle H_V\rangle^{(0)}$

$$\begin{aligned}\langle H_V\rangle^{(0)} &= \int \frac{d\varepsilon}{2\pi} 2f(\varepsilon)\Gamma\,\mathrm{Re}\,G^R(\varepsilon) \qquad \text{(B.21)}\\ &= 2\int \frac{d\varepsilon}{2\pi} f(\varepsilon)(\varepsilon-\varepsilon_d)A\,, \qquad \text{(B.22)}\end{aligned}$$

which leads, using the result for $\langle H_D\rangle^{(0)} = \varepsilon_d\langle d^\dagger d\rangle^{(0)}$ from Eq. (3.45), to the quasistatic internal energy of the extended resonant level given in the main text Eq. (3.18)

$$E^{(0)} = \langle H_D\rangle^{(0)} + \frac{1}{2}\langle H_V\rangle^{(0)} = \int \frac{d\varepsilon}{2\pi}\varepsilon f A\,. \qquad \text{(B.23)}$$

The first order correction to the coupling energy is obtained from the second term on the right of Eq. (B.20) and takes the form

$$\begin{aligned}\langle H_V\rangle^{(1)} &= \int \frac{d\varepsilon}{2\pi}\partial_\varepsilon f\Gamma\,\mathrm{Im}\,\partial_t G^R(\varepsilon) \qquad \text{(B.24)}\\ &= \frac{\dot\varepsilon_d}{2}\int \frac{d\varepsilon}{2\pi}\partial_\varepsilon f\Gamma\partial_\varepsilon A\,. \qquad \text{(B.25)}\end{aligned}$$

With $\langle H_D\rangle^{(1)} = \varepsilon_d\langle d^\dagger d\rangle^{(1)}$ from Eq. (3.45) we obtain the correction to the

internal energy Eq. (3.51) from the main text

$$E^{(1)} = \langle H_D \rangle^{(1)} + \frac{1}{2} \langle H_V \rangle^{(1)} = \dot{\varepsilon}_d \int \frac{d\varepsilon}{2\pi} \left(-\frac{\varepsilon_d}{2} \partial_\varepsilon f A^2 + \frac{1}{4} \Gamma \partial_\varepsilon f \partial_\varepsilon A \right) \tag{B.26}$$

$$= \frac{-\dot{\varepsilon}_d}{2} \int \frac{d\varepsilon}{2\pi} \varepsilon \partial_\varepsilon f A^2 \,, \tag{B.27}$$

where we used $\partial_\varepsilon A = \frac{-2(\varepsilon - \varepsilon_d)}{\Gamma} A^2$. Taking the time derivative of this correction leads to the second order contribution to the internal energy change per unit time

$$\frac{d}{dt} E^{(1)} = \dot{E}^{(2)} = \frac{\dot{\varepsilon}_d^2}{2} \int \frac{d\varepsilon}{2\pi} \varepsilon \partial_\varepsilon f \partial_\varepsilon A^2 \tag{B.28}$$

$$= \frac{\dot{\varepsilon}_d^2}{2} \int \frac{d\varepsilon}{2\pi} \left(-\partial_\varepsilon f A^2 - \varepsilon \partial_\varepsilon^2 f \, A^2 \right) \,, \tag{B.29}$$

where we integrated by parts. Note again that throughout the entire paper we assume a linear motion of the dot level $\ddot{\varepsilon}_d = 0$. With the corresponding expressions given in the main text Eq. (3.49), (3.52) and (3.48) it can be seen that the derived corrections satisfy the first law $\dot{E}^{(2)} = \dot{W}^{(2)} + \dot{Q}^{(2)} + \mu \, \dot{N}^{(2)}$.

Note however that even though the symmetric splitting into effective system and bath gives a correct representation of the ε_d-dependent part of the internal energy (the internal energy of the extended resonant level model), it does not mean that $\langle H_B \rangle$ has no ε_d-dependent part. This can be seen explicitly by calculating the ε_d-dependent part of the lead Hamiltonian, which we call $\langle H_B \rangle_{\varepsilon_d}$ in the following, via a scaled version of the grand potential of the extended resonant level Ω Eq. (3.15) (the ε_d-dependent part of the grand potential). We use the scaled Hamiltonian

$$H_\lambda = H_D + \lambda H_B + H_V \tag{B.30}$$

to calculate $\langle H_B \rangle_{\varepsilon_d}$ from the associated scaled grand potential Ω_λ

$$\langle H_B \rangle_{\varepsilon_d} = \frac{\partial \Omega_\lambda}{\partial \lambda} \big|_{\lambda=1}, \tag{B.31}$$

evaluated at $\lambda = 1$. The scaled lead Hamiltonian changes the density of states of the bath electrons $\nu_\lambda(\varepsilon) = \nu(\varepsilon)/\lambda$ and the scaled spectral function of the dot electrons A_λ reads

$$A_\lambda = \frac{\Gamma}{(\varepsilon - \varepsilon_d)^2 + \left(\frac{\Gamma}{2\lambda}\right)^2} \,. \tag{B.32}$$

This sets the form of the scaled grand potential Ω_λ from which we obtain

$$\langle H_B\rangle_{\varepsilon_d} = \frac{-1}{\beta}\frac{\partial}{\partial\lambda}\int\frac{d\varepsilon}{2\pi}\frac{\Gamma}{(\varepsilon-\varepsilon_d)^2+\left(\frac{\Gamma}{2\lambda}\right)^2}\ln\left(1+e^{-\beta(\varepsilon-\mu)}\right) \tag{B.33}$$

$$= -\frac{1}{\beta}\left(-\frac{\Gamma}{\lambda^2}\right)\int\frac{d\varepsilon}{2\pi}\underbrace{\frac{(\varepsilon-\varepsilon_d)^2-\left(\frac{\Gamma}{2\lambda}\right)^2}{\left[(\varepsilon-\varepsilon_d)^2+\left(\frac{\Gamma}{2\lambda}\right)^2\right]^2}}_{-\partial_\varepsilon Re G^R(\varepsilon)}\ln\left(1+e^{-\beta(\varepsilon-\mu)}\right)\quad \lambda\to 1 \tag{B.34}$$

$$= \frac{1}{\beta}\int\frac{d\varepsilon}{2\pi}\Gamma\,\mathrm{Re}\,G^R(\varepsilon)\;\partial_\varepsilon\ln\left(1+e^{-\beta(\varepsilon-\mu)}\right) \tag{B.35}$$

$$= -\int\frac{d\varepsilon}{2\pi}(\varepsilon-\varepsilon_d)\;Af(\varepsilon)\;. \tag{B.36}$$

Note that an analogous calculation for H_D and H_V reproduces the direct expectation values $\langle H_V\rangle_{\varepsilon_d} = \langle H_V\rangle^{(0)}$ Eq. (B.21) and $\langle H_D\rangle_{\varepsilon_d} = \varepsilon_d\langle d^\dagger d\rangle^{(0)}$ from Eq. (3.45). Thus the ε_d-dependent part of all three Hamiltonian reproduces the adiabatic internal energy of the extended resonant level from above

$$\langle H_D\rangle^{(0)} + \langle H_V\rangle^{(0)} + \langle H_B\rangle^{(0)}_{\varepsilon_d} = \int\frac{d\varepsilon}{2\pi}\varepsilon f A\,, \tag{B.37}$$

while the sum $\langle H_V\rangle^{(0)} + \langle H_B\rangle^{(0)}_{\varepsilon_d}$ gives the 'half splitting' contribution $\frac{1}{2}\langle H_V\rangle^{(0)}$.

B.4 Calculation of the energy fluxes

Using the results of Section 3.3.1, we calculate the different energy fluxes contributing to the heat current at different orders from the non-equilibrium Green's functions formalism. Since the energy fluxes $W_\alpha = i\langle[H_{\mathrm{tot}}, H_\alpha]\rangle$ between the different parts of the system α must satisfy

$$W_B + W_V + W_D = 0\,, \tag{B.38}$$

and because the energy change of the *total* system is given by the power provided by the external driving $\dot{E}_{\mathrm{tot}} = \langle\frac{\partial H_d}{\partial t}\rangle$, there are in principle two ways of calculating the energy flow into the effective bath (needed for the evaluation of the heat flow at different orders):

$$\dot{Q} = -\left(\frac{1}{2}W_V - W_B\right) - \mu\dot{N} \quad \text{or} \tag{B.39}$$

$$\dot{Q} = W_D + \frac{1}{2}W_V - \mu\dot{N}\,. \tag{B.40}$$

We present the calculation via the energy flux leaving the effective system $W_D + \frac{1}{2}W_V$, since it takes a simpler form in the non-equilibrium Green's functions

formalism. Note however that a calculation via W_B is also possible and leads to the same result.

We calculate the heat flux via

$$\begin{aligned}\dot{Q} &= W_D + \frac{1}{2}W_V - \mu\dot{N} \\ &= \varepsilon_d\dot{N} + \frac{1}{2}\frac{d}{dt}\langle H_V\rangle - \mu\dot{N}\,. \end{aligned} \tag{B.41}$$

This leads with $\dot{N}^{(1)}$ Eq. (3.22) and $\langle H_V\rangle^{(0)}$ Eq. (B.21) to the quasistatic heat current linear in the velocity

$$\begin{aligned}\dot{Q}^{(1)} &= \varepsilon_d\dot{N}^{(1)} + \frac{1}{2}\frac{d}{dt}\langle H_V\rangle^{(0)} - \mu\dot{N}^{(1)} \\ &= \varepsilon_d\dot{\varepsilon}_d\int\frac{d\varepsilon}{2\pi}A\,\partial_\varepsilon f - \dot{\varepsilon}_d\int\frac{d\varepsilon}{2\pi}f\Gamma\partial_\varepsilon\,\mathrm{Re}\,G^R - \mu\int\frac{d\varepsilon}{2\pi}A\,\partial_\varepsilon f\,(\varepsilon) \\ &= \dot{\varepsilon}_d\int\frac{d\varepsilon}{2\pi}\,(\varepsilon-\mu)\,A\,\partial_\varepsilon f\,(\varepsilon)\;, \end{aligned} \tag{B.42}$$

where we used $\Gamma\,\mathrm{Re}\,G^R = (\varepsilon-\varepsilon_d)\,A$ and integrated by parts. Therefore the calculation of the first order heat current via the energy flux into the effective bath reproduces the adiabatic heat current Eq. (3.21) from the main text. To calculate the non-equilibrium correction we use $\dot{N}^{(2)}$, Eq. (3.48), and $\langle H_V\rangle^{(1)}$, Eq. (B.24), and obtain

$$\begin{aligned}\dot{Q}^{(2)} &= \varepsilon_d\dot{N}^{(2)} + \frac{1}{2}\frac{d}{dt}\langle H_V\rangle^{(1)} - \mu\dot{N}^{(2)} \\ &= -\varepsilon_d\int\frac{d\varepsilon}{2\pi}\frac{\dot{\varepsilon}_d^2}{2}\,\partial_\varepsilon^2 f\,A^2 - \frac{\dot{\varepsilon}_d^2}{4}\int\frac{d\varepsilon}{2\pi}\Gamma\partial_\varepsilon f\partial_\varepsilon^2 A - \mu\int\frac{d\varepsilon}{2\pi}\frac{\dot{\varepsilon}_d^2}{2}\,\partial_\varepsilon^2 f\,A^2 \\ &= -\int\frac{d\varepsilon}{2\pi}(\varepsilon-\mu)\frac{\dot{\varepsilon}_d^2}{2}\,\partial_\varepsilon^2 f\,A^2\,, \end{aligned} \tag{B.43}$$

where we integrated by parts and used $\Gamma\partial_\varepsilon A = -2(\varepsilon-\varepsilon_d)A^2$. This is the form of the non-equilibrium correction to the heat current given in the main text Eq. (3.52).

B.5 Particle conservation of the finite speed current

In the following we show that the correction $\dot{N}^{(2)} = \frac{d}{dt}N^{(1)}$ to the quasistatic current is obeying particle conservation upon moving on a path between two states with a well defined particle number. We need to show that

$$\Delta N^{(2)} = \int_{t_1}^{t_2} dt\dot{N}^{(2)} = 0\,, \tag{B.44}$$

with $\varepsilon_d(t_1)$ well below and $\varepsilon_d(t_2)$ well above μ. Assuming a constant velocity $\dot{\varepsilon}_d$ we obtain

$$\begin{aligned}\Delta N^{(2)} &= -\int_{t_1}^{t_2} dt \int \frac{d\varepsilon}{2\pi} \frac{\dot{\varepsilon}_d^2}{2} \partial_\varepsilon^2 f \, A^2 \\ &= \int_{\varepsilon_1}^{\varepsilon_2} d\varepsilon_d \frac{\dot{\varepsilon}_d}{2} \int \frac{d\varepsilon}{2\pi} \, \partial_\varepsilon f \partial_\varepsilon A^2, \end{aligned} \tag{B.45}$$

where we did an integration by parts in the second line. Now we use that A is a function of $\varepsilon - \varepsilon_d$ and therefore $\partial_\varepsilon A = -\partial_{\varepsilon_d} A$ to obtain

$$\begin{aligned}\Delta N^{(2)} =& -\frac{\dot{\varepsilon}_d}{2} \int \frac{d\varepsilon}{2\pi} \, \partial_\varepsilon f \int_{\varepsilon_1}^{\varepsilon_2} d\varepsilon_d \frac{\partial A^2}{\partial \varepsilon_d} \\ =& -\frac{\dot{\varepsilon}_d}{2} \int \frac{d\varepsilon}{2\pi} \, \partial_\varepsilon f A^2 |_{\varepsilon-\varepsilon_1}^{\varepsilon-\varepsilon_2} \\ =& 0 \, , \end{aligned}$$

where we used that the derivative of the fermi distribution $\partial_\varepsilon f$ restricts the ε-interval in which the integrand is non-zero to a finite range $\sim T$ around μ. As long as ε_1 is well below and ε_2 is well above it, $A^2(\varepsilon, \varepsilon_{1/2})$ is zero everywhere, where $\partial_\varepsilon f$ is nonzero, from which follows the last line.

B.6 Energy conservation of the corrections to heat current and the extra work

In the following we show that all the extra work paid for moving the level at finite speed is given as extra heat to the leads

$$\int_{t_1}^{t_2} dt \dot{W}^{(2)} = -\int_{t_1}^{t_2} dt \dot{Q}^{(2)} \, , \tag{B.46}$$

(6.3)where again $\varepsilon_d(t_1)$ is well below and $\varepsilon_d(t_2)$ is well above μ. With analogous steps as above we obtain assuming a constant level speed

$$\begin{aligned}
\int_{t_1}^{t_2} dt \dot{W}^{(2)} &= -\int_{t_1}^{t_2} dt \dot{Q}^{(2)} \\
-\int_{t_1}^{t_2} dt \int \frac{d\varepsilon}{2\pi} \frac{\dot{\varepsilon}_d^2}{2} \partial_\varepsilon f \, A^2 &= \int_{t_1}^{t_2} dt \int \frac{d\varepsilon}{2\pi} \varepsilon \left(\frac{\dot{\varepsilon}_d^2}{2} \partial_\varepsilon^2 f \, A^2 \right) \\
\dot{\varepsilon}_d \int_{\varepsilon_1}^{\varepsilon_2} d\varepsilon_d \int \frac{d\varepsilon}{2\pi} \varepsilon \partial_\varepsilon \left(\partial_\varepsilon f \, A^2 \right) &= \dot{\varepsilon}_d \int_{\varepsilon_1}^{\varepsilon_2} d\varepsilon_d \int \frac{d\varepsilon}{2\pi} \varepsilon \partial_\varepsilon^2 f \, A^2 \\
\int_{\varepsilon_1}^{\varepsilon_2} d\varepsilon_d \int \frac{d\varepsilon}{2\pi} \varepsilon \partial_\varepsilon f \, \partial_\varepsilon A^2 &= 0 \\
-\int \frac{d\varepsilon}{2\pi} \varepsilon \partial_\varepsilon f \int_{\varepsilon_1}^{\varepsilon_2} d\varepsilon_d \partial_{\varepsilon_d} A^2 &= 0 \\
-\int \frac{d\varepsilon}{2\pi} \varepsilon \partial_\varepsilon f \, A^2 |_{\varepsilon-\varepsilon_1}^{\varepsilon-\varepsilon_2} &= 0 \,,
\end{aligned}$$

where the last equality is fulfilled due to the finite range where $\partial_\varepsilon f$ is non-zero, as above.

C | Appendices: The extended resonant level model: Energy fluctuations and behavior beyond the wide band limit

C.1 Derivation of Eqs. 4.3 and 4.6

In this Appendix we derive the expression for the local energy fluctuations of the extended resonant level. We consider the rescaled Hamiltonian in Eq. (4.2) and grand potential in Eq. (4.5), with rescaling parameter λ and evaluate

$$-\frac{1}{\beta}\frac{\partial^2}{\partial\lambda^2}\Omega(\lambda) = -\frac{1}{\beta^2}\left(\frac{1}{\Xi}\frac{\partial\Xi}{\partial\lambda}\right)^2 + \frac{1}{\beta^2}\frac{1}{\Xi(\lambda)}\frac{\partial^2\Xi(\lambda)}{\partial\lambda^2} \tag{C.1}$$

Setting $\lambda = 1$ we obtain Eq. (4.3). Next, we notice that the rescaled Hamiltonian has effective level energy $\lambda\varepsilon_d$, system-bath coupling parameter λV_k and bath electron energies $\lambda\varepsilon_k$. Accordingly, the rescaled electron decay rate $\tilde{\Gamma}$ in the wide band limit is $\tilde{\Gamma} = 2\pi\sum_k |\lambda V_k|^2\delta(\varepsilon-\lambda\varepsilon_k) = 2\pi\lambda^2\times(\lambda^{-1})\sum_k |V_k|^2\delta(\lambda^{-1}\varepsilon-\varepsilon_k) = \lambda\Gamma$, and the level spectral function depends on λ as follows

$$A = \frac{\lambda\Gamma}{(\varepsilon-\lambda\varepsilon_d)^2 + (\lambda\Gamma/2)^2}. \tag{C.2}$$

Evaluating the derivatives of A with respect to λ, as well as the derivatives of A and $\mathrm{Re}G^R$ with respect to the energy ε we obtain Eq. (4.4). Also, Eqs. (4.5), (4.3) and (4.4) readily yield

$$\frac{\partial^2}{\partial\lambda^2}\Omega\bigg|_{\lambda=1} = \int\frac{d\varepsilon}{2\pi}\varepsilon^2 A\frac{\partial}{\partial\varepsilon}f(\varepsilon), \tag{C.3}$$

which is Eq. (4.6) of the main text.

More generally, the above discussion shows that by identifying how the parameters of the Hamiltonian change after rescaling, we can determine the functional form of the spectral function A on the rescaling parameters λ_i, then use its derivatives with respect to these scaling parameters to find averages and higher moments of other relevant local quantities expressed in terms of energy derivatives of A and $\mathrm{Re}G^R$.

C.2 Derivation of Eqs. 4.26 and 4.31

Here we derive the relation $\frac{\partial}{\partial\varepsilon_d}\rho_{\varepsilon_d}(\varepsilon) = -\frac{\partial}{\partial\varepsilon}\tilde{A}(\varepsilon)$ used in Sec. 4.2. Let $B(\varepsilon) = (\varepsilon - \varepsilon_d - \Lambda)^2 + (\Gamma/2)^2$, such that $\tilde{A} = \Gamma/B$ and $\mathrm{Re}G^R = (\varepsilon - \varepsilon_d - \Lambda)/B$. Thus

$$\frac{\partial}{\partial\varepsilon_d}\tilde{A} = \frac{1}{B^2}2\left(\varepsilon - \varepsilon_d - \Lambda\right)\Gamma, \tag{C.4}$$

$$\frac{\partial}{\partial\varepsilon_d}\mathrm{Re}G^R = \frac{1}{B^2}\left\{\left(\varepsilon - \varepsilon_d - \Lambda\right)^2 - \left(\Gamma/2\right)^2\right\}. \tag{C.5}$$

The energy derivative of the extended resonant level spectral function $\tilde{A}$ is

$$\begin{aligned}\frac{\partial}{\partial\varepsilon}\tilde{A} =& \frac{1}{B^2}\left\{\left(\left(\varepsilon - \varepsilon_d - \Lambda\right)^2 + \left(\Gamma/2\right)^2\right)\partial_\varepsilon\Gamma\right. \\ &\left. - \left(2\left(\varepsilon - \varepsilon_d - \Lambda\right)\left(1 - \partial_\varepsilon\Lambda\right)\Gamma + 2(\Gamma/2)^2\partial_\varepsilon\Gamma\right)\right\} && \text{(C.6)}\\ =& \partial_\varepsilon\Gamma\frac{\partial}{\partial\varepsilon_d}\mathrm{Re}G^R - \left(1 - \partial_\varepsilon\Lambda\right)\frac{\partial}{\partial\varepsilon_d}\tilde{A} && \text{(C.7)}\\ =& -\frac{\partial}{\partial\varepsilon_d}\rho_{\varepsilon_d}(\varepsilon)\,, && \text{(C.8)}\end{aligned}$$

where we used Eq. (C.4) and (C.5) in (C.6) in order to identify $\rho_{\varepsilon_d}(\varepsilon)$ as given by Eq. (4.23).

To obtain $\langle\hat{H}_D\rangle$ in Eq. (4.31), just notice that $\langle\hat{H}_D\rangle = \varepsilon_d\langle\hat{d}^\dagger\hat{d}\rangle = \varepsilon_d\partial_{\varepsilon_d}\tilde{\Omega} = \varepsilon_d\int\frac{d\varepsilon}{2\pi}\tilde{A}f(\varepsilon)$, where we have used (4.26).

C.3 Derivation of Eq. 4.32

To obtain the expression for $\langle H_V\rangle$ in Eq. (4.32) we defined the rescaled Hamiltonian

$$\hat{H}(\lambda) = \hat{H}_D + \lambda_V H_V + \hat{H}_B, \tag{C.9}$$

and observe that Γ and Λ rescale as $\Gamma = \lambda_V^2\Gamma$ and $\Lambda = \lambda_V^2\Lambda$, respectively. The rescaled retarded Green function and spectral density are

$$\mathrm{Re}G^R(\varepsilon, \varepsilon_d, \Gamma, \Lambda; \lambda_V) = \frac{\varepsilon - \varepsilon_d - \lambda_V^2\Lambda}{(\varepsilon - \varepsilon_d - \lambda_V^2\Lambda)^2 + (\lambda_V^2\Gamma/2)^2} \tag{C.10}$$

$$\tilde{A}(\varepsilon; \varepsilon_d, \Gamma, \Lambda; \lambda_V) = \frac{\lambda_V^2\Gamma}{(\varepsilon - \varepsilon_d - \lambda_V^2\Lambda)^2 + (\lambda_V^2\Gamma/2)^2} \tag{C.11}$$

and the derivative of ρ_{ε_d} with respect to the rescaling parameter λ_V is

$$\begin{aligned}\frac{\partial}{\partial\lambda_V}\rho_{\varepsilon_d}(\varepsilon) = &\left(\frac{\partial}{\partial\lambda_V}\tilde{A}\right)(1 - \partial_\varepsilon\Lambda) - \tilde{A}(2/\lambda_V)\partial_\varepsilon\Lambda \\ &- \left(\frac{\partial}{\partial\lambda_V}\mathrm{Re}G^R\right)\partial_\varepsilon\Gamma - \mathrm{Re}G^R(2/\lambda_V)\partial_\varepsilon\Gamma.\end{aligned} \tag{C.12}$$

Equations (C.10) - (C.12) lead to

$$\begin{aligned}\frac{\partial}{\partial\lambda_V}\rho_{\varepsilon_d}(\varepsilon) = &\frac{2}{B^2}\Gamma(\varepsilon - \varepsilon_d - \Lambda)(2/\lambda_V)\Lambda(1 - \partial_\varepsilon\Lambda) \\ &- (2/\lambda_V)\frac{\partial}{\partial\varepsilon}\left(\tilde{A}\Lambda\right) \\ &+ (2/\lambda_V)\Lambda\left(\frac{\partial}{\partial\varepsilon}\tilde{A}\right) \\ &- (2/\lambda_V)\frac{\partial}{\partial\varepsilon}\left(\Gamma\,\mathrm{Re}G^R\right) \\ &- \frac{1}{B^2}(2/\lambda_V)\left[(\varepsilon - \varepsilon_d - \Lambda)^2 - (\Gamma/2)^2\right]\Lambda\partial_\varepsilon\Gamma.\end{aligned} \tag{C.13}$$

The first, third and fifth terms in the r.h.s of Eq. (C.13) mutually cancel. Therefore

$$\frac{\partial}{\partial\lambda_V}\rho_{\varepsilon_d}(\varepsilon) = -\frac{2}{\lambda_V}\left\{\frac{\partial}{\partial\varepsilon}\left(\Gamma\,\mathrm{Re}G^R\right) + \frac{\partial}{\partial\varepsilon}\left(\tilde{A}\Lambda\right)\right\}. \tag{C.14}$$

Finally, the expression in Eq. (C.14) can be used to calculate $\langle H_V\rangle$:

$$\langle H_V\rangle = \frac{\partial}{\partial\lambda_V}\tilde{\Omega}\bigg|_{\lambda_V=1} \tag{C.15}$$

$$= -\frac{1}{\beta}\int\frac{d\varepsilon}{2\pi}\left(\frac{\partial}{\partial\lambda_V}\rho_{\varepsilon_d}(\varepsilon)\right)_{\lambda_V=1}\ln\left(1 + e^{-\beta(\varepsilon-\mu)}\right) \tag{C.16}$$

$$= 2\int\frac{d\varepsilon}{2\pi}(\varepsilon - \varepsilon_d)\tilde{A}f(\varepsilon), \tag{C.17}$$

which is the result in Eq. (4.32). This result can also be derived from the Green's functions formalism (see Sec. B.3).

D | Appendices: Landauer-Büttiker approach to strongly coupled quantum thermodynamics

D.1 Calculation of the outgoing distribution matrix in the gradient expansion

In the following we derive the adiabatic expansion for the outgoing distribution matrix Eq. (5.21). With the expression of the outgoing operators b in terms of the incoming ones a via exact scattering matrix of the time-dependent problem $\mathcal{S}$, Eq. (5.14), we obtain

$$\langle b_\beta^\dagger(\epsilon_2)\, b_\alpha(\epsilon_1)\rangle = \sum_{\gamma\delta}\int\frac{d\epsilon_3}{2\pi}\int\frac{d\epsilon_4}{2\pi}\left\langle\, \mathcal{S}^*_{\beta\gamma}(\epsilon_2,\epsilon_3)a^\dagger_\gamma(\epsilon_3)\mathcal{S}_{\alpha\delta}(\epsilon_1,\epsilon_4)a_\delta(\epsilon_4)\,\right\rangle.$$

We use that the incoming scattering states are uncorrelated equilibrium channels

$$\langle a_i^\dagger(\epsilon_1)a_j(\epsilon_2)\rangle = \delta_{ij}2\pi\delta(\epsilon_1-\epsilon_2)f_i(\epsilon_1) \tag{D.1}$$

and get

$$\langle b_\beta^\dagger(\epsilon_2)\, b_\alpha(\epsilon_1)\rangle = \sum_{\gamma}\int\frac{d\epsilon_3}{2\pi}\int\frac{d\epsilon_4}{2\pi}\left\{\mathcal{S}_{\alpha\gamma}(\epsilon_1,\epsilon_3)\tilde{f}_\gamma(\epsilon_3,\epsilon_4)\,\mathcal{S}^\dagger_{\gamma\beta}(\epsilon_4,\epsilon_2)\right\}, \tag{D.2}$$

with $\tilde{f}_\gamma(\epsilon_3,\epsilon_4)\equiv 2\pi\delta(\epsilon_3-\epsilon_4)\,f(\epsilon_3)$. The Wigner transform of a convolution

$$G(\epsilon_1,\epsilon_2) = \int\frac{d\epsilon_3}{2\pi}C(\epsilon_1,\epsilon_3)D(\epsilon_3,\epsilon_2) \tag{D.3}$$

takes the form of a Moyal product of Wigner transforms

$$G(\epsilon,t) = C(\varepsilon,t) * D(\varepsilon,t) \tag{D.4}$$

where $C(\varepsilon,t) * D(\varepsilon,t) = C(\varepsilon,t) \exp\left[\frac{i}{2}\left(\overleftarrow{\partial}_\varepsilon \vec{\partial}_t - \overleftarrow{\partial}_t \vec{\partial}_\varepsilon\right)\right] D(\varepsilon,t)$. Hence, we get

$$\phi^{\text{out}}_{\alpha\beta}(\epsilon,t) = \int \frac{d\tilde{\epsilon}}{2\pi} e^{-i\tilde{\epsilon}t} \left\langle b^\dagger_\beta(\epsilon - \tilde{\epsilon}/2) b_\alpha(\epsilon + \tilde{\epsilon}/2) \right\rangle \tag{D.5}$$

$$= \sum_\gamma \left[\mathcal{S}_{\alpha\gamma}(\epsilon,t) * \tilde{f}_\gamma(\epsilon,t)\right] * \mathcal{S}^\dagger_{\gamma\beta}(\epsilon,t)\,. \tag{D.6}$$

Expanding the exponential gives the different orders of velocity, which is called the gradient expansion. The Wigner transform of the incoming distribution in channel γ $\tilde{f}_\gamma(\epsilon_3,\epsilon_4) = 2\pi\delta(\epsilon_3 - \epsilon_4) f_\gamma(\epsilon_3)$ is just the Fermi function of the associated reservoir $\tilde{f}_\gamma(\epsilon,t) = f_\gamma(\epsilon)$. The Wigner transform of the full scattering matrix

$$\mathcal{S}(\epsilon,t) = \int \frac{d\tilde{\epsilon}}{2\pi} \mathrm{e}^{-i\tilde{\epsilon}t} \mathcal{S}(\epsilon + \frac{\tilde{\epsilon}}{2}, \epsilon - \frac{\tilde{\epsilon}}{2}) \tag{D.7}$$

can be written as an expansion in powers of velocity (assuming $\ddot{X} = 0$)[Moskalets and Büttiker, 2004b; Bode et al., 2011]

$$\mathcal{S}(\epsilon,t) = S_t(\epsilon) + \dot{X} A_t(\epsilon) + \dot{X}^2 B_t(\epsilon)\,, \tag{D.8}$$

where S is the frozen scattering matrix, A is the A-matrix, its first order correction, and B is its second order correction. All these matrices depend parametrically on time and from now on we drop their energy and time labels for better readability. The second order contribution to the scattering matrix B never contributes to the distribution matrix up to second order in $\dot{X}$ in absence of a bias $f_\alpha = f \forall \alpha$, as we show below.

In the setting of a quantum dot $H_D = \sum_{n,n'} d^\dagger_n h_{n,n'}(X) d_{n'}$ coupled to leads $H_L = \sum_\eta \epsilon_\eta c^\dagger_\eta c_\eta$ via a coupling Hamiltonian $H_T = \sum_{\eta,n} c^\dagger_\eta W_{\eta n} d_n + h.c.$, the frozen scattering matrix S can be expressed in terms of the frozen retarded Green's function of the of the quantum dot G^R and the coupling matrices W between the dot and the attached leads

$$S = 1 - 2\pi i \nu W G^R W^\dagger\,, \tag{D.9}$$

where ν is the density of states in the leads. This formula is called the Mahaux-Weidenmueller formula.

In the case of an energy-independent hybridization the A-matrix can be written as [Bode et al., 2011]

$$A = \pi\nu W \left(\partial_\epsilon G^R \Lambda_X G^R - G^R \Lambda_X \partial_\epsilon G^R\right) W^\dagger\,, \tag{D.10}$$

where $\Lambda_X = \partial h(X)/\partial X$.

D.1.1 Zeroth order

At zeroth order only the frozen scattering matrix in the zeroth order gradient expansion contributes

$$\phi^{\text{out}(0)}_{\alpha\beta} = \sum_\gamma S_{\alpha\gamma} f_\gamma S^\dagger_{\gamma\beta} \,. \tag{D.11}$$

In the absence of voltage and temperature bias $f^{\text{in}}_\alpha = f \forall \alpha$, this simplifies to

$$\phi^{\text{out}(0)}_{\alpha\beta} = f \sum_\gamma S_{\alpha\gamma} S^\dagger_{\gamma\beta} = f \, \left[S S^\dagger\right]_{\alpha\beta} \,. \tag{D.12}$$

For $f^{\text{in}}_\alpha = f \forall \alpha$, we can at each order simplify the expression for the outgoing distribution function $\phi^{\text{out}}_{\alpha\beta}$ by the unitarity of the scattering matrix at different orders. At zeroth order this condition is just the unitarity of the frozen scattering matrix

$$S S^\dagger = \hat{1} \,, \tag{D.13}$$

which leads to the zeroth order outgoing distribution matrix diagonal in channel lead space, identical to the incoming distribution matrix

$$\phi^{\text{out}(0)}_{\alpha\beta} = \delta_{\alpha\beta} f = \phi^{\text{in}}_{\alpha\beta} \,. \tag{D.14}$$

We derive the unitarity conditions for the first and second order below in Sec. D.1.4.

D.1.2 First order

At first order there are contributions both from the zeroth order gradient expansion with the first order correction to $\mathcal{S}(\epsilon, t)$, $\dot{X} A^X_t$ in Eq. (D.8), and the first order gradient expansion with the frozen scattering matrix S, which is simplified by the fact that the incoming distribution function f_γ has no time dependency. We obtain

$$\begin{aligned}
\phi^{\text{out}(1)}_{\alpha\beta} = \dot{X} \sum_\gamma \Big[& A_{\alpha\gamma} f_\gamma S^\dagger_{\gamma\beta} + S_{\alpha\gamma} f_\gamma A^\dagger_{\gamma\beta} \\
& + \frac{i}{2} \left\{ \partial_\epsilon S_{\alpha\gamma} \partial_X S^\dagger_{\gamma\beta} - \partial_X S_{\alpha\gamma} \partial_\epsilon S^\dagger_{\gamma\beta} \right\} f_\gamma \\
& + \frac{i}{2} \left\{ -\partial_X S_{\alpha\gamma} \partial_\epsilon f_\gamma S^\dagger_{\gamma\beta} + S_{\alpha\gamma} \partial_\epsilon f_\gamma \partial_X S^\dagger_{\gamma\beta} \right\} \Big] \,,
\end{aligned} \tag{D.15}$$

where we used $\partial_t S = \dot{X} \partial_X S$.
If we assume $f_\alpha = f \forall \alpha$ we get

$$\begin{aligned}
\frac{\phi^{\text{out}(1)}_{\alpha\beta}}{\dot{X}} = & f \sum_\gamma \left[A_{\alpha\gamma} S^\dagger_{\gamma\beta} + S_{\alpha\gamma} A^\dagger_{\gamma\beta} + \frac{i}{2} \left\{ \partial_\epsilon S_{\alpha\gamma} \partial_X S^\dagger_{\gamma\beta} - \partial_X S_{\alpha\gamma} \partial_\epsilon S^\dagger_{\gamma\beta} \right\} \right] \\
& + \partial_\epsilon f \sum_\gamma \frac{i}{2} \left\{ -\partial_X S_{\alpha\gamma} S^\dagger_{\gamma\beta} + S_{\alpha\gamma} \partial_X S^\dagger_{\gamma\beta} \right\} \,.
\end{aligned} \tag{D.16}$$

This can be simplified by the unitarity condition at first order Eq. (D.23)

$$\begin{aligned}\phi^{\mathrm{out}(1)}_{\alpha\beta} &= \dot{X}\partial_\epsilon f \sum_{\beta=LR} \frac{i}{2}\left\{-\partial_X S_{\alpha\gamma} S^\dagger_{\gamma\beta} + S_{\alpha\gamma}\partial_X S^\dagger_{\gamma\beta}\right\} \\ &= \dot{X}\partial_\epsilon f\, i\left[S\partial_X S^\dagger\right]_{\alpha\beta} \end{aligned} \tag{D.17}$$

where we used $\partial_X\left(SS^\dagger\right) = \partial_X \hat{I} = 0$.

D.1.3 Second order

At second order there are contributions by the zeroth order gradient expansion with $\dot{X}^2 B$ in Eq. (D.8), the first order gradient expansion with $\dot{X}A$ and the second order gradient expansion with S. Using Eq. (D.24) we can simplify the expression to

$$\begin{aligned}&\frac{\phi^{\mathrm{out}(2)}_{\alpha\beta}}{\dot{X}^2} = \frac{1}{2}\partial_\epsilon^2 f\left[\partial_X S\partial_X S^\dagger\right]_{\alpha\beta} \\ &+ \partial_\epsilon f\frac{i}{2}\left[A\partial_X S^\dagger + S\partial_X A^\dagger + \frac{i}{2}\left(\partial_X^2 S\partial_\epsilon S^\dagger + \partial_\epsilon S\partial_X^2 S^\dagger - \partial_\epsilon\partial_X S\partial_X S^\dagger - \partial_X S\partial_X\partial_\epsilon S^\dagger\right)\right]_{\alpha\beta} .\end{aligned} \tag{D.18}$$

D.1.4 Unitarity condition at different orders

The unitarity of the full scattering matrix

$$\sum_n \int \frac{d\epsilon}{2\pi}\mathcal{S}_{mn}(\epsilon',\epsilon)\mathcal{S}^\dagger_{nk}(\epsilon,\epsilon'') = 2\pi\delta(\epsilon'-\epsilon'')\delta_{mk} \tag{D.19}$$

leads to different conditions at each order in velocity. Taking the Wigner transform of this expression leads to

$$1\delta_{mk} = \sum_n \mathcal{S}_{mn}(\epsilon,t) * \mathcal{S}^\dagger_{nk}(\epsilon,t)\,. \tag{D.20}$$

We insert the adiabatic expansion of the scattering matrix Eq. (D.8) and consistently collect the terms order by order in the velocity.

Zeroth order To zeroth order in the velocity we obtain the unitarity condition for the frozen scattering matrix

$$\delta_{mk} = \sum_n S_{mn} S^\dagger_{nk}\,. \tag{D.21}$$

First order Up to first order in the velocity Eq. (D.20) reads

$$\delta_{mk} = \sum_n \Big[S_{mn} S^\dagger_{nk} + \dot{X} A_{mn} S^\dagger_{nk} + \dot{X} S_{mn} A^{,\dagger}_{nk}(\epsilon) + \frac{i}{2} \left(\frac{\partial S_{mn}}{\partial \epsilon} \frac{\partial S^\dagger_{nk}}{\partial t} - \frac{\partial S_{mn}}{\partial t} \frac{\partial S^\dagger_{nk}}{\partial \epsilon} \right) \Big] . \tag{D.22}$$

Using that the frozen scattering matrix S is unitary and $\partial_t S = \dot{X} \partial_X S$ this yields

$$\sum_n \left[A^X_{mn} S^\dagger_{nk} + S_{mn}(\epsilon) A^{X,\dagger}_{nk} \right] = - \sum_n \frac{i}{2} \left(\frac{\partial S_{mn}}{\partial \epsilon} \frac{\partial S^\dagger_{nk}}{\partial X} - \frac{\partial S_{mn}}{\partial X} \frac{\partial S^\dagger_{nk}}{\partial \epsilon} \right) . \tag{D.23}$$

Second order Up to second order in the velocity one obtains upon using Eqs. (D.21) and (D.23)

$$\begin{aligned} 0 = \dot{X}^2 \sum_n \Big[& A_{mn} A^\dagger_{nk} + S_{mn} B^{,\dagger}_{nk}(\epsilon) + B_{mn} S^\dagger_{nk} \\ & + \frac{i}{2} \left(\frac{\partial A_{mn}}{\partial \epsilon} \frac{\partial S^\dagger_{nk}}{\partial X} - \frac{\partial A_{mn}}{\partial X} \frac{\partial S^\dagger_{nk}}{\partial \epsilon} \right) + \frac{i}{2} \left(\frac{\partial S_{mn}}{\partial \epsilon} \frac{\partial A^\dagger_{nk}}{\partial X} - \frac{\partial S_{mn}}{\partial X} \frac{\partial A^\dagger_{nk}}{\partial \epsilon} \right) \\ & - \frac{1}{8} \left(\partial^2_\epsilon S_{mn} \partial^2_X S^\dagger_{nk} + \partial^2_X S_{mn} \partial^2_\epsilon S^\dagger_{nk} - 2 \partial_\epsilon \partial_X S_{mn} \, \partial_X \partial_\epsilon S^\dagger_{nk} \right) \Big] . \end{aligned} \tag{D.24}$$

Bibliography

S. Ajisaka, F. Barra, C. Mejía-Monasterio, and T. Prosen. Nonequlibrium particle and energy currents in quantum chains connected to mesoscopic Fermi reservoirs. *Phys. Rev. B*, 86(12):125111, 2012.

A. E. Allahverdyan and T. M. Nieuwenhuizen. Extraction of work from a single thermal bath in the quantum regime. *Phys. Rev. Lett.*, 85:1799–1802, 2000.

B. L. Altshuler and L. I. Glazman. Pumping electrons. *Science*, 283(5409): 1864–1865, 1999.

S. An, J.-N. Zhang, M. Um, D. Lv, Y. Lu, J. Zhang, Z.-Q. Yin, H. T. Quan, and K. Kim. Experimental test of the quantum Jarzynski equality with a trapped-ion system. *Nat. Phys.*, 11(2):193–199, 2014.

L. Arrachea and F. von Oppen. Nanomagnet coupled to quantum spin Hall edge: An adiabatic quantum motor. *Phys. E Low-dimensional Syst. Nanostructures*, 74:596–602, 2015.

O. M. Auslaender, A. Yacoby, R. de Picciotto, K. W. Baldwin, L. N. Pfeiffer, and K. W. West. Experimental Evidence for Resonant Tunneling in a Luttinger Liquid. *Phys. Rev. Lett.*, 84(8):1764–1767, 2000.

O. M. Auslaender, A. Yacoby, R. de Picciotto, K. W. Baldwin, L. N. Pfeiffer, and K. W. West. Tunneling spectroscopy of the elementary excitations in a one-dimensional wire. *Science*, 295(5556):825–828, 2002.

O. M. Auslaender, H. Steinberg, A. Yacoby, Y. Tserkovnyak, B. I. Halperin, K. W. Baldwin, L. N. Pfeiffer, and K. W. West. Spin-charge separation and localization in one dimension. *Science*, 308(5718):88–92, 2005.

J. E. Avron, A. Elgart, G. M. Graf, and L. Sadun. Optimal Quantum Pumps. *Phys. Rev. Lett.*, 87(23):236601, 2001.

R. Balian. *From Microphysics to Macrophysics*. Theoretical and Mathematical Physics. Springer Berlin Heidelberg, 2007.

T. B. Batalhão, A. M. Souza, L. Mazzola, R. Auccaise, R. S. Sarthour, I. S. Oliveira, J. Goold, G. De Chiara, M. Paternostro, and R. M. Serra. Experimental Reconstruction of Work Distribution and Study of Fluctuation Relations in a Closed Quantum System. *Phys. Rev. Lett.*, 113(14):140601, 2014.

C. W. J. Beenakker, C. Emary, M. Kindermann, and J. L. van Velsen. Proposal for Production and Detection of Entangled Electron-Hole Pairs in a Degenerate Electron Gas. *Phys. Rev. Lett.*, 91(14):147901, 2003.

A. Benyamini, A. Hamo, S. Viola Kusminskiy, F. von Oppen, and S. Ilani. Real-space tailoring of the electron-phonon coupling in ultraclean nanotube mechanical resonators. *Nat. Phys.*, 10(2):151–156, 2014.

N. Bode, S. Viola Kusminskiy, R. Egger, and F. von Oppen. Scattering Theory of Current-Induced Forces in Mesoscopic Systems. *Phys. Rev. Lett.*, 107(3): 036804, 2011.

N. Bode, L. Arrachea, G. S. Lozano, T. S. Nunner, and F. von Oppen. Current-induced switching in transport through anisotropic magnetic molecules. *Phys. Rev. B*, 85(11):1–13, 2012a.

N. Bode, S. Viola Kusminskiy, R. Egger, and F. von Oppen. Current-induced forces in mesoscopic systems: A scattering-matrix approach. *Beilstein J. Nanotechnol.*, 3:144–162, 2012b.

P. W. Brouwer. Scattering approach to parametric pumping. *Phys. Rev. B*, 58 (16):R10135–R10138, 1998.

A. Bruch, M. Thomas, S. Viola Kusminskiy, F. von Oppen, and A. Nitzan. Quantum thermodynamics of the driven resonant level model. *Phys. Rev. B*, 93:115318, 2016.

A. Bruch, C. Lewenkopf, and F. von Oppen. Landauer-Büttiker approach to strongly coupled quantum thermodynamics: inside-outside duality of entropy evolution. *arXiv:1709.06043*, 2017.

R. Bustos-Marún, G. Refael, and F. von Oppen. Adiabatic Quantum Motors. *Phys. Rev. Lett.*, 111(6):060802, 2013.

M. Büttiker. Scattering theory of current and intensity noise correlations in conductors and wave guides. *Phys. Rev. B*, 46(19):12485–12507, 1992.

M. Campisi, P. Talkner, and P. Hänggi. Fluctuation theorem for arbitrary open quantum systems. *Phys. Rev. Lett.*, 102:210401, 2009.

S. Carnot. *Réflexions sur la puissance motrice du feu et sur les machines propres à développer atte puissance.* Bachelier Libraire, 1824.

A. H. Castro Neto and M. P. A. Fisher. Dynamics of a heavy particle in a Luttinger liquid. *Phys. Rev. B*, 53(15):9713–9718, 1996.

B. S. L. Collins, J. C. M. Kistemaker, E. Otten, and B. L. Feringa. A chemically powered unidirectional rotary molecular motor based on a palladium redox cycle. *Nat. Chem.*, 2016.

H. G. Craighead. Nanoelectromechanical Systems. *Science*, 290(5496):1532–1535, 2000.

G. E. Crooks. Entropy production fluctuation theorem and the nonequilibrium work relation for free energy differences. *Phys. Rev. E*, 60(3):2721–2726, 1999.

S. Deffner and E. Lutz. Nonequilibrium entropy production for open quantum systems. *Phys. Rev. Lett.*, 107:140404, 2011.

C. Dekker, Z. Yao, H. W. C. Postma, and L. Balents. Carbon nanotube intramolecular junctions. *Nature*, 402(6759):273–276, 1999.

K. L. Ekinci and M. L. Roukes. Nanoelectromechanical systems. *Rev. Sci. Instrum.*, 76(6):061101, 2005.

M. Esposito, K. Lindenberg, and C. Van den Broeck. Entropy production as correlation between system and reservoir. *New J. Phys.*, 12(1):013013, 2010.

M. Esposito, M. A. Ochoa, and M. Galperin. Nature of heat in strongly coupled open quantum systems. *Phys. Rev. B*, 92:235440, 2015a.

M. Esposito, M. A. Ochoa, and M. Galperin. Quantum thermodynamics: A nonequilibrium green's function approach. *Phys. Rev. Lett.*, 114:080602, 2015b.

L. J. Fernández-Alcázar, R. A. Bustos-Marún, and H. M. Pastawski. Decoherence in current induced forces: Application to adiabatic quantum motors. *Phys. Rev. B*, 92(7):075406, 2015.

M. P. A. Fisher and L. I. Glazman. Transport in a One-Dimensional Luttinger Liquid. In L. L. Sohn, L. P. Kouwenhoven, and G. Schön, editors, *Mesoscopic Electron Transport*. NATO ASI (Springer Netherlands), 1997.

R. Gallego, A. Riera, and J. Eisert. Thermal machines beyond the weak coupling regime. *New J. Phys.*, 16(12):125009, 2014.

M. Galperin, M. a. Ratner, and A. Nitzan. Molecular transport junctions: vibrational effects. *J. Phys. Condens. Matter*, 19(10):103201, 2007.

T. Giamarchi. *Quantum Physics in One Dimension*. International Series of Monographs on Physics. Clarendon Press, 2004.

G. Giuliani and G. Vignale. *Quantum Theory of the Electron Liquid*. Masters Series in Physics and Astronomy. Cambridge University Press, 2005.

F. D. M. Haldane. 'Luttinger liquid theory' of one-dimensional quantum fluids. I. Properties of the Luttinger model and their extension to the general 1D interacting spinless Fermi gas. *J. Phys. C Solid State Phys.*, 14(19):2585–2609, 1981.

P. Hänggi and P. Talkner. The other QFT. *Nat. Phys.*, 11(2):108–110, 2015.

P. Hänggi, G.-L. Ingold, and P. Talkner. Finite quantum dissipation: the challenge of obtaining specific heat. *New J. Phys.*, 10(11):115008, 2008.

H. Haug and A. Jauho. *Quantum Kinetics in Transport and Optics of Semiconductors, Springer*, 1996.

S. Hilt and E. Lutz. System-bath entanglement in quantum thermodynamics. *Phys. Rev. A - At. Mol. Opt. Phys.*, 79(1):4–7, 2009.

C. Jarzynski. Nonequilibrium equality for free energy differences. *Phys. Rev. Lett.*, 78(14):2690–2693, 1997.

C. Jarzynski. Equalities and Inequalities: Irreversibility and the Second Law of Thermodynamics at the Nanoscale. *Annu. Rev. Condens. Matter Phys.*, 2 (1):329–351, 2011.

A.-P. Jauho, N. S. Wingreen, and Y. Meir. Time-dependent transport in interacting and noninteracting resonant-tunneling systems. *Phys. Rev. B*, 50: 5528–5544, 1994.

E. T. Jaynes. Information Theory and Statistical Mechanics. *Phys. Rev.*, 106 (4):620–630, 1957.

I. Junier, A. Mossa, M. Manosas, and F. Ritort. Recovery of free energy branches in single molecule experiments. *Phys. Rev. Lett.*, 102(7):2–5, 2009.

A. Kamenev. *Field Theory of Non-Equilibrium Systems*. Cambridge University Press, Cambridge, 2011.

C. L. Kane and M. P. A. Fisher. Transport in a one-channel Luttinger liquid. *Phys. Rev. Lett.*, 68(8):1220–1223, 1992.

T. Karzig, G. Refael, L. I. Glazman, and F. von Oppen. Energy Partitioning of Tunneling Currents into Luttinger Liquids. *Phys. Rev. Lett.*, 107(17):176403, 2011.

T. Kita. Introduction to nonequilibrium statistical mechanics with quantum field theory. *Prog. Theor. Phys.*, 123(4):581–658, 2010.

M. Klok, N. Boyle, M. T. Pryce, A. Meetsma, W. R. Browne, and B. L. Feringa. MHz Unidirectional Rotation of Molecular Rotary Motors. *J. Am. Chem. Soc.*, 130(32):10484–10485, 2008.

J. Koch and F. von Oppen. Franck-Condon Blockade and Giant Fano Factors in Transport through Single Molecules. *Phys. Rev. Lett.*, 94(20):206804, 2005.

J. Koch, F. von Oppen, and A. V. Andreev. Theory of the Franck-Condon blockade regime. *Phys. Rev. B*, 74(20):205438, 2006.

J. V. Koski, T. Sagawa, O.-P. Saira, Y. Yoon, A. Kutvonen, P. Solinas, M. Möttönen, T. Ala-Nissila, and J. P. Pekola. Distribution of entropy production in a single-electron box. *Nat. Phys.*, 9(10):644–648, 2013.

J. V. Koski, V. F. Maisi, T. Sagawa, and J. P. Pekola. Experimental observation of the role of mutual information in the nonequilibrium dynamics of a Maxwell demon. *Phys. Rev. Lett.*, 113(3):1–5, 2014.

N. Koumura, R. W. Zijlstra, R. A. van Delden, N. Harada, and B. L. Feringa. Light-driven monodirectional molecular rotor. *Nature*, 401(6749):152–155, 1999.

L. P. Kouwenhoven, C. M. Marcus, P. L. McEuen, S. Tarucha, R. M. Westervelt, and N. S. Wingreen. *Electron Transport in Quantum Dots*, pages 105–214. Springer Netherlands, Dordrecht, 1997.

T. Kudernac, N. Ruangsupapichat, M. Parschau, B. Maciá, N. Katsonis, S. R. Harutyunyan, K.-H. Ernst, and B. L. Feringa. Electrically driven directional motion of a four-wheeled molecule on a metal surface. *Nature*, 479(7372): 208–211, 2011.

L. Landau. The theory of a fermi liquid. *Soviet Physics Jetp-Ussr*, 3(6):920–925, 1957.

B. Lassagne, Y. Tarakanov, J. Kinaret, D. Garcia-Sanchez, and A. Bachtold. Coupling Mechanics to Charge Transport in Carbon Nanotube Mechanical Resonators. *Science*, 325(5944):1107–1110, 2009.

J.-T. Lü, M. Brandbyge, P. Hedegård, T. N. Todorov, and D. Dundas. Current-induced atomic dynamics, instabilities, and Raman signals: Quasiclassical Langevin equation approach. *Phys. Rev. B*, 85(24):245444, 2012.

M. F. Ludovico, J. S. Lim, M. Moskalets, L. Arrachea, and D. Sánchez. Dynamical energy transfer in ac-driven quantum systems. *Phys. Rev. B*, 89:161306, 2014.

D. L. Maslov and M. Stone. Landauer conductance of Luttinger liquids with leads. *Phys. Rev. B*, 52(8):R5539–R5542, 1995.

Q. Meng, S. Vishveshwara, and T. L. Hughes. Spin-transfer torque and electric current in helical edge states in quantum spin Hall devices. *Phys. Rev. B*, 90 (20):205403, 2014.

M. Moskalets. *Scattering Matrix Approach to Non-stationary Quantum Transport*. Imperial College Press, 2012.

M. Moskalets and M. Büttiker. Dissipation and noise in adiabatic quantum pumps. *Phys. Rev. B*, 66(3):35306, 2002.

M. Moskalets and M. Büttiker. Floquet scattering theory for current and heat noise in large amplitude adiabatic pumps. *Phys. Rev. B*, 70(24):245305, 2004a.

M. Moskalets and M. Büttiker. Adiabatic quantum pump in the presence of external ac voltages. *Phys. Rev. B*, 69(20):205316, 2004b.

A. Mossa, M. Manosas, N. Forns, J. M. Huguet, and F. Ritort. Dynamic force spectroscopy of DNA hairpins: I. Force kinetics and free energy landscapes. *J. Stat. Mech. Theory Exp.*, 2009(02):P02060, 2009.

A. K. Naik, M. S. Hanay, W. K. Hiebert, X. L. Feng, and M. L. Roukes. Towards single-molecule nanomechanical mass spectrometry. *Nat. Nanotechnol.*, 4(7): 445–450, 2009.

H. T. M. Nghiem, D. M. Kennes, C. Klöckner, V. Meden, and T. A. Costi. Ohmic two-state system from the perspective of the interacting resonant level model: Thermodynamics and transient dynamics. *Phys. Rev. B*, 93:165130, 2016.

M. A. Ochoa, A. Bruch, and A. Nitzan. Energy distribution and local fluctuations in strongly coupled open quantum systems: The extended resonant level model. *Phys. Rev. B*, 94:035420, 2016.

A. D. O'Connell, M. Hofheinz, M. Ansmann, R. C. Bialczak, M. Lenander, E. Lucero, M. Neeley, D. Sank, H. Wang, M. Weides, J. Wenner, J. M. Martinis, and a. N. Cleland. Quantum ground state and single-phonon control of a mechanical resonator. *Nature*, 464(7289):697–703, 2010.

H. Park, J. Park, A. K. L. Lim, E. H. Anderson, A. P. Alivisatos, and P. L. McEuen. Nanomechanical oscillations in a single-C60 transistor. *Nature*, 407 (6800):57–60, 2000.

J. B. Pendry. Quantum limits to the flow of information and entropy. *J. Phys. A: Math. Gen.*, 16(10):2161, 1983.

M. Perarnau-Llobet, A. Riera, R. Gallego, H. Wilming, and J. Eisert. Work and entropy production in generalised Gibbs ensembles. *New J. Phys.*, 18 (12):123035, 2016.

M. Perarnau-Llobet, H. Wilming, A. Riera, R. Gallego, and J. Eisert. Fundamental corrections to work and power in the strong coupling regime. pages 1–17, 2017.

I. Peschel. Calculation of reduced density matrices from. *J. Phys. A. Math. Gen.*, 36:205–208, 2003.

I. Peschel. Special Review: Entanglement in Solvable Many-Particle Models. *Brazilian J. Phys.*, 42(3-4):267–291, 2012.

X.-L. Qi and S.-C. Zhang. Field-induced gap and quantized charge pumping in a nanoscale helical wire. *Phys. Rev. B*, 79(23):235442, 2009.

R. Rajaraman. *Solitons and Instantons: An Introduction to Solitons and Instantons in Quantum Field Theory*. North-Holland, Amsterdam, 1987.

D. Rugar, R. Budakian, H. J. Mamin, and B. W. Chui. Single spin detection by magnetic resonance force microscopy. *Nature*, 430(6997):329–332, 2004.

O.-P. Saira, Y. Yoon, T. Tanttu, M. Möttönen, D. V. Averin, and J. P. Pekola. Test of the Jarzynski and Crooks Fluctuation Relations in an Electronic System. *Phys. Rev. Lett.*, 109(18):180601, 2012.

P. Samuelsson, E. V. Sukhorukov, and M. Büttiker. Two-Particle Aharonov-Bohm Effect and Entanglement in the Electronic Hanbury Brown?Twiss Setup. *Phys. Rev. Lett.*, 92(2):026805, 2004.

P. G. Silvestrov, P. Recher, and P. W. Brouwer. *Phys. Rev. B*, 93(20):205130, 2016.

G. A. Steele, A. K. Huttel, B. Witkamp, M. Poot, H. B. Meerwaldt, L. P. Kouwenhoven, and H. S. J. van der Zant. Strong Coupling Between Single-Electron Tunneling and Nanomechanical Motion. *Science*, 325(5944):1103–1107, 2009.

P. Strasberg, G. Schaller, N. Lambert, and T. Brandes. Nonequilibrium thermodynamics in the strong coupling and non-Markovian regime based on a reaction coordinate mapping. *New J. Phys.*, 18(7):073007, 2016.

P. Talkner, E. Lutz, and P. Hänggi. Fluctuation theorems: Work is not an observable. *Phys. Rev. E*, 75(5):050102, 2007.

M. Thomas, T. Karzig, S. V. Kusminskiy, G. Zaránd, and F. von Oppen. Scattering theory of adiabatic reaction forces due to out-of-equilibrium quantum environments. *Phys. Rev. B*, 86(19):195419, 2012.

M. Thomas, T. Karzig, and S. Viola Kusminskiy. Langevin dynamics of a heavy particle and orthogonality effects. *Phys. Rev. B*, 92(24):245404, 2015.

D. J. Thouless. Quantization of particle transport. *Phys. Rev. B*, 27(10):6083–6087, 1983.

H. L. Tierney, C. J. Murphy, A. D. Jewell, A. E. Baber, E. V. Iski, H. Y. Khodaverdian, A. F. McGuire, N. Klebanov, and E. C. H. Sykes. Experimental demonstration of a single-molecule electric motor. *Nat. Nanotechnol.*, 6(10):625–629, 2011.

Y. Tserkovnyak, B. I. Halperin, O. M. Auslaender, and A. Yacoby. Finite-Size Effects in Tunneling between Parallel Quantum Wires. *Phys. Rev. Lett.*, 89 (13):136805, 2002.

Y. Tserkovnyak, B. I. Halperin, O. M. Auslaender, and A. Yacoby. Interference and zero-bias anomaly in tunneling between Luttinger-liquid wires. *Phys. Rev. B*, 68(12):125312, 2003.

A. Tsvelick and P. Wiegmann. Exact results in the theory of magnetic alloys. *Adv. Phys.*, 32(4):453–713, 1983.

U. Weiss. *Quantum Dissipative Systems, World Scientific, 3rd Edition*, 2008.

M. R. Wilson, J. Solà, A. Carlone, S. M. Goldup, N. Lebrasseur, and D. A. Leigh. An autonomous chemically fuelled small-molecule motor. *Nature*, 534 (7606):235–240, 2016.

E. Wolf. *Nanophysics and Nanotechnology: An Introduction to Modern Concepts in Nanoscience*. Wiley, 2015.

C. Wu, B. A. Bernevig, and S.-C. Zhang. Helical Liquid and the Edge of Quantum Spin Hall Systems. *Phys. Rev. Lett.*, 96(10):106401, 2006.

L. H. Yu, Z. K. Keane, J. W. Ciszek, L. Cheng, M. P. Stewart, J. M. Tour, and D. Natelson. Inelastic Electron Tunneling via Molecular Vibrations in Single-Molecule Transistors. *Phys. Rev. Lett.*, 93(26):266802, 2004.

X. C. Zhang, E. B. Myers, J. E. Sader, and M. L. Roukes. Nanomechanical torsional resonators for frequency-shift infrared thermal sensing. *Nano Lett.*, 13(4):1528–1534, 2013.

Publications

This thesis is based on the following publications:

- *Quantum thermodynamics of the driven resonant level model.*
  A. Bruch, M. Thomas, S. Viola Kusminskiy, F. von Oppen, and A. Nitzan.
  Phys. Rev. B **93**, 115318, 2016. http://dx.doi.org/10.1103/PhysRevB.93.115318
- *Energy distribution and local fluctuations in strongly coupled open quantum systems: The extended resonant level model.*
  M. A. Ochoa, A. Bruch, and A. Nitzan.
  Phys. Rev. B, **94**, 035420, 2016. http://dx.doi.org/10.1103/PhysRevB.94.035420
- *Landauer-Büttiker approach to strongly coupled quantum thermodynamics: inside-outside duality of entropy evolution.*
  A. Bruch, C. Lewenkopf, and F. von Oppen.
  arXiv:1709.06043, 2017.
- *An interacting adiabatic quantum motor.*
  A. Bruch, S. Viola Kusminskiy, G. Refael, and F. von Oppen.
  In preparation.

The following publication is not subject of this thesis:

- *Effect of interactions on quantum-limited detectors.*
  G. Skorobagatko, A. Bruch, S. Viola Kusminskiy, and A. Romito.
  Phys. Rev. B **95**, 205402, 2017. http://dx.doi.org/10.1103/PhysRevB.95.205402

Acknowledgements

First of all I would like to thank my advisor, Felix von Oppen, for his support and guidance throughout the last years. His way of tackling physics problems had a great influence on me and significantly shaped, how I will address complicated problems in the future. Also his effort to connect me to other scientists, which sparked fruitful international collaborations (see below), led to a very exciting time, scientifically and beyond. Thanks for that.

Throughout the past years I had the chance to work with a number of great scientists, of which I want to address a few individually in the following. Right in the beginning of my PhD I started to work with Abe Nitzan. His immense kindness and patience really gave me a good start and I am very grateful for his immense hospitality during my visit in the *City of Brotherly Love*. Towards the second half I started working with Caio Lewenkopf, which culminated in a wonderful time in the *Cidade Maravilhosa*. And I want to thank Silvia Viola Kusminskiy for her extensive support throughout the entire PhD and for making all of our collaborations so much fun.

Furthermore, I am grateful for having met all the people of the Dahlem center for Complex Quantum systems, which gave this place here such a cheerful atmosphere and were always there for discussions and support—especially Yang (Bob) Peng, Yuval Vinkler and Clemens Meyer zu Rheda, who started as colleagues and are now good friends.

Moreover, I want to thank Piet Brouwer for co-refereeing this thesis and putting me on the path of Condensed Matter Theory.

I am also indebted to Gabi Herrmann, Brigitte Odeh and Marietta Wissmann for their overall support.

Finally, I want to acknowledge the financial support by the SFB 658 of the Deutsche Forschungsgemeinschaft.

Curriculum Vitae

Der Lebenslauf ist in der Online-Version aus Gründen des Datenschutzes nicht enthalten.

Selbstständigkeitserklärung

Hiermit versichere ich, dass ich in meiner Dissertation alle Hilfsmittel und Hilfen angegeben habe, und auf dieser Grundlage die Arbeit selbstständig verfasst habe. Diese Arbeit habe ich nicht schon einmal in einem früheren Promotionsverfahren eingereicht.

Berlin, Oktober 2017